Accelerating phytoplankton phenomics through FTIR spectroscopy

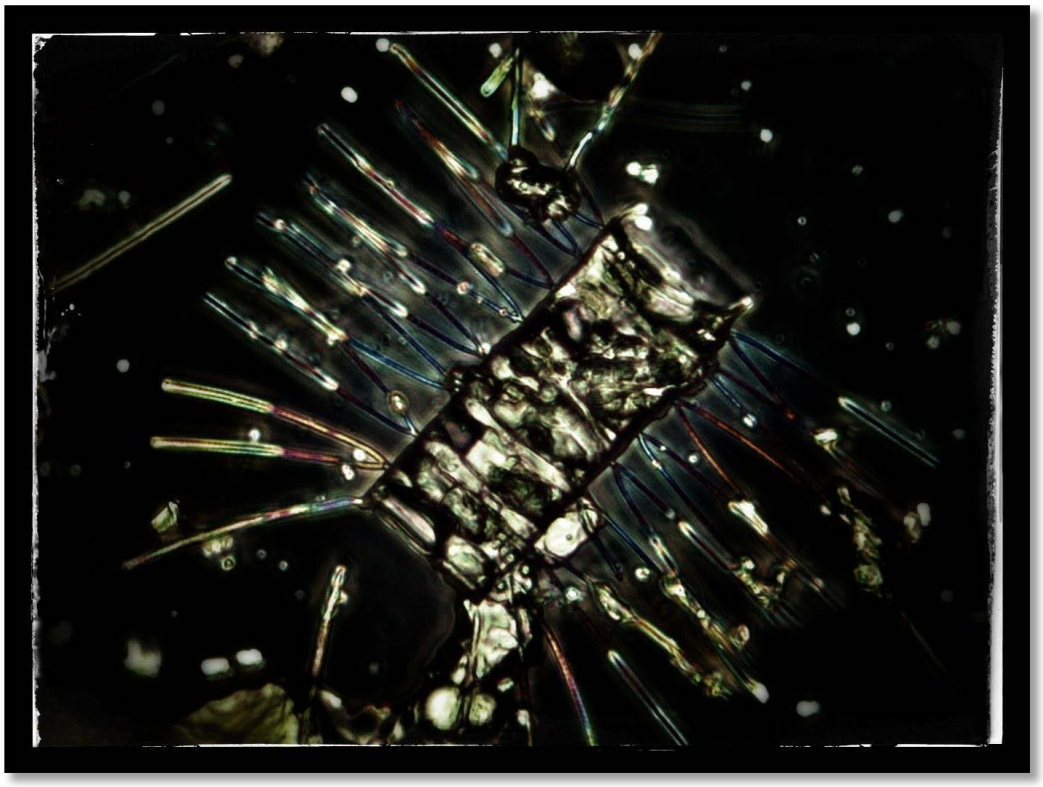

Olivia Sackett

Doctoral Thesis, February 2015

Supervisors:

Professor Peter Ralph, Professor John Beardall, Dr Philip Heraud,

Dr Martina Doblin and Dr Ross Hill

Prediction is difficult, particularly if it involves the future.

— Uncertain…depends on whom you ask.

Certificate of original authorship

I certify that the work in this thesis has not previously been submitted for a degree nor has it been submitted as part of requirements for a degree except as fully acknowledged within the text.
I also certify that the thesis has been written by me. Any help that I have received in my research work and the preparation of the thesis itself has been acknowledged. In addition, I certify that all information sources and literature used are indicated in the thesis.

Production Note:
Signature removed prior to publication.

Olivia Sackett

February 15, 2015

Acknowledgements

To John Beardall and Phil Heraud, thank you for a decade of education, encouragement, mentoring, facilitation, relentless reviewing skills and friendship. Learning from you has been an honour and a privilege. I hope to continue to work with you both for many more years.

Thank you to Peter Ralph, Martina Doblin and Ross Hill for making my candidature at the University of Technology, Sydney possible, and for facilitating my doctoral degree. Ross, your enthusiasm, attention to detail and rapid turn-around-time never cease to impress me.

To Katherina Petrou, thanks for your friendship and guidance. You have provided focus, direction, humour, cups of tea and soothing words during tough times. I will miss our many hours in the lab together. Thank you to my fellow PhD candidates (Sutinee Sinutok, Verena Schrameyer, Ying Hong and Noni Dowsett) for all the great times we've had.

Finally, this project would not have been possible without the seemingly limitless support of my family and friends. In particular, my partner Wayne Vest has played a critical role by providing technical, moral, emotional and financial support. Thank you, Wayne, for encouraging and enabling me to follow my dreams. Thanks to Mum and Dad (Na-Na and Gan-Pa) for making education such a high priority in our family, for providing enthusiasm and for helping us to bring up our two beautiful daughters. I would especially like to thank Gan-Pa for cheerfully providing porridge and wheat bix to Merren at 5 am during winter. Thank you to Christine Connelly for endless PhD pep-talks over coffee and chai, and for technical assistance at the Australian Synchrotron.

Thank you all once again, what a fabulous time it's been!

List of Figures

List of Tables

Abstract

Marine phytoplankton play a driving role in global biogeochemical cycling, providing fuel for marine and terrestrial ecosystems, and removing substantial quantities of CO_2 from the atmosphere. Phytoplankton respond to environmental change by varying their phenotypes, including photophysiology, macromolecular composition and morphology. Southern Ocean phytoplankton are subjected to one of the most extreme habitats on earth, resulting in great phenotypic variation between and within taxonomic groups. Given they provide a significant net sink of atmospheric CO_2 and support the most biologically productive ecosystem on earth, improving our ability to predict the responses of Southern Ocean phytoplankton to environmental change is of global importance. At present, our ability to predict the responses of these critical organisms to environmental change, including climate change, is limited by a bottleneck in the efficiency with which we can characterise phytoplankton phenotypes.

This thesis demonstrates the feasibility of accelerating phytoplankton phenomics using Fourier Transform Infrared (FTIR) microspectroscopy, a powerful yet under-utilised frontier technology. The extensive phenotypic variation shown by Southern Ocean phytoplankton provided excellent scope for demonstrating the power of the microspectroscopic approach. Coupling the microspectroscopic approach with multivariate modeling tools enabled the characterisation of phenotypic plasticity from cell FTIR spectra. When combined with mass spectrometry data, cell FTIR spectra provided accurate estimates of multiple phenotypic parameters including cellular protein, carbon and energy. Of particular value, spectroscopic models were able to accurately estimate rates of carbon production from samples taken at a single time-point, circumventing the need to take measurements over time. Further, the high spatial resolution achievable with microspectroscopy enabled the analysis of individual cells, revealing taxon-specific responses to iron availability within samples taken from a mixed natural Southern Ocean phytoplankton bloom. This work demonstrates that incorporating FTIR microspectroscopy into the phenomics toolbox will improve the efficiency of phenotypic data collection and, in combination with multivariate modeling, will enable the development of powerful, taxon-specific predictive phenomic models.

Table of Contents

1 Introduction

1.1 Importance of marine phytoplankton

Each year, photosynthesis by marine phytoplankton converts about 58 gigatonne of atmospheric carbon dioxide into organic carbon molecules, equivalent in magnitude to the productivity of terrestrial vegetation, creating half the oxygen we breathe as a by-product (Field et al. 1998). As phytoplankton assimilate CO_2 and a proportion of the fixed carbon sinks to the deep ocean, more CO_2 then diffuses into surface waters from the atmosphere. This process, known as the "biological pump", is estimated to have redistributed nearly half the CO_2 released by human activites from the atmosphere into the ocean (Richardson 2009). Phytoplankton perform two major functions within the network of global biogeochemical cycles. The first is the photosynthetic transformation of inorganic forms of carbon into organic molecules and the second being the capture and temporary storage of nutrients and trace metals. The portion of organic carbon made available to higher trophic levels as a result of the first function, is known as *primary production* (Falkowski *et al.* 1998). Approximately 4% of marine primary production is contributed by the Southern Ocean, albeit at rates that can double those measured at subtropical sites (Westberry et al. 2008; Ducklow et al. 2007). Southern Ocean phytoplankton constitute an important component of the global carbon cycle, support the most biologically productive ecosystem on earth and constitute a significant net sink of atmospheric CO_2 (Busalacchi 2004).

High genetic diversity, combined with a collection of flexible biogeochemical processes, has ensured the success of the phytoplankton for at least the last one thousand-million years, despite earth's considerable climatic variation (Falkowski et al. 1998). Phytoplankton cells have evolved a number of unique characteristics, which enable them to capitalise on the dynamic physical and chemical marine environment. For example, phytoplankton are able to take advantage of transient nutrient fluxes by storing excess nutrients for later growth (Geider & La Roche 2002). Additionally, the small size (and therefore high surface area to volume ratio) of phytoplankton cells enables them to capture nutrients and trace metals that are unavailable to larger organisms. Phytoplankton in surface waters accumulate nutrients and trace metals, including N, P, Si, Fe, Mn, Ni, Cu and Zn, which can then be exported to depth as sinking biogenic particles or consumed by higher trophic levels (Twining et al. 2008). In order to cope with environmental change, phytoplankton must adopt strategies to regulate metabolic processes. Short-term physiological and metabolic adjustments in response to transitory changes in environmental conditions are known as *acclimation*, whereas adjustments which occur over many generations and confer some kind of genetic change are known as *adaptation* (Morgan-Kiss *et al* 2006). Acclimation can result

in substantial changes to the macromolecular composition of phytoplankton. Variations in the relative proportions of proteins, lipids and carbohydrates in microalgae may have dramatic implications for grazers. For example, as lipids contain ~2 and 2.3 times as many calories per unit biomass as proteins and carbohydrates (respectively), algal cells rich in lipids may contain more energy per unit biomass than those rich in proteins or carbohydrates (Whyte 1987). Further, the total amount of carbon stored is highly dependent on the macromolecular composition of the biomass (Geider & La Roche 2002). The ratio of carbon to other elements (elemental stoichiometry) is known to influence both the carbon-use efficiency and the carbon-sequestering potential of marine ecosystems (Hessen et al. 2004). In other words, changes in the phenotypes of phytoplankton communities directly affect biogeochemical cycling (including carbon and bio-limiting elements) in the sea, as well as ecosystem structure and function (Finkel et al. 2010).

Contemporary phytoplankton living in extreme habitats demonstrate a remarkable resilience to environmental change. In the Southern Ocean, the annual cycle of sea ice formation causes the Antarctic continent to increase five-fold in size from 4 x 10^6 km^2 to 20 x 10^6 km^2 each year (Horner *et al* 1992). The ice brings with it a number of challenges for phytoplankton including extremes in temperature, salinity, light, pH and nutrient availability. Ranging from 0 to -35°C, sea ice represents one of the coldest marine habitats on earth (Mock & Thomas 2005), while salinity levels can reach 200 ‰, nearly 7 times those of seawater (Eicken et al. 2000). Perhaps surprisingly, some species of phytoplankton can survive and even thrive under these conditions, leading to the development of sea ice microbial communities within sea ice brine channels. Algae living within sea ice contribute a modest 5% of total annual primary production for the sea ice zone, though the ecological importance of the sea ice microalgae is of far greater significance than such figures suggest (Lizotte 2001). In winter, sea ice algae are a critical food resource for grazers, including juvenile krill and larvae, and as such play a key ecological role in the success of the Southern Ocean food web (Arrigo & Thomas 2004). In spring, when the ice starts to melt, the phytoplankton experience an influx of cool, low salinity meltwater from the ice into the surface ocean. This promotes stratification and shallow mixing which increases the exposure of phytoplankton to sunlight. In addition, micronutrients such as iron, which have been collecting on the surface of ice and snow throughout the sea ice season, are released into the stratified layer and rapidly consumed by phytoplankton. In response to these conditions, massive blooms of phytoplankton (up to 45,000 km^2) form throughout spring months (Quéguiner et al. 2007). The annual cycle completes as stratified layers begin to break down, promoting a pelagic habitat, which is characterised by the circulation of phytoplankton into deeper water, average salinity levels and warmer temperatures.

The Southern Ocean ecosystem is profoundly affected by the seasonal duration and extent of winter sea ice. Changes to Sothern Ocean sea ice algae communities due to altered seasonal duration and extent of sea ice are likely to impact higher trophic levels since sea ice algae are a key component of the Antarctic food web (Smetacek & Nicol 2005; McMinn et al. 2007). Indeed, reduced duration and extent of winter sea ice along the West Antarctic Peninsula have been correlated with a decline in krill abundance and increased abundance of salps (planktonic tunicates) the following summer, though the mechanisms behind these trends are yet to be elucidated (Atkinson et al. 2004). Laboratory studies have demonstrated that zooplankton growth rate and reproductive success can be directly affected by the growth phase and macromolecular composition of their phytoplankton food source (Long & Hay 2006; Diekmann et al. 2009a). In combination with observations from the West Antarctic Peninsula, these studies indicate that further examination of phytoplankton responses to environmental conditions and the flow-on effects to higher trophic levels is warranted.

Chapter 2 of this thesis examines the macromolecular responses of three key species of Southern Ocean phytoplankton, *Fragilariopsis cylindrus*, *Chaetoceros simplex* and *Pseudo-nitzschia subcurvata*, to conditions encountered during the annual sea ice cycle. To compare the phenotypic plasticity of the three species in response to conditions encountered in the Southern Ocean, laboratory cultures were exposed to salinity and temperature conditions characteristic of sea ice, meltwater and pelagic habitats and changes in macromolecular composition of individual cells were measured using synchrotron FTIR microspectroscopy (discussed below). Significant differences in macromolecular plasticity were measured and correlated with the organisms' known distributions within the Southern Ocean. The study demonstrates a methodology based on multivariate modeling techniques which quantifies the degree of phenotypic plasticity displayed by each species. This chapter introduces the concept of phenotypic plasticity and explores how measurements of phenotypic plasticity may assist us to predict which species may cope best under rapid environmental change, as is currently being experienced by the Southern Ocean and Antarctica. Further, some potential implications of phytoplankton responses to environmental change, such as alterations to energy and nutrient flows throughout the Southern Ocean ecosystem, are discussed.

The Southern Ocean is the largest upwelling region in the world, resulting in an abundant supply of inorganic nutrients including phosphates, nitrates and silicates (Smetacek et al. 2004; Falkowski et al. 1998; El-Sayed 2005). Despite the abundance of nutrients, Antarctic phytoplankton seldom achieve high growth rates (El-Sayed 2005). For this reason, the Southern Ocean is recognised as the world’s largest high nutrient-low chlorophyll (HNLC) ocean

(Tomczak & Godfrey 2003; El-Sayed 2005). The main factor known to limit photosynthetic growth in the Southern Ocean is iron limitation. Although it is widely accepted that iron availability has profound effects on the growth rate and productivity of phytoplankton (Assmy & Smetacek 2009; Pankowski & McMinn 2009; Pollard et al. 2009; Cochlan et al. 2000), there is uncertainty about broader phenotypic responses, such as the influence of iron availability on diatom silicification (Twining et al. 2008). Further, although changes in phytoplankton phenotypes are expected to affect trophic dynamics, the nature of flow-on effects for marine ecosystems remain poorly understood (Finkel et al. 2010). In response to this knowledge gap, Chapter 3 of this thesis presents a study of diatoms sampled near the Kerguelen Islands in November 2011. Upwelling along the plateau and coastal areas provides naturally iron enriched waters which stimulate the largest bloom of phytoplankton south of the polar front (Quéguiner et al. 2007). Synchrotron FTIR microspectroscopy was used to analyse the macromolecular composition of individual diatom cells, generating the first known taxon-specific dataset of its kind. The study revealed taxon-specific phenotypic responses to iron availability and challenged the generally held view that iron limitation stimulates increased silicification in marine diatoms.

1.2 Infrared spectroscopy-based phenomics: strengths, prospects

Infrared spectroscopy essentially involves illuminating a sample with infrared radiation, then measuring the absorbance of that radiation by macromolecules in the sample. Although there are a variety of other methods available for the detection and measurement of macromolecules (e.g. mass spectrometry, chromatography, UV-visible spectroscopy), infrared spectroscopy offers many distinct advantages over more traditional approaches. Firstly, the cost of acquiring infrared data is generally a small fraction of the cost of alternative methods. Further, most alternative methods involve significant sample preparation (such as chemical digestion) and subsequent chemical assays for measurement with colorimetric instruments. Differences in cell morphology and composition can result in differences in the efficiency of digestion and extraction processes (Barbarino & Lourenço 2005). Such variations are very difficult to quantify, meaning that extraction methods tend to introduce uncertainties into the calculation of the concentrations of macromolecules. Methods that involve minimal sample processing have obvious appeal as the potential for experimental artefacts and biases inherent in complex and lengthy extraction and measurement of biochemical components are greatly reduced (Hirschmugl et al. 2005; Montechiaro et al. 2006). As a result, Fourier Transform Infrared Spectroscopy (FTIR) is becoming a widely used tool for determining the macromolecular composition of a variety of microbiological samples including microalgae (Giordano et al. 2001; Kansiz et al. 1999; Heraud et al. 2007; Sackett et al. 2013). The characteristics that make this method appealing include

minimal sample preparation, repeatability of measurements, rapid acquisition of data and the high spatial resolution achievable with FTIR microspectroscopy. Further enhanced spatial resolution is achieved by coupling of the FTIR microscope with a synchrotron light source. Studies utilising synchrotron light sources have achieved sub-cellular resolution and have successfully probed the physiological response of large algal cells (~300 μm) to nutrient replenishment in real time (Heraud et al. 2005). Like all new methods, early studies using FTIR spectroscopy encountered technical challenges such as inaccuracies related to sample preparation, including sample thickness. These types of artefacts have been well characterised and accounted for through the use of data pre-processing techniques for normalisation and to account for minor shifts peak position (Heraud & Wood 2013).

FTIR spectroscopic studies of algae have covered a diversity of applications and purposes including (but not limited to): phosphorus limitation (Sigee et al. 2007; Dean, Nicholson, et al. 2008; Dean, Estrada, et al. 2008; Philip Heraud et al. 2008); biodiversity (Domenighini and Giordano 2009); spatial metabolic fingerprinting (Patel et al. 2008); nutritional content (Murdock et al. 2008); metabolic costs of carbon assimilation (Jakob *et al* 2007); and cell sheath silicification (Benning et al. 2004). A further, particularly valuable, characteristic of FTIR spectroscopy, is its ability to measure multiple phenotypic traits simultaneously. Building on this previous ground-work, Chapter 4 of this thesis presents an overview of the phenotypic traits that have been measured thus far using spectroscopy and introduces several new traits (including carbon productivity, carbon and protein content) which can be also be probed using the technique. To my knowledge, this study is the first to demonstrate a method to estimate the rate of carbon production from samples collected at a single time-point, as opposed to using the traditional method of incubating samples over time and taking several measurements to determine a rate. In summary, Figure 1-1 outlines the research questions addressed by this thesis.

Figure 1-1 Key Research Questions

Southern Ocean microalgae show great resilience to environmental stress.

i. Is this resilience related to phenotypic plasticity?
ii. Are taxon-specific phenotypic changes related to observed biogeography?
iii. Do such changes in microalgal phenotypes have the potential to affect the Southern Ocean ecosystem and biogeochemical cycling?
iv. Do bulk-community phenotypic measurements reflect those of key taxa?

There is currently a bottleneck in the rate of acquisition of phenotypic data.

Can FTIR Spectroscopy be used to:

v. increase the efficiency and cost-effectiveness of phenotypic data collection?
vi. measure taxon-specific traits in phytoplankton?

Chapter 2 provides a demonstration of the power of FTIR microspectroscopy to measure changes in macromolecular composition and phenotypic plasticity in ecologically significant species of Southern Ocean phytoplankton; Chapter 3 provides a field-validation of this method using phytoplankton collected from the Kerguelen Island bloom and demonstrates taxon-specific responses to iron availability in a natural population; and Chapter 4 demonstrates some new and powerful applications of FTIR microspectroscopy to the field of phytoplankton phenomics. Collectively, this work demonstrates that incorporating FTIR spectroscopy into the phenomics toolbox will substantially improve the efficiency of phenotypic data collection and, in combination with multivariate modeling, will enable the development of powerful, taxon-specific predictive phenomic models. Such models have the potential to enhance our ability to predict the responses of marine ecosystems to future environmental conditions and assist with modeling the likely flow-on effects for biogeochemical cycling.

2 Phenotypic plasticity of Southern Ocean diatoms: key to success in the sea ice habitat?

In response to research questions i-iii and v (Figure 1-1), an experiment was designed to test the phenotypic plasticity of three key species (*Fragilariopsis cylindrus, Pseudo-nitzschia subcurvata* and *Chaetoceros simplex*) of Southern Ocean diatom. Phenotypic plasticity was measured in the form of overall changes in macromolecular composition between treatments, which were designed to reflect salinity and temperature regimes characteristic of those experienced by algae during the Southern Ocean sea ice cycle. This chapter is a reformatted version of the published manuscript Sackett, O. et al., 2013. Phenotypic plasticity of Southern Ocean diatoms: key to success in the sea ice habitat? *PLoS ONE*, 8(11).

2.1 Introduction

Macromolecules, including proteins, lipids and carbohydrates are the building blocks of life. Microalgae are the primary source of macromolecules in marine ecosystems through their photosynthetic assimilation of dissolved inorganic carbon into organic carbon biomass that is then consumed by higher trophic levels. In the Antarctic, greater than 50% of this production is contributed by diatoms, which dominate the microalgal assemblage, ultimately providing food for krill, fish, whales, penguins, and seabirds (Sarthou et al. 2005). This capacity to synthesise macromolecules enables microalgae to acclimate to prevailing environmental conditions. For example, lipids are synthesised to sustain membrane structure and function and for energy storage, while proteins and carbohydrates have wide-ranging uses including maintenance of cell walls, membrane structure and function, mucus production, and osmoregulation (Tang et al. 2009; Mock & Kroon 2002a; Krell et al. 2008). Such responses to environmental conditions have trophic implications because microalgal macromolecular composition affects herbivore assimilation efficiencies and reproductive success (Diekmann et al. 2009a).

The Southern Ocean is characterised by the seasonal formation and decay of sea ice, which produces a range of environmental conditions from deeply mixed waters in summer to solid ice sheets in winter (Lizotte 2001; Horner et al. 1992). Consequently, diatoms experience rapid fluctuations in physical and chemical conditions associated with the transition from sea ice to meltwater and pelagic habitats (Figure 2-1) (Petrou & Ralph 2011). This highly variable habitat has driven the evolutionary adaptation of extremophile diatoms, which are capable of growing and photosynthesising under conditions that lie at the ends of temperature, pH and salinity tolerance scales (Petrou & Ralph 2011; Ralph et al. 2007).

Phenotypic plasticity refers to an organisms' ability to change their chemistry, physiology, development, morphology or behaviour, to maximise fitness in variable environments (Agrawal 2001). Photophysiological plasticity in Southern Ocean diatoms in response to short term changes in salinity and temperature has previously been reported by Petrou at al. (Petrou et al. 2011; Petrou & Ralph 2011). This study builds on the work conducted by Petrou et al. by investigating whether such environmental changes are also associated with plasticity in macromolecular composition.

Lipid accumulation has frequently been reported in sea ice microalgal communities from both the Arctic and the Southern Ocean and is thought to provide an important source of nutrition and energy to higher trophic levels (Fahl & Kattner 1993; Lee et al. 2008). Although phytoplankton blooms in the pelagic habitat usually contribute a greater percentage of annual primary production, sea ice microalgal communities are thought to provide a vital injection of lipid-rich biomass during the winter-months, when production by phytoplankton is limited by low light conditions under the sea ice (Lizotte 2001; Diekmann et al. 2009a). The average caloric value of lipid biomass in microalgae is reportedly 1.98 and 2.26 times higher than that of protein and carbohydrate biomass, respectively (Whyte 1987). Therefore factors that affect the production of these compounds can influence the overall caloric value of the cell (Jakob et al. 2007). Here we show that the magnitude of change in cellular lipid content is highly species-specific, demonstrating that shifts in community composition have the potential to alter the supply of energy to higher trophic levels (Suárez & Marañón 2003; Diekmann et al. 2009a). Understanding such variability in macromolecular composition provides important information about adaptation strategies of microalgae. It is also essential if we are to understand how the nutritional value of the microalgal community may respond to environmental change, which has implications for the productivity of the entire Antarctic ecosystem.

Despite its importance, we have little understanding of macromolecular composition of individual microalgal species within natural assemblages. This is primarily due to technical limitations of traditional bulk analysis techniques, which do not have the capacity to target individual species within mixed communities. Fourier Transform Infrared (FTIR) microspectroscopy is a vibrational spectroscopic technique becoming increasingly popular amongst microbial ecologists (Murdock & Wetzel 2009; Heraud et al. 2007). The technique measures concentrations of macromolecules and can be used for the classification of samples based on their infrared spectral "fingerprint" (Xie et al. 2012). When coupled with a synchrotron light source, infrared microspectroscopy achieves high sensitivity and spatial resolution (~3 μm for lipids), enabling the analysis of individual microalgal cells (Heraud et al. 2005; Twining, Baines & Fisher 2004; P. Heraud et al. 2008). FTIR microspectroscopy is therefore an excellent candidate for collecting species-specific

data from natural populations, because it allows the targeting of individual species within a mixed sample.

To improve our understanding of macromolecular plasticity and associated changes in nutritional value in response to salinity and temperature regimes characteristic of sea ice, meltwater and pelagic habitats, FTIR microspectroscopy was used to measure macromolecular concentrations in three Antarctic diatoms: *Fragilariopsis cylindrus,* a dominant species in the sea ice and ice-edge habitats of both polar regions (Mock et al. 2007); *Chaetoceros simplex*, which is found in great abundance in pelagic and meltwater habitats around Antarctica and belongs to the most abundant algal genus on the planet (Armand et al. 2005); and *Pseudo-nitszchia subcurvata*, typically found in meltwater habitats of coastal Antarctic waters (Lizotte 2001; Almandoz et al. 2008). This study tests the hypotheses: i. that species well adapted to life in the sea ice demonstrate high phenotypic plasticity in terms of changes in macromolecular composition in response to the highly variable polar marine environment, and ii. that the nutritional value of Antarctic diatoms is influenced by the fluctuating salinity and temperature conditions experienced during an annual cycle. For the first time, synchrotron FTIR microspectroscopy and multivariate data analysis and modelling are used to measure the macromolecular composition of individual Antarctic diatom cells and quantitatively assess the degree of phenotypic plasticity of cell populations in response to conditions characteristic of sea ice meltwater and pelagic habitats.

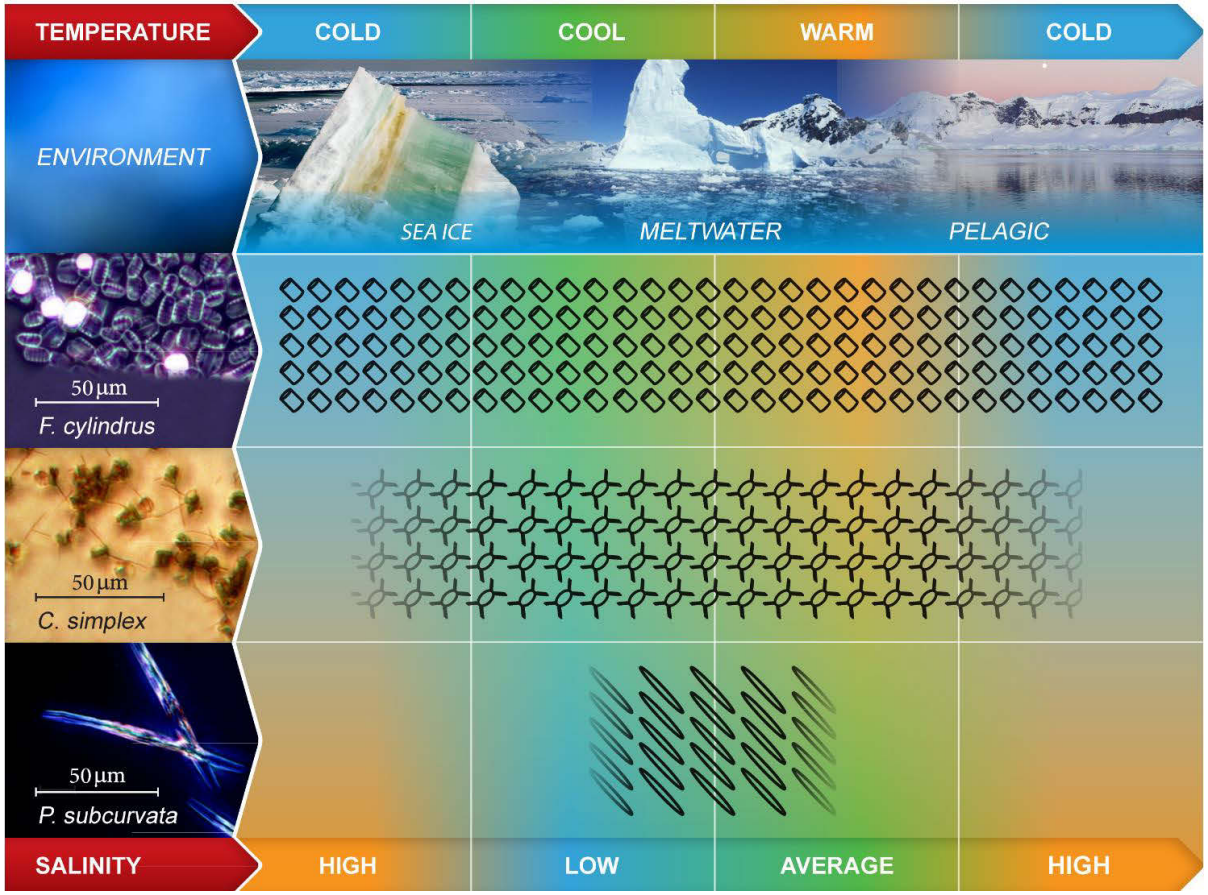

Figure 2-1 Major Southern Ocean habitats and related distribution of diatom species.

The seasonal cycle of sea ice formation and decay produces three major habitats: sea ice, meltwater and pelagic. Sea ice brine channels contain cold, highly saline water within which extremophile microalgae, such as *F. cylindrus*, are able to flourish (visible as brown coloured regions within the sea ice). The melting sea ice produces a stable layer of cool, low salinity water to which species such as *P. subcurvata* have adapted. Once the stratified meltwater layer has broken down, deeper mixing returns and the pelagic habitat prevails. *C. simplex* is most successful in the pelagic and meltwater habitats, but also manages to survive the winter months within the sea ice. *F. cylindrus* is abundant in all three habitats but frequently dominates the sea ice microalgal community

2.2 Materials and Methods

2.2.1 Culturing

F. cylindrus (Grunow) was collected from ice cores (66°S, 147°E) taken in November 2001. Cultures of the Antarctic diatom *C. simplex* were isolated from the coastal waters of Antarctica, Prydz Bay (CS 624, Australian National Algae Culture Collection, CSIRO, Hobart, Australia) and *P. subcurvata* (Hasle) Fryxell was collected from the subpolar South Atlantic Ocean. No permission was necessary for the collection of the algal samples from the Southern Ocean, however permits were obtained from the Australian Quarantine and Inspection Service (AQIS) for the import of samples into Australia. The taxonomic classification of all species was confirmed, based on analysis of frustule morphology by light microscopy. All species were maintained in approximate pelagic conditions at 4°C in natural Antarctic filtered seawater (0.2 µm, 0.28 nM Fe, 145.9 °S 54.0 °S, 72 m), collected during SAZ-Sense, Jan.- Feb. 2007, RV Aurora Australis. Culturing was conducted in specially designed 1 L glass culturing vessels using natural seawater (salinity 34) enriched with F/2 nutrients, with continuous air bubbling and maintained at +4°C (Guillard and Ryther 1962). Cultures received a 16:8 h light:dark cycle at 50 µmol photons m-2 s-1 (Grolux, GMT lighting, Northmead, Australia). Exponential growth phase (confirmed with regular in vivo auto-fluorescence measurements as a proxy for biomass (Wood et al. 2005); Trilogy, Turner Designs Inc., Sunnyvale CA, USA) was maintained for the duration of the experiment by diluting (up to 90%) with fresh medium every 3-5 days. Cultures were concentrated by gentle vacuum filtering using 2 µm polycarbonate membrane filters (Millipore, MA, USA). Concentrated cultures were re-suspended in approximately 150 mL of medium in 250 mL culture flasks at three different salinities (31, 34 and 70 (± 0.5), approximating the characteristics of meltwater, pelagic and sea ice brine channels respectively) and stoppered with gauze (n=4). The salinity of the F/2 medium was adjusted either by the addition of MilliQ water or sodium chloride salt (Sigma, USA) and measured by refractometer. Flasks were then transferred to a temperature-controlled incubator and maintained at one of three temperatures (-1.8, +2 and +5°C (± 0.3°C), simulating characteristic of sea ice, meltwater and pelagic habitats) where the cells were given 72 h (well within the previously reported 7-day cold acclimation phase for *F. cylindrus*) to acclimate before samples were removed and analysed (Mock & Valentin 2004). Pulse amplitude modulated (PAM) fluorometry was used to confirm the algae were extant and photosynthetically active prior to all other measurements being taken.

2.2.2 FTIR microspectroscopy

Approximately 15 mL of cell suspension was filtered through 1 µm polycarbonate filter membranes using a hand-operated vacuum filter tower. Cells collected on the filter were then

resuspended in isotonic saline solution (NaCl (Sigma, USA) and MilliQ water) to wash the cells to remove F/2 medium which contains compounds that can absorb infrared radiation and possibly confound the FTIR measurements (Heraud et al. 2007). The saline solution was kept at the same temperature as the incubation temperature of the cells. This rinsing process was repeated three times for each replicate. Washed cells were deposited on Kevley MirrIR Low-e Microscope Slides (Kevley Technologies, Ohio, USA) using a Shandon Cytospin Centrifuge (Cytospin III, Thermo Fischer Scientific, Waltham, MA) and immediately stored in a vacuum desiccator at room temperature until analysis (Heraud et al. 2007).

Spectral data were collected on the Infrared Microspectroscopy Beamline (2BM1B) at the Australian Synchrotron, Melbourne, Australia in August 2010. Spectra were acquired over the measurement range 4000-800 cm^{-1} with a Vertex 80v FTIR spectrometer (Bruker Optics, Ettlingen, Germany) coupled with an IR microscope (Hyperion 2000, Bruker) with a Mercury Cadmium Telluride detector cooled with liquid nitrogen. The microscope was connected to a computer-controlled microscope stage and placed in a specially designed box which was purged with dehumidified air. The measurements were performed in the mapping mode, using a nominal aperture size of 5 µm × 5 µm with a spectral resolution of 8 cm^{-1}, with 64 scans co-added. Adjusting the aperture for each species provided spectra that were representative unambiguously of individual cells (not clumps of cells) for *C. simplex* and *P. subcurvata.* However, for *F. cylindrus* spectra were acquired from groups of 5-10 cells due to a lower signal to noise ratio compared with the other species. The number of co-added scans was chosen as a good compromise between achieving spectra with good signal to noise characteristics and the rapid acquisition of data. Spectra were processed using Happ-Genzel appodization and 2 levels of zero-filling. Spectral acquisition and instrument control was performed using Opus 6.5 software (Bruker).

FTIR spectral data was exported from the OPUS 6.5 for multivariate analysis using The Unscrambler X v 10.2 (Camo Inc., Oslo, Norway). An initial quality control procedure was performed over the range 3000-950 cm^{-1} where spectra with maximum absorbance greater than 0.85, which resulted from spectral acquisition of regions of the sample where cells were clumped, were rejected. Spectra were then pre-processed taking the second derivative using the Savitzky-Golay algorithm with 9 smoothing points, and normalization using Extended Multiplicative Signal Correction (EMSC).

2.2.3 Multivariate modeling

Partial Least Squares Discrimination Analysis (PLS-DA) modelling was used to classify samples by experimental treatment conditions and species based on their spectra using the Non-linear

Iterative Partial Least Squares (NIPALS) algorithm on mean-centred data. For PLS-DA, infrared spectra from 200-300 individual cells was used to generate a PLS-DA model which was then validated using a test set of 200-300 individual cell spectra which were not used to generate the PLSDA models. The PLSDA training data matrix comprised the spectra (X-variables) and three Y variables with integer values of 0 or +1 coding for the three modelled spectral classes (sea ice, melt water or pelagic conditions, respectively; or the three different species)[49,50]. PLSDA used the spectral ranges containing bands of biological origin between 3050-2800 and 1780-1000 cm^{-1}. Spectra with a predicted Y-value of ≥0.5 were accepted as being from cells of the relevant species or treatment; spectra with predicted Y-values ≤0.5 were rejected. To assess the validity (accuracy) of each model, s*ensitivity* and *specificity* statistics were calculated using the equations True Positives/(True Positives+False Negatives) and True Negatives/(False Positives+True Negatives) respectively (Bylesjö et al. 2006).

Partial Least Squares Regression (PLSR) analysis was used to compare variations in infrared spectra between the ranges 3050-2800 and 1780-1000 cm^{-1} from 200-300 individual cells (X-variables) in response to both temperature and salinity conditions (Y-variables). PLSR analyses were conducted on mean-centred data using the NIPALS algorithm and validated using an independent test set of 200-300 samples which were not used to generate the PLSR models.

Relative changes in the concentration of lipids, carbohydrates, amino acids and phosphorylated molecules were estimated based on proportionality between absorbance and analyte concentration according to the Beer-Lambert Law, previously demonstrated with diatoms and other types of microlagal cells (Jungandreas et al. 2012; Wagner et al. 2010; Giordano et al. 2001). Protein concentration was determined using a combination of mass spectrometry and FTIR spectroscopy to build a predictive PLSR model. Firstly, protein concentration was determined in a subset of *C. simplex* samples using mass spectrometry based on the previously reported nitrogen to protein conversion factor for microalgae of 4.78 (Saibo et al. 2009). Because protein represents a small fraction of the dry mass of diatoms relative to the mass of the silicate frustule, protein was reported as the percentage of total carbon contributed by protein. Protein from *C. simplex* was previously reported to consist of 52% carbon (Laws 1991). The calculation of the percentage total carbon contributed by protein was as follows:

$$C_{Protein}\ (g) = \frac{N\ (g) \times 4.78}{0.52}$$

$$C_{Protein}\ (\%\ C_{Total}) = \frac{C_{Protein}\ (g)}{C_{Total}\ (g)} \times 100$$

Where $C_{Protein}$ is the mass of C from protein, C_{Total} is the total mass of carbon and N is the mass of nitrogen per unit dry weight.

Protein measurements were then used as a training set to build a PLSR model based on 499 cell spectra. A further 295 cell spectra were used to validate the model. Experimental replicates that were used in the training data set were not used in the validation data set. This PLSR model was subsequently used to predict the protein carbon (as percent of total carbon) for the remainder of the samples.

2.2.4 Statistical analyses

Statistical analyses were conducted using SigmaPlot for Windows version 11.0 (Systat Software, Inc). The cell size and cellular chlorophyll a and c content of different groups were compared using one and two-way Analysis of Variance (ANOVA) followed by Tukey's post-hoc tests. If the data did not meet the assumption of homoscedasticity then a Kruskal Wallis on ranked data was used to replace the one-way ANOVA. In the case of a two-way ANOVA where data did not meet the assumption of homoscedasticity or normality, a non-parametric Scheirer-Ray-Hare test was used on ranked data instead. The Scheirer-Ray-Hare test was performed on Predictive Analytical Software (Version 18, SPSS Inc, Chicago, IL, USA) with additional calculations by hand and a Chi-squared table for determining the P-value. Given the reduced power of the S-R-H test, a more conservative significance level was set at $\alpha = 0.01$ for these data. For all other analyses, significance level was set to $\alpha = 0.05$.

2.3 Results

Microalgal cells from each of the three species (*F. cylindrus, C. simplex and P. subcurvata*) were exposed to three levels of salinity and temperature in order to simulate sea ice (70, -1.8°C), meltwater (30, 2°C) and pelagic (34, 5°C) habitats. Changes in macromolecular composition were then measured using FTIR spectroscopy.

2.3.1 Degree of phenotypic plasticity varies between diatom species

The degree of plasticity was determined by comparing the accuracy of Partial Least Squares Discriminant Analysis (PLSDA) models used to classify "unknown" samples by treatment conditions. Samples which had a macromolecular composition more highly differentiated would be classified with a higher degree of accuracy than those which were more similar. Although this method did not provide a direct measure of plasticity, by presenting the discriminant analysis scores plot and the model validation statistics together, the reader is provided with a complete picture of the variability within and between sample groupings. *F. cylindrus* and *C. simplex* displayed a higher degree of macromolecular plasticity (sensitivity of classification 85.7-97.6%; Table 2-1) in response to changes in salinity and temperature conditions, relative to *P. subcurvata* (sensitivity of classification 42.8-77.9%). This was indicative of a greater magnitude of change

in macromolecular composition in *F. cylindrus* and *C. simplex* than *P. subcurvata*, as outlined below.

Table 2-1 PLSDA Classification by Treatment Summary Statistics

Species	n	Treatment	R2	Sensitivity (%)	Specificity (%)
F. cylindrus	201	Meltwater	0.754	94.9	99.4
		Pelagic	0.715	95.4	99.3
		Sea ice	0.591	97.6	91.2
C. simplex	295	Meltwater	0.560	96.7	89.5
		Pelagic	0.651	96.5	92.3
		Sea ice	0.782	85.7	100.0
P. subcurvata	294	Meltwater	0.268	77.9	86.4
		Pelagic	0.249	42.8	93.1
		Sea ice	0.532	74.0	97.2

2.3.2 Source of plasticity: changes in macromolecular composition

Macromolecular composition was different between treatments for all three species, with variations in maximum absorbance for bands corresponding to biological macromolecules (Figure 2-2; for band assignments see Appendix I). *F. cylindrus* and *C. simplex* showed broad-scale changes in macromolecular composition including variation in levels of lipids (~1730 cm^{-1}), proteins (~1650 cm^{-1}), amino acids (~1400 cm^{-1}) and phosphorylated molecules (~1250 cm^{-1}), with a particularly strong increase in amino acid content evident for both species in the sea ice treatment (Figure 2-2a & b). Additionally, the appearance of a second peak in the Amide I region at ~1630 cm^{-1} indicated that *C. simplex* underwent distinctive changes in protein composition (Figure 2-2b). In contrast, changes in macromolecular composition in *P. subcurvata* were mainly restricted to proteins, which were at highest concentration in the pelagic and lowest in the sea ice treatment (Figure 2-2c).

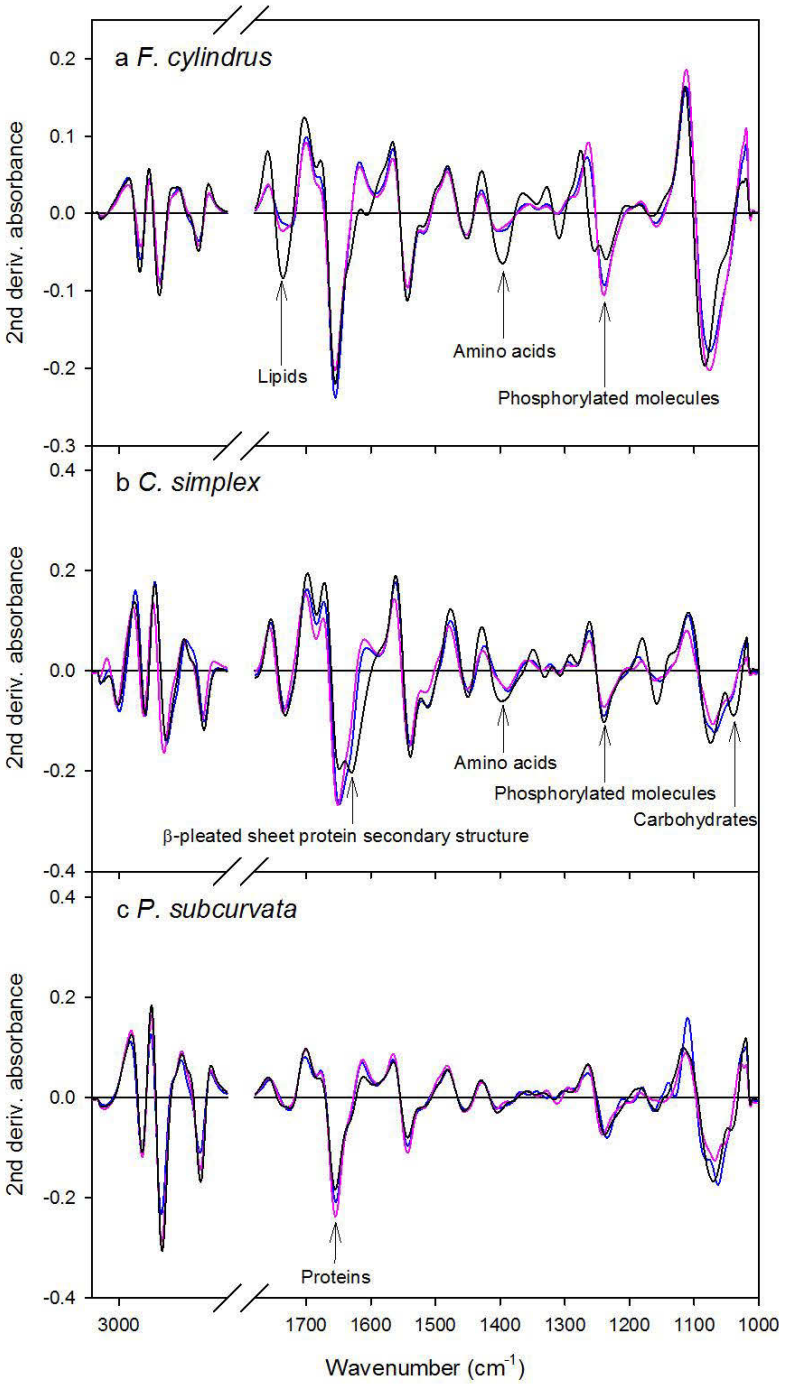

Figure 2-2 Average second derivative spectra of *F. cylindrus*, *C. simplex* and *P. subcurvata*. The average second derivative spectra of *F. cylindrus* (a), *C. simplex* (b) and *P. subcurvata* (c) from meltwater (—), pelagic (—) and sea ice (—) treated cells. Labels indicate the macromolecular pool represented by peaks in each spectrum. Standard error ranged from 9.16×10^{-7} to 1.76×10^{-4} absorbance units for the pooled dataset. Negative peaks correspond to positive absorbance.

PLSDA scores plots provided a visualisation of clustering patterns in the data set, intrapopulation variability (where each point represented an entire spectrum from an individual cell, or in the case of *F. cylindrus* a cluster of a few cells) and revealed more details about patterns of variation in macromolecular composition than could be determined from the average spectra (see Figure 2-3a, d & g). The PLSDA factors summarised variation in the data set, with the largest amount of variance being captured by Factor-1 and each subsequent factor capturing a lesser amount of variation. The loadings plots associated with the clustering patterns observed in the scores plots indicated which peaks in the spectrum drove variability between samples (Figure 2-3b,c,e,f,h, & i). For *F. cylindrus*, the Factor-1 loadings plot explained 39% of variation between cells and confirmed that levels of lipids (1730 cm^{-1}), amino acids (1400 cm^{-1}) and phosphorylated molecules (1260 cm^{-1}) were higher in cells from the sea ice treatment compared to the meltwater or pelagic treatments, as shown in the average second derivative spectra (Figure 2-3a & b). Additionally, a prominent and broad band at 1620 cm^{-1} indicted that changes in protein composition occurred between treatments. The Factor-2 loadings plot explained 19% of variation between cells and indicated that cells from the meltwater treatment had increased protein (1660-1540 cm^{-1}) and carbohydrate (1040cm^{-1}) content and decreased levels of phosphorylated molecules (1250cm^{-1}) compared to the pelagic treated cells (Figure 2-3a & c).

Loadings plots for *C. simplex* showed fewer prominent peaks than for *F. cylindrus*, indicating that differences between cells were related to variations in fewer macromolecular pools. Factor-1 explained 34% of the variation between cells and was consistent with the average second derivative spectra (Figure 2-2b), whereby cells from the sea ice treatment showed higher levels of lipids (1731 cm^{-1}) and distinct changes in protein composition (1668-1558 cm^{-1}; Figure 2-3e). Factor-2, which explained 28% of the variation between cells, showed that protein compositional changes occurred between meltwater and pelagic treatments (Figure 2-3f). In the PLSDA scores plot for *P. subcurvata*, clustering of points by treatment was less distinct than for the other two species, indicating that much of the variability between cells was related to intra-population variation (Figure 2-3g). The loadings plots for *P. subcurvata* were characterised by fewer prominent peaks than either of the other two species, confirming that changes were limited to fewer macromolecular pools (Figure 2-3h & i). In combination, Factors-1 and 2 explained only 31% of variation between cells with moderate peaks at 1241, 1654, 1545 and 1020 cm^{-1} indicative of small variations in phosphorylated molecules, proteins and carbohydrates relative to the other two species.

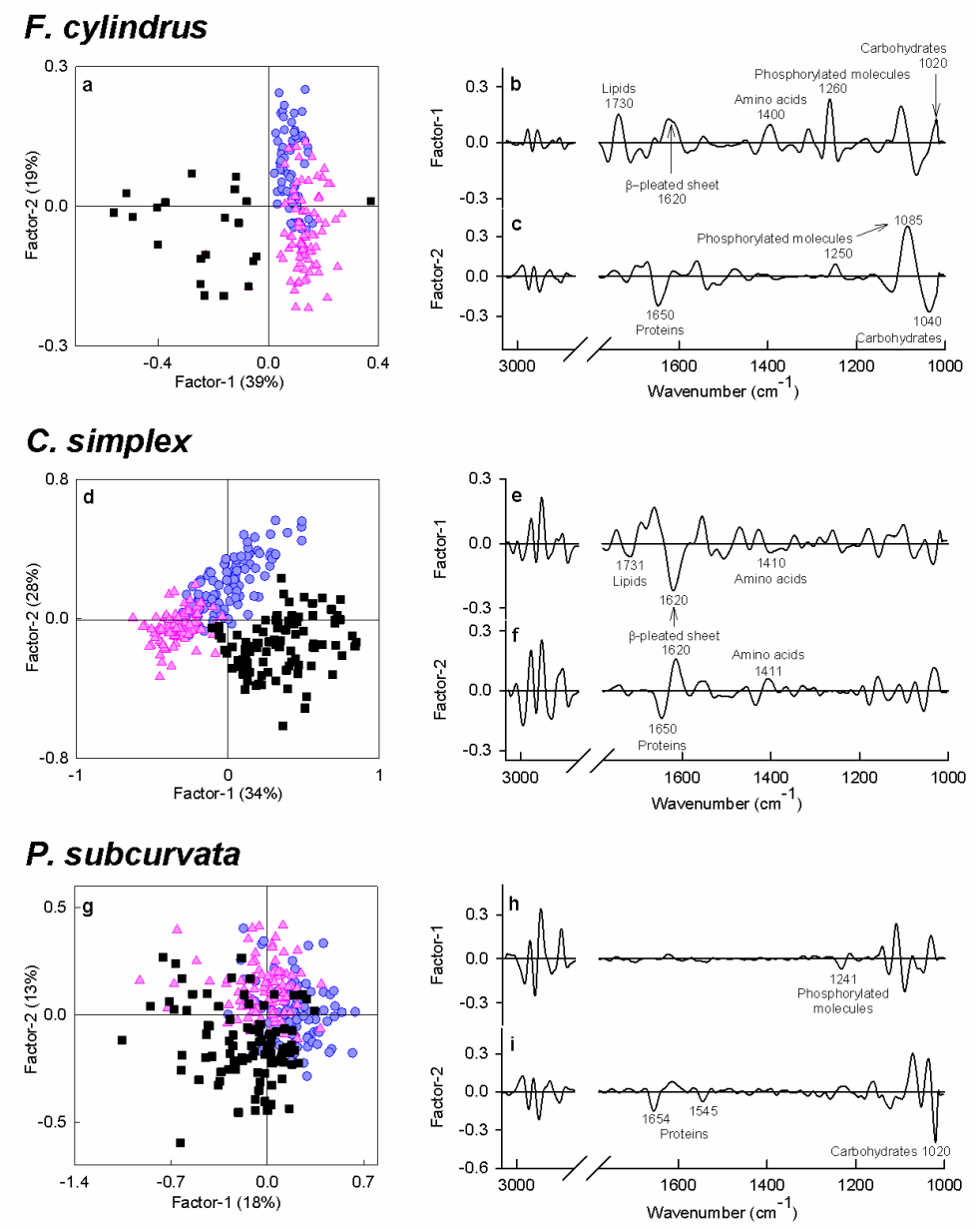

Figure 2-3 Discrimination of cell spectra by treatment condition.

PLSDA modelling was used to classify samples by meltwater (●), pelagic (▲) and sea ice (■) treatment conditions based on their infrared spectra. Scores plots for *F. cylindrus* and *C. simplex* (a & d) clearly show three clusters of cell spectra, indicating that the macromolecular composition was distinctly different between treatments, whereas *P. subcurvata* showed minimal plasticity (g). Because the data were second derivative transformed, a positive peak in the loadings plot indicates a decrease in absorbance for points that have positive scores in the PLSDA scores plots.

2.3.3 Predictions of environmental history of cells

To further quantify the degree to which macromolecular composition varied with treatment for each species, Partial Least Squares Regression (PLSR) modelling was used to predict salinity and temperature levels based on cell spectra. A higher degree of accuracy indicated a more dissimilar macromolecular composition between treatments and hence a higher degree of plasticity for that species. Salinity and temperature could be predicted with accuracies of ± 12.1 and ± 2.6 °C, respectively, for *F. cylindrus* and ± 13.2 and ± 2.7 °C for *C. simplex* (Table 2-2). In contrast, models for *P. subcurvata* were almost 50% less accurate (± 25.7 and ± 4.2 °C for salinity and temperature, respectively), suggesting a lower degree of plasticity in macromolecular composition in response to environmental changes in this organism.

Table 2-2 Salinity and Temperature Prediction Summary Statistics

Variable	N	Species	R^2	Accuracy (±)
Salinity	203	*F. cylindrus*	0.811	12.1
	295	*C. simplex*	0.776	13.2
	295	*P. subcurvata*	0.604	25.7
Temperature (°C)	201	*F. cylindrus*	0.756	2.6
	295	*C. simplex*	0.753	2.7
	295	*P. subcurvata*	0.556	4.2

2.3.4 Change in concentration of macromolecules

Lipid content increased under sea ice conditions in all three species (SRH test, P<0.001). *F. cylindrus* showed the greatest magnitude of change, with lipid content nearly doubling in the sea ice treatment compared to the meltwater and pelagic treatments (Figure 2-4a). *C. simplex* had the highest lipid content of the three species, regardless of treatment (SRH test, P<0.001). Protein content varied between treatments with the pattern of variation being different for each species (Figure 2-4b).Protein content was lowest in the sea ice treatment for all three species (two-way ANOVA, P<0.001). Sea ice conditions resulted in the lowest carbohydrate content for all three species (SRH test, P=0.010). *P. subcurvata* had the highest and *C. simplex* the lowest carbohydrate content regardless of treatment (Figure 2-4c; SRH test, P<0.001). Amino acid content was significantly higher under sea ice conditions for both *F. cylindrus* and *C. simplex* (Figure 2-4d; SRH test, P<0.001) whereas *P. subcurvata* showed minimal variation in amino acid content. *F. cylindrus* demonstrated the greatest magnitude of change in amino acid content with levels more than doubling in the sea ice treatment compared to the meltwater and pelagic treatments. Phosphorylated molecules varied with both species and treatment (Figure 2-4e; SRH test, P < 0.001). The lowest levels of phosphorylated molecules occurred in the sea ice treatment

for *F. cylindrus* and the pelagic treatment for *C. simplex*, whereas *P. subcurvata* showed minimal variation between treatments.

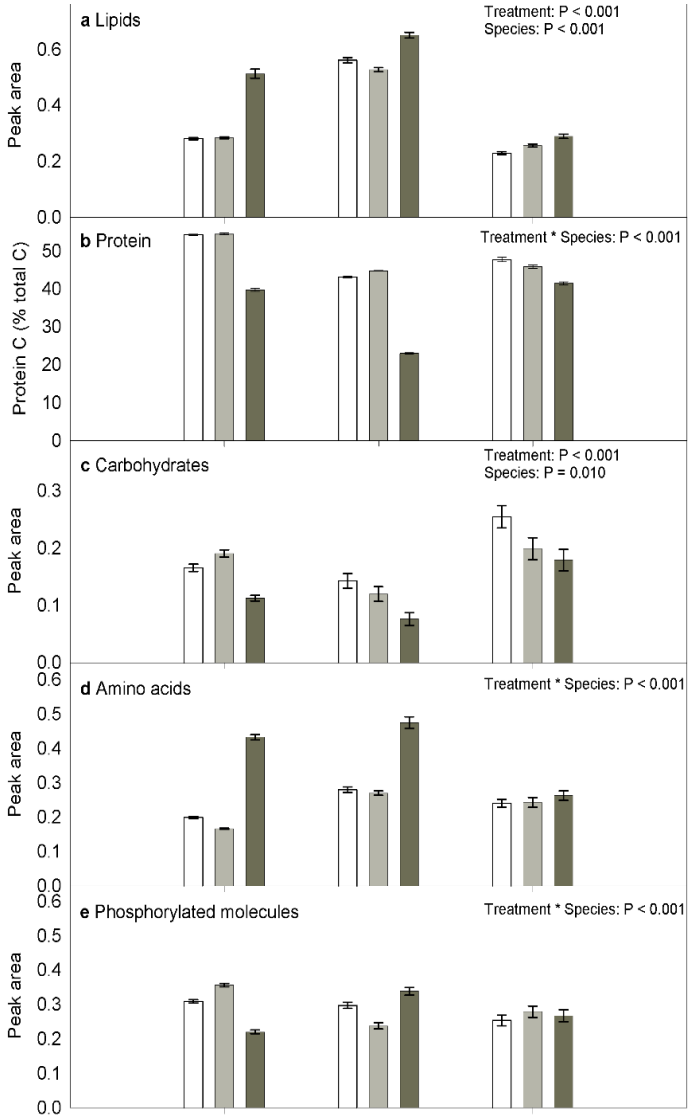

Figure 2-4 Cellular concentrations of macromolecules under treatment conditions.
Concentration is proportional to the area under the peak in the infrared spectrum corresponding to each macromolecule, according to the Beer-Lambert Law proportionality between concentration and absorbance. For all parameters excluding protein, bars show the mean peak area. Protein is expressed as the percentage of total carbon contributed by protein, determined by mass spectrometry for a subset of *C. simplex* samples (pelagic and sea ice treated samples). This mass spectrometry data was used as a Partial Least Squares Regression (PLSR) calibration data set (499 spectra) to predict protein content in the remaining samples based on their FTIR spectrum (1328 spectra). Key: meltwater (□), pelagic (▒) and sea ice (■) treatments. Error bars indicate the standard error. Results from Scheirer-Ray-Hare two-way non-parametric statistical tests are shown in the top right corner of each plot.

2.4 Discussion

This study compared the phenotypic plasticity of three ecologically important species of Southern Ocean diatoms in response to salinity and temperature regimes characteristic of the highly variable polar marine environment. Photophysiological plasticity in response to these conditions was previously reported in Petrou et al. (Petrou et al. 2011). This paper builds on Petrou et al. by showing that phenotypic plasticity was also manifest as changes in macromolecular composition. Responses were species-specific in terms of which macromolecular pools varied (proteins, lipids, carbohydrates, amino acids and/or phosphorylated molecules) and the degree of plasticity. *F. cylindrus* and *C. simplex*, two diatom species with widespread distribution in diverse habitats in the Southern Ocean, each displayed a high degree of phenotypic plasticity, in terms of macromolecular composition, in response to changing temperature and salinity. In contrast, *P. subcurvata*, a meltwater specialist (Almandoz et al. 2008), displayed a comparatively low degree of plasticity. Additionally, reduced photosynthetic efficiency in *P. subcurvata* under sea ice treatment conditions provided further evidence that this species is less well adapted to the sea ice environment (see Supplementary Table S3). Together, these results suggest that phenotypic plasticity as shown here by *F. cylindrus* and *C. simplex* is advantageous under the highly variable physicochemical conditions associated with the seasonal formation and decay of sea ice.

Microalgae vary macromolecular pools to satisfy physiological requirements. Lipids are used as storage products, for the repair and maintenance of membranes (Fahl & Kattner 1993; Mock & Kroon 2002a; Mock & Kroon 2002b; Falk-Petersen et al. 1998; Nichols et al. 1989; Thomas & Dieckmann 2002). Macromolecules such as anti-freeze proteins, ice-binding proteins and ice-active substances are known to be critical for osmoregulation and cryoprotection (preventing injury to cells due to ice crystal formation) (Mock et al. 2007; Krell et al. 2008; Gwak et al. 2010; Bayer-Giraldi et al. 2010; Raymond 2000). The elevated lipid levels displayed by *F. cylindrus* and *C. simplex* in response to the sea ice treatment are consistent with previous observations of lipid accumulation by diatoms in the sea ice. *P. subcurvata* did not display a similar increase in lipid concentration.

Protein concentration decreased in all three species in the sea ice treatment. In addition, *C. simplex* and *F. cylindrus* showed a distinct change in protein secondary structure (indicated by a shift in the Amide I peak maxima from 1650 to between 1630 and 1616 cm^{-1}) attributed to a decrease in α-helix dominated proteins and an increase in proteins with β-pleated sheet. Antarctic microalgae have previously been reported to contain high amounts of Ribulose-1,5-bisphosphate carboxylase/oxygenase (RUBISCO), the enzyme which catalyses carboxylation and oxygenation of ribulose-1,5-bis- phosphate (RuBP) in the chloroplast (Devos et al. 1998). The authors

suggested that the increased production of RUBISCO in psychrophilic species, relative to mesophilic microalgae, compensates for the reduced activity of the enzyme at low temperatures. Given that RUBISCO is dominated by beta-pleated sheet structure (Laskowski 2001) the observed shift in the Amide I peak maxima in *F. cylindrus* and *C. simplex* (the two psychrophilic diatoms) cell spectra in the sea ice treatment is consistent with an increased proportion of RUBISCO in the protein pool. Cell spectra from *P. subcurvata* did not indicate similar changes in protein secondary structure.

Both *F. cylindrus* and *C. simplex* showed elevated levels of free amino acids under sea ice treatment conditions, whereas *P. subcurvata* did not. Proline is known to be a key osmoregulator in *Fragilaropsis sp.* and sea ice diatoms in general (Bayer-Giraldi et al. 2010). Hence, the increase in amino acid content shown by *F. cylindrus and C. simplex* in study is consistent with previous research indicating that proline production is likely to be another important adaptive response to life in the sea ice habitat. Additionally, the catabolism of proline upon cessation of salt stress releases a great deal of energy which is thought to assist with the cells' physiological recovery (Trovato et al. 2008).

Phenotypic plasticity can have significant ecological and genetic costs, which can reduce a species' fitness in comparison to a species with a less plastic phenotype (Agrawal 2001). The costs relate to the maintenance of genetic material encoding particular traits. Just as environmental instability has selected for phenotypic plasticity in *F. cylindrus* and *C. simplex*, the stability of the meltwater habitat may have selected against phenotypic plasticity in *P. subcurvata*, resulting in a reduced capacity to vary macromolecular composition in response to environmental conditions, as shown in this study. Recent research highlights that some species have the ability to sustain long-term adaptation to environmental change through phenotypic variation alone (Green et al. 2008; Charmantier et al. 2008). Therefore, species with higher levels of phenotypic plasticity, such as *F. cylindrus* and *C. simplex*, may have greater capacity to adapt to environmental change than species such as *P. subcurvata*.

As the Antarctic region warms due to global climate change, polar inhabitants will experience warmer winters with thinning and retreat of sea ice cover (Smetacek & Nicol 2005). Such environmental change will likely alter the species assemblage composition, as conditions become more or less favourable to individual species (Arrigo 2005; Flynn et al. 2012). Indeed, 'massive' blooms of *Chaetoceros* and *Fragilariopsis* species have already been observed in the Arctic growing under ice between 0.5 and 1.8 m thick in the Chukchi Sea (Arrigo 2012). The authors concluded that the under ice bloom was facilitated by increased penetration of light through the ice, which was thinner than previous years, had a high surface melt pond fraction and transmitted

four-fold more incident irradiance than adjacent, melt pond-free ice. The elemental stoichiometry of the microalgal community is known to reflect the average stoichiometry of individual species (Arrigo 2005). Similarly, the average macromolecular composition of the microalgal community is determined by the macromolecular composition of the constituent species, which has been shown here to be highly species-specific. Hence, shifts in the assemblage composition will likely alter the average macromolecular composition of the microalgal community with potential implications for the quality of food supplied to the Southern Ocean ecosystem. Indeed, recently observed shifts in microalgal and zooplankton community composition along the West Antarctic Peninsula, one of the most rapidly warming regions on earth, have coincided with changes in krill recruitment, abundance and availability to predators (Ducklow et al. 2007).

Taxon-specific studies of microalgal physiology and associated effects on the nutritional value of natural populations are rare, particularly from the Southern Ocean (Twining, Baines & Fisher 2004; Rivkin 1985; Rivkin & Voytek 1987; Carr et al. 2006). Such data is in great demand for the calibration and validation of plankton functional type models used to predict how microalgal assemblages will respond to climate change (Boyd et al. 2010). This research demonstrates high-throughput and highly sensitive measurements of the nutritional value of individual diatom cells, highlighting the potential for studies of macromolecular compositional changes in mixed natural populations, at the level of individual species (Domenighini & Giordano 2009). Additionally, the single-cell approach has the ability to classify cells by taxon with sensitivity and specificity of up to 97.6% and 100%, respectively (see Supplementary Table S2), corroborating studies with other prokaryotic and eukaryotic organisms (Xie et al. 2012; Naumann et al. 1991). Given that leading semi-automated plankton classification systems currently achieve accuracies of between 70-80%, incorporating the synchrotron FTIR approach into the taxonomic classification tool-box will facilitate progress in this field (MacLeod et al. 2010). Moreover, increasing the efficiency of data collection by simultaneously measuring macromolecular composition and taxonomically classifying cells is particularly innovative and valuable.

This study identified species-specific variations in cellular levels of all four major classes of macromolecules (lipids, proteins, carbohydrates and phosphorylated molecules) in response to salinity and temperature regimes characteristic of sea ice meltwater and pelagic habitats. For *F. cylindrus* and *C. simplex*, which belong to two of the most abundant genera in the Southern Ocean, lipid content was highest in cells from the sea ice treatment. Lipid accumulation has previously been reported in Antarctic sea ice algal communities due to the enhanced production of polyunsaturated fatty acids, resulting in a different quality of food being released into the food web in winter compared to other seasons (Thomas & Dieckmann 2002). Given that lipids have

the highest caloric value of the macromolecular pools, the enhanced production of lipids by microalgae in sea ice habitats may also influence the quantity of calories available to the food web. Such changes in microalgal nutritional value may help to explain observations that summer krill densities within the southwest Atlantic Ocean correlate positively with sea-ice extent the previous winter (Atkinson et al. 2004). However, since cellular protein content in *F. cylindrus* and *C. simplex* was lower in treatment conditions characteristic of the sea ice habitat, years with reduced duration and extent of sea ice may be associated with increased protein production by sea ice microalgae. Given that microalgae are the major primary source of protein for the Southern Ocean food web, a macromolecule that is essential for growth at higher trophic levels (Lohrenz & Taylor 1987), the relationship between sea ice duration and extent, and microalgal protein production merits further investigation. Presently, the likelihood and potential consequences of such changes in macromolecular composition and energy production on the Southern Ocean ecosystem remain unknown.

2.5 Acknowledgments

We would like to thank Dr Scarlett Trimborne (Alfred Wegener Institute for Polar and Marine Research) for cultures of *P. subcurvata* and the species identification of *Chaetoceros simplex* by electron microscopy. Thanks to Dr Andrew Pankowski and Professor Andrew McMinn (University of Tasmania) for the collection and isolation of *F. cylindrus*. Thanks to Richard Jardine for assistance with Figure 2.1.

3 Taxon-specific responses of Southern Ocean diatoms to Fe-enrichment revealed by FTIR microspectroscopy

In response to research questions iii-vi (Figure 1-1), an experiment was designed whereby samples of Southern Ocean diatoms collected during the Kerguelen Ocean Plateau Study 2 (KEOPS2) voyage were analysed for taxon-specific phenotypic changes. Synchrotron FTIR microspectroscopy was used to probe changes in the overall macromolecular composition of cells in response to differences in Fe availability between stations. A reformatted version of this chapter has been published in the international journal *Biogeosciences Discussions*. The paper is listed in Appendix II as Sackett, O., Beardall, J., Armand, L., Connelly, C., Howes, J., Hill, R., Doblin, M., Ralph, P. and Heraud, P.: Taxon-specific responses of Southern Ocean diatoms to Fe enrichment revealed by synchrotron radiation FTIR microspectroscopy, Biogeosciences, 11, 5795-5808, doi:10.5194/bg-11-5795-2014, 2014. Please see www.biogeosciences.net/special_issue164 for further studies resulting from KEOPS-2, including phytoplankton community composition.

3.1 Introduction

Growth of diatoms in the global ocean is estimated to contribute ~ 20% of the total primary productivity on Earth, thereby supporting substantial marine and terrestrial ecosystems, including fisheries which supply 15% of the world's animal protein for human consumption (Nelson et al. 1995; Armbrust 2009; Mora et al. 2009). As their frustules rain down to the deep ocean, diatoms export substantial quantities of C, Fe and Si from surface waters and determine the nutrient budget of the global ocean (Le Quere et al. 2005; Arrigo 2005; Ingall et al. 2013). Diatoms are very sensitive to changes in Fe availability and rapidly form expansive blooms when the trace metal becomes available (Marchetti & Cassar 2009). Fe limitation is known to cause changes in diatom morphology (such as reduced cell size), reduced photosynthetic efficiency, pigment levels and growth rates (Marchetti & Cassar 2009). The critical role of diatoms in ocean biogeochemistry and ecosystem functioning merits further investigation of their phenotypic responses to environmental change.

Naturally Fe-enriched water near the Kerguelen Island supports the largest annual phytoplankton bloom (45,000 km^2) in the high nutrient, low chlorophyll Southern Ocean (Quéguiner et al. 2007). The natural phenomenon of Fe enrichment in this region presents a valuable opportunity to study the effects of Fe perturbations on diatom growth, productivity, community composition, biogeochemistry and carbon export (Blain et al. 2007). Little is currently known about the effects

of Fe on the macromolecular composition (i.e. carbohydrates, lipids, proteins and nucleic acids) of diatoms. The macromolecular composition is an important component of the phenotype, determining energy and nutrient fluxes available for higher trophic levels and influencing cellular carbon productivity (Kroon & Thoms 2006; Andersen et al. 2004; Sackett et al. 2013). Given the importance of diatoms to elemental cycling and marine ecosystem productivity, this study aimed to investigate the macromolecular responses of major groups of diatoms in waters near Kerguelen Island in relation to differences in Fe availability. Further, we demonstrate a novel, microspectroscopy-based approach to *phenomics*, a discipline that has been flagged as critical to enhancing our ability to untangle the complex interaction of genotype and environment, and allow us to predict phenotypic traits such as species fitness (Houle et al. 2010).

Although it is generally accepted that the responses of phytoplankton communities to environmental factors vary between species, to date phenotypic (e.g. macromolecular, elemental and physiological) data from natural populations has been largely limited to bulk community or size fractionated measurements. The lack of taxon-specific macromolecular data relates to the large quantities of biomass generally required for biochemical analyses, difficulty sorting algal cells into taxonomic groupings, and to the time and financial costs associated with available measurement techniques. Recently however, elemental analysis of individual Southern Ocean phytoplankton cells using X-ray Fluorescence Microprobe Analysis has revealed species-specific changes in elemental composition with Fe availability (Twining, Baines & Fisher 2004; Twining, Baines, Fisher, et al. 2004). Here we used synchrotron radiation Fourier Transform Infrared (SR-FTIR) microspectroscopy to analyse taxon-specific changes in macromolecular composition with Fe availability in individual diatom cells. SR-FTIR microspectroscopy is a powerful, non-invasive technique generating multivariate data on the total macromolecular composition of cells. The approach is growing in popularity among microbial ecologists and biomedical researchers (Murdock & Wetzel 2009). The technique provides information on the macromolecular composition and physiological status of biological samples, without the need for lengthy extraction protocols because cells can be analysed non-invasively. The power of the technique relates not only to its high precision, but its ability to simultaneously provide information about the macromolecular composition and phenotypic parameters such as growth rate and phenotypic plasticity (Giordano et al. 2001; Sackett et al. 2013; Jebsen et al. 2012; Heraud, Wood, et al. 2007; Marchetti et al. 2010). In addition, FTIR microspectroscopy has shown great promise as a tool for semi-automated taxonomic classification of microorganisms down to sub-species level (Naumann et al. 1991; Giordano et al. 2009; Domenighini & Giordano 2009).

Here we present the first published macromolecular data collected from individual phytoplankton cells from the Southern Ocean using SR-FTIR spectroscopy. Cells were analysed in hydrated form directly from sea water plankton haul samples, thereby minimizing artefacts related to sample preparation. The study aimed to measure phytoplankton macromolecular composition of cells of different taxa collected from stations with contrasting Fe levels. The macromolecular composition of individual cells from four dominant groups of phytoplankton (*Fragilariopsis kerguelensis, Pseudo-nitzschia* spp., *Chaetoceros* spp. and *Eucampia antarctica v. antarctica*) at four different sampling stations is compared (Table 3-1). The first two stations (E-1 and E-5) were sited within a complex recirculation system located in a stationary meander of the Polar Front, characterised by moderate phytoplankton biomass, moderate Fe levels and relatively low productivity and growth rates (S. Blain, I. Obernosterer, B. Quéguiner, T. Trull, this issue). The second two stations (E4-W and TEW-8) received Fe-rich waters from the Kerguelen Island and Plateau, resulting in high phytoplankton biomass, high productivity and growth rates (S. Blain, I. Obernosterer, B. Quéguiner, T. Trull, this issue). Additionally, the spectroscopic data was used to investigate the accuracy of the method for simultaneously classifying cells by taxa.

Table 3-1 Description of sampling stations and associated biogeochemical characteristics.

Station	*dFe (nM)	dSi ($\mu molL^{-1}$)	POC (μM)	PBSi (μM)	BSi/POC (mol)	[a,b]13C-POC (‰VPDB)	[b]Growth rate (%)	$Productivity_{Ez}$ ($mgC/m^2/d$)
E-1	*0.06 – 0.38	~15	0.57	0.36	0.63	+1.63	25	578
E-5	^0.06 - 0.43	~10	0.44	0.28	0.63	+1.46	25	1064
E-4W	^0.11–0.61	~17	1.18	0.67	0.57	+2.83	50	3287
TEW-8	*~0.26 nM	NA	7.1	1.65	0.23	+4.67	75	No data
Ref.	(*Trull et al. 2014, ^unpublished A. Bowie)	(Closset et al. 2014)	(Trull et al. 2014)	(Trull et al. 2014)	(Trull et al. 2014)	(Trull et al. 2014)	(Trull et al. 2014)	(Jacquet et al. 2014)

Notes on station locations: E1 and E5 situated in a complex recirculation system located in a stationary meander of the Polar Front; E-4W located in a region receiving Plateau waters; TEW-8 located in region receiving Kerguelen Island waters (Trull et al. 2014; Stéphane Blain et al. 2014).
Notes on values reported for POC and PBSi: values from Trull et al. (2014) are for size fraction 20 µm, which is composed of diatoms and other microalgae.
Abbreviations: Particulate Organic Carbon (POC), Particulate Biogenic Silicate (PBSi), Not Available (NA)
Key: *approximations based on measurements at nearby sites
[a] isotopic indices of growth rate
[b] increase relative to reference station
[ez] euphotic zone
[VPDB] Vienna Pee Dee Belemnite standard

3.2 Materials and Methods

3.2.1 Sampling

Twenty phytoplankton net stations (Phytonet stations 7 to 27, excluding station 23) were sampled (by L. Armand) for the purpose of SR-FTIR microspectroscopy analysis from Oct-Dec 2011 (S. Blain, I. Obernosterer, B. Quéguiner, T. Trull, this issue). A 35 µm meshed phytoplankton net was deployed from the RV *Marion Dufresne II* to sample the top 100 m of the surface waters. Hauling speed was minimised to around 5 $m.mn^{-1}$. 100 mL samples were taken from each station immediately after the haul and fixed with formaldehyde (1-2% final conc.). Fixed samples were kept at room temperature in the dark until analysis by SR-FTIR microspectroscopy. Comparison of FTIR spectra from fixed samples with those observed before from fresh microalgal samples did not show any pronounced differences. Additional 100 mL samples were preserved with Lugol's iodine solution and analysed for diatom composition (Armand unpublished). Taxonomic identification followed modern authority descriptions summarised in Hasle and Syvertsen (1997).

3.2.2 Microspectroscopy

Four taxa were selected for analysis based on their abundance within the samples at each site. These were *Fragilariopsis kerguelensis*, *Eucampia antarctica*, *Chaetoceros* spp. (at stations E-1 and E4-W these were mostly *C. decipiens*, at TEW-8 these were mostly *C. criophilus*) and *Pseudo-nitzschia* spp. Cells were analysed in hydrated form within 1 µL of sea water pipetted directly onto the measurement substrate (calcium fluoride). A compression chamber with IR transparent calcium fluoride windows (0.5 mm thick) was used to hold each sample and prevent the sea water from evaporating prior to measurements being taken (Tobin et al. 2010). The use of the wet chamber meant that differences in the refractive index of the hydrated cells and the measurement medium (seawater) were less than would have been the case for dried cells in air resulting in much less light scattering effects on spectra (Bassan et al. 2009). Spectral data were collected on the Infrared Microspectroscopy Beamline (2BM1B) at the Australian Synchrotron, Melbourne, Australia in July 2013 (approximately 2 years after sample collection). Spectra were acquired over the measurement range 4000-800 cm^{-1} with a Vertex 80v FTIR spectrometer (Bruker Optics, Ettlingen, Germany) coupled to an IR microscope (Hyperion 2000, Bruker) fitted with a mercury cadmium telluride detector cooled with liquid nitrogen. The microscope was connected to a computer-controlled microscope stage and placed in a specially designed box purged with dehumidified air. The measurements were performed in transmission via the mapping mode, using an aperture size of 5 µm × 5 µm with a spectral resolution of 8 cm^{-1}, with 64 scans co-added. This aperture size, employed for all species, provided spectra that were unambiguously representative of individual cells (not clumps of cells; Fig. 3-1). The selected aperture size enabled

targeting of the cell interior and avoidance of the cell edge which could cause pronounced light scattering. Additionally, maintaining a consistent aperture size avoided variations in signal to noise ratio throughout the experiment. Although the small aperture size did not cover the entire interior of the cell, we attempted to overcome heterogeneity across the cell by capturing large numbers of cells (20-50) and varying the measurement position across the cell in a random fashion. Further, a consistent aperture size helps to avoid variation in the signal to noise ratio. Given that the spectral data in this study is used to probe relative changes in the proportions of cellular macromolecules, it is unlikely the measurement strategy would overestimate cellular macromolecules. Were the data to be converted into quantitative measures (e.g. grams of protein per unit biomass or cell quotas), this method would likely result in overestimates. The number of co-added scans was chosen as a good compromise between achieving spectra with good signal to noise ratios and the rapid acquisition of data. Spectra were processed using Happ-Genzel appodization and 2 levels of zero-filling. Spectral acquisition and instrument control was performed using Opus 6.5 software (Bruker).

3.2.3 Multivariate Modeling

A multivariate modeling approach was selected for data analysis for two reasons. Firstly spectral data is inherantly highly multivariate (containing thousands of variables) and therefore well suited to multivariate analysis. Secondly, the multivariate approach is more robust than univariate methods (such as comparison of peak-height/area ratios) because it detects co-variation across large numbers of variables and is less susceptible to experimental artefacts including baseline effects. SR-FTIR microspectroscopy is a semi-quantitative technique whereby changes in macromolecular absorbance are proportional to changes in the concentrations of those macromolecules. According to the the Beer-Lambert Law, absorbance is proportional to the path length through the sample and the concentration of light absorbing molecules, as has been validated for diatoms and other microalgae (Heraud, Wood, et al. 2007; Jungandreas et al. 2012; Wagner et al. 2010). Given that no independent data was available for the calibration of the SR-FTIR spectral data, we do not report changes in macromolecules in absolute units, however a doubling of absorbance at a particular wavenumber, for example, is indicative of a doubling in concentration of the macromolecules which absorb at those wavenumbers, given adherence to the Beer-Lambert Law. The multivariate modeling approach (including pre-processing methods) described below allows for normalisation of differences in sample thickness, hence changes in the absorbance bands at particular wavenumbers indicate proportional changes in the concentration of the macromolecules associated with those wavenumbers (Heraud et al. 2005).

SR-FTIR spectral data were exported from the OPUS 6.5 for multivariate analysis using The Unscrambler X v 10.3 (Camo Inc., Oslo, Norway). An initial quality control procedure was performed over the range 3000-950 cm^{-1}. Spectra with maximum absorbance greater than 0.85 (resulting from relatively thick regions of the sample) were excluded from further analyses. The regions 3050-2800, 1770-1730 and 1560-950 cm^{-1} were selected for analysis since they contain all the major biological bands, but avoided possible issues related to spurious absorbance values for the amide I band region (1730-1560 cm^{-1}) due to the intense absorbance by water in this region (Vaccari et al. 2012). Firstly, data was smoothed (8 points either side) and second derivative transformed (3rd order polynomial) using the Savitzky-Golay function (to account for differences in samples thickness, minimise baseline differences and aid visual interpretation of spectra) (Heraud et al. 2005). Secondly, the Multiplicative Scattering Correction (MSC) function was applied to the dataset for the purposes of reducing any remaining light scattering and to normalize the data.

Data were initially screened for quality using Principal Component Analysis (PCA) to remove obvious outliers, prior to the calculation of average spectra and analysis by Partial Least Squares Discriminant Analysis (PLSDA) (Wold et al. 2001; Sackett et al. 2013; P. Heraud et al. 2008). Outliers were identified using the Leverage versus Residual X-variance plots, with a threshold of 5% set nominally. Models were validated using a set of samples not used to build the PLSDA model (i.e. a test set). The calibration and test sets were chosen by randomly assigning two thirds and one third of the samples to each, respectively. The classification accuracy of each model was compared using sensitivity and specificity metrics (Bylesjö et al. 2006).

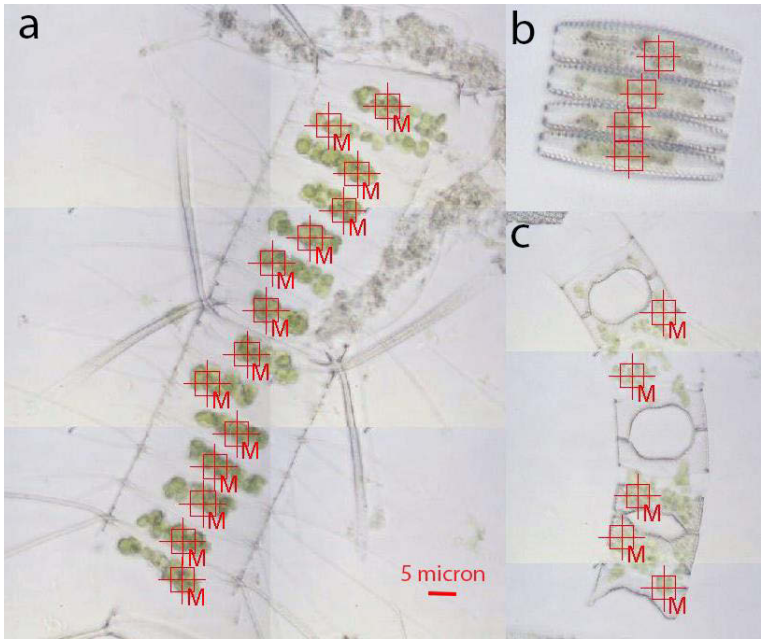

Figure 3-1 Visible images of *Chaetoceros* spp. (a), *F. kerguelensis* (b) and *E. antarctica* (c) cells showing the infrared measurement positions (indicated by cross hairs).
The red square around the crosshairs indicates that the aperture size on the infrared microscope was set to 5 × 5 μm.

3.3 Results

3.3.1 Stations E-1 and E-5 (moderate Fe availability)

Spectra were interpreted based on published literature for band assignments (Appendix I)). Visual inspection of the average second derivative spectra showed bands characteristic of microalgal samples, with those in the lower region (1250-1000 cm^{-1}) dominating the spectra (Fig. 3-2). Differences in the height and position of the peaks indicated that the macromolecular composition varied between taxa. Cell spectra from sites E-1 and E-5 had the strongest absorbance by bands associated with proteins (1540 cm^{-1}), lipids (3050-2800 cm^{-1}, 1745 cm^{-1}, and 1450 cm^{-1}), phosphorylated molecules (~1240 cm^{-1}) and carbohydrates (~1150 cm^{-1}) compared to stations EW-4 and TEW-8 (Fig. 3-2 a&b). At station E-1 (Fig. 3-2 a), *Pseudo-nitzschia* spp. showed the highest absorbance by proteins and lipids and *E. antarctica* the lowest. Also at station E-1, *F. kerguelensis* cells had the highest absorbance by phosphorylated molecules, followed by *E. antarctica*, *Pseudo-nitzschia* spp. then *Chaetoceros* spp.. At station E-5 (Fig. 3-2 b), *Pseudo-nitzschia* spp. and *F. kerguelensis* cells showed the highest absorbance by proteins and lipids, whereas *E. antarctica* had the lowest. Another notable feature of the cell spectra from station E-5 (Fig. 3-2 c) was the relatively low variability in the region 3050-2800 cm^{-1}, as indicated by small error bars compared to cell spectra from the other stations.

3.3.2 Stations E4-W and TEW-8 (higher Fe availability)

Cells from the stations with higher levels of Fe availability (E4-W and TEW-8) showed spectra with weaker absorbance from bands above 1250 cm^{-1} compared to those from stations E-1 and E-5 (Fig. 3-2 c&d). As with the other stations, *F. kerguelensis* cell spectra showed the strongest absorbance by phosphorylated molecules (~1240 cm^{-1}) and the weakest by silicate/silicic acid and carbohydrates (1160-1040 cm^{-1}) relative to the other taxa.

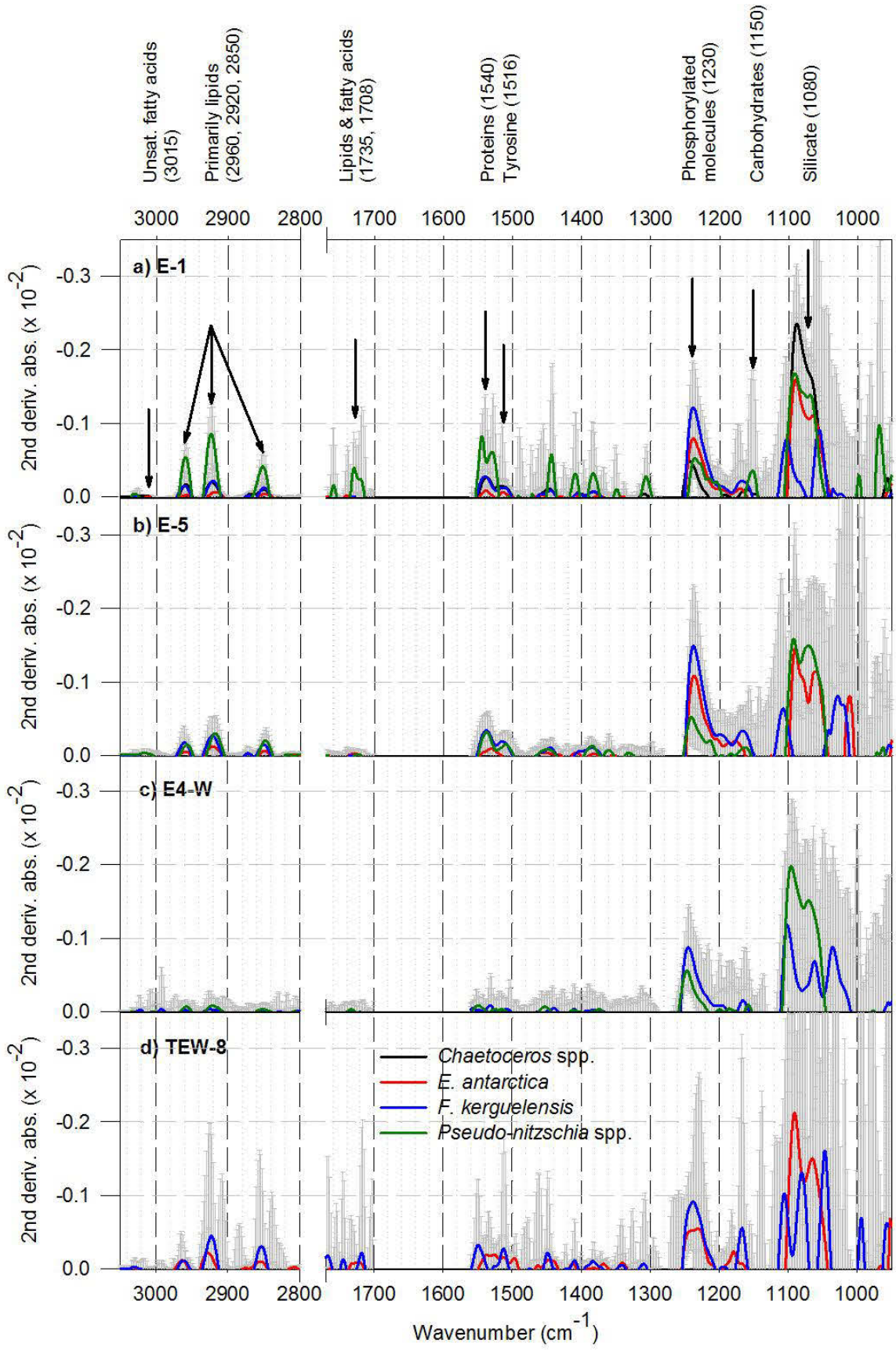
Unsat. fatty acids (3015)
Primarily lipids (2960, 2920, 2850)
Lipids & fatty acids (1735, 1708)
Proteins (1540) Tyrosine (1516)
Phosphorylated molecules (1230)
Carbohydrates (1150)
Silicate (1080)
a) E-1
b) E-5
c) E4-W
d) TEW-8
2nd deriv. abs. (x 10-2)
Chaetoceros spp.
E. antarctica
F. kerguelensis
Pseudo-nitzschia spp.
Wavenumber (cm-1)

Figure 3-2 Average second derivative cell spectra from four common genera: Chaetoceros, Eucampia, Fragilariopsis and Pseudo-nitzschia.

Taxonomic abundance varied between stations hence there is no data for *Chaetoceros* spp. and *Eucampia antarctica* at station E4-W, or *Chaetoceros* spp. and *Pseudo-nitzschia* spp. at station TEW-8. Panels a-d show four different stations. Peaks show the macromolecular composition of cells which is dominated by phosphorylated molecules (1240 cm^{-1}), carbohydrates (~1150 cm^{-1}) and silicate (1080 cm^{-1}). Peaks found in the spectral region 3050-2800 cm^{-1}, ~1735 cm^{-1} and ~1450 cm^{-1} indicate the presence of lipids. Additionally, peaks at 1540 and 1515 cm^{-1} indicate the presence of proteins and the amino acid tyrosine, respectively. Error bars indicate one standard deviation from the mean. Note: the Y-axis has been reversed to ease examination of the negative peaks (which are the relevant peaks after second derivative transformation).

3.3.3 Multivariate modeling and taxonomic classification

Partial Least Squares Discriminant Analysis (PLSDA) is a multivariate modeling process enabling the modeling and classification of spectral datasets. In this study, PLSDA served to both validate the visual observations made from the average second derivative spectra and to assess the power of SR-FTIR microspectroscopy to taxonomically classify cell spectra from the mixed, natural diatom communities. PLSDA scores plots showed distinct clustering of cell spectra by taxonomic grouping at all four sites (Fig. 3-3). PLSDA results supported observations made from average second derivative spectra. For example, interpretation of the scores and corresponding loading weights plots showed strong peaks at ~1240 cm^{-1}, indicating that *F. kerguelensis* cell spectra had the highest levels of phosphorylated molecules at all four sites. In addition, the PLSDA loading weights plots revealed a consistent anti-correlation between phosphorylated molecules and peaks corresponding to silicate/silicic acid and carbohydrates (bands at ~1240 and 1080 cm^{-1} had opposite correlation indicated in all four loading weights plots). Classification of cell spectra by taxon using PLSDA demonstrated a high level of accuracy (Table 3-2), performing at >90% specificity and sensitivity for all species at the single cell level. Moreover, cell spectra clustered well by taxonomic group even after pooling the data across the four stations (Fig. 3-4), indicating that inter-species spectral variability was greater than the environmentally-induced spectral variability.

Table 3-2 Taxonomic Classification Summary Statistics for PLSDA models

Station	PLSDA Model	n (cal)	n (val)	Factors	RMSEP	R-square	Sensitivity	Specificity
E-1	*Chaetoceros*	3	0	3	0.131	0.067	0%	100%
E-1	*Eucampia*	15	2	3	0.284	0.088	40%	96%
E-1	*Fragilariopsis*	48	35	3	0.256	0.735	100%	84%
E-1	*Pseudo-nitzschia*	28	12	3	0.229	0.719	92%	100%
E-1	**Total**	**94**	**54**	**3**	**-**	**-**	**91%**	**97%**
TEW-8	*Eucampia*	3	2	4	0.175	0.674	100%	100%
TEW-8	*Fragilariopsis*	26	17	4	0.175	0.674	100%	100%
TEW-8	**Total**	**29**	**19**	**4**	**-**	**-**	**100%**	**100%**
E-4W	*Fragilariopsis*	34	15	1	0.264	0.713	93%	100%
E-4W	*Pseudo-nitzschia*	36	30	1	0.264	0.713	100%	93%
E-4W	**Total**	**71**	**45**	**1**	**-**	**-**	**98%**	**98%**
E-5	*Eucampia*	13	7	5	0.251	0.494	86%	98%
E-5	*Fragilariopsis*	58	32	5	0.225	0.763	100%	93%
E-5	*Pseudo-nitzschia*	14	9	5	0.272	0.470	75%	98%
E-5	**Total**	**85**	**48**	**5**	**-**	**-**	**94%**	**97%**

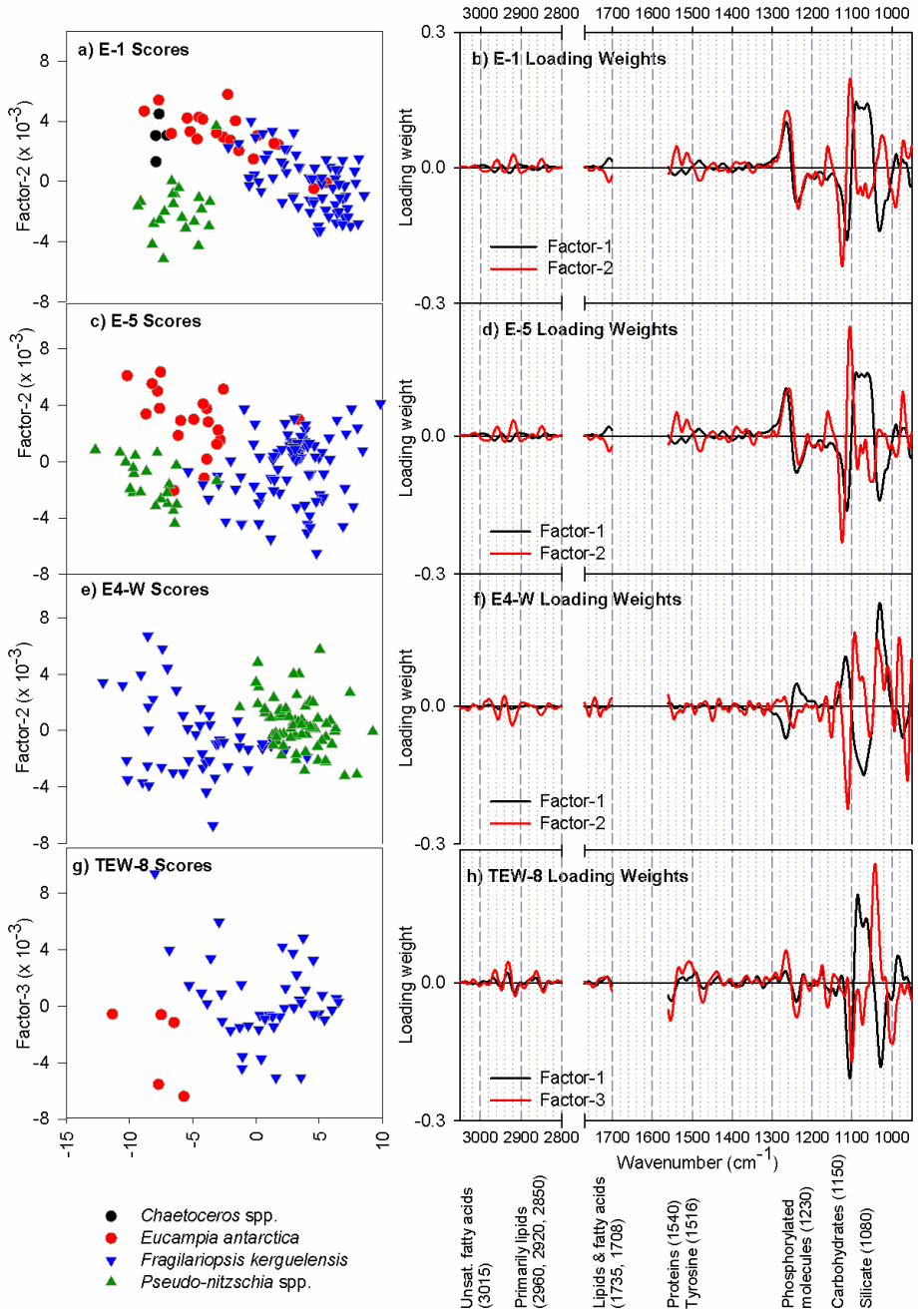

Figure 3-3 Taxonomic Classification by PLSDA results for four common genera: *Chaetoceros* spp, *Eucampia antarctica, Fragilariopsis kerguelensis* and *Pseudo-nitzschia* spp. Panels a-h show four different stations. Scatter plots on the left hand side shows scores and line plots on the right hand side show the associated loading weights. The scores plots indicate that the cell spectra cluster well by taxonomic grouping at each site. The loading weights plots indicate that the source of the variation between cell spectra is largely from the lower wavenumber region (~1240-1000 cm^{-1}).

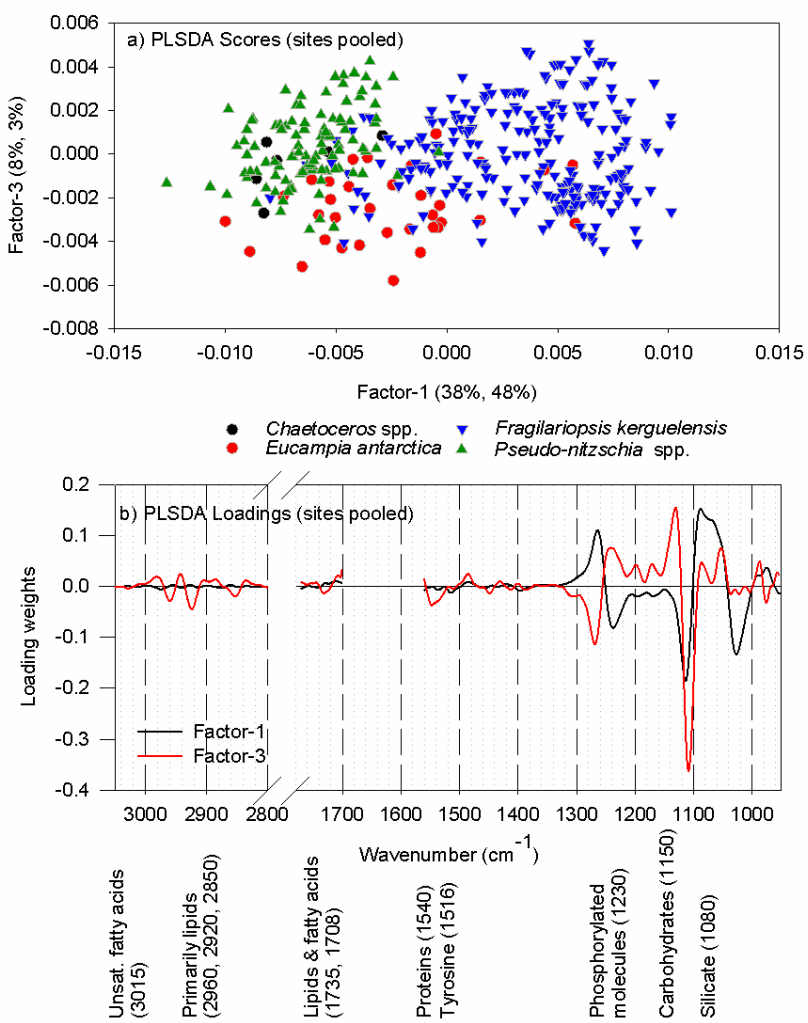

Figure 3-4 Classification of cell spectra by PLSDA with data pooled across stations. PLSDA scores plot (a) shows clustering of cell spectra by taxon.

PLSDA Loading weights plot (b) shows spectral bands which drive variation between cell spectra - primarily phosphorylated molecules (1230 cm^{-1}), carbohydrates (1150 cm^{-1}) and silicate (1080 cm^{-1}).

3.3.4 Community averages compared to individual taxon

Changes in macromolecular composition for the four taxa pooled were compared to those for *F. kerguelensis* alone to see how well community average measurements reflected those of the dominant taxa (Fig. 3-5). Inspection of the average second derivative spectra (Fig. 3-5 a & d) showed that some trends observed for *F. kerguelensis* were reflected in the bulk averages; however, there were other notable differences in both peak position and intensity. Protein (1540 cm^{-1}) and phosphorylated molecule (~1240 cm^{-1}) levels were lowest and silicate/silicic acid levels

(~1080 cm^{-1}) were highest at site E4-W for both the pooled taxonomic group and for *F. kerguelensis*. Yet, stronger clustering occurred in the scores plots between the high (E4-W & TEW-8) and moderate (E-1 and E-5) Fe stations for *F. kerguelensis* alone than within the pooled taxa. The PLSDA scores plots (Fig. 3-5 b & e) confirmed this observation whereby cell spectra from high Fe stations clustered tightly on the same side of the plot for *F. kerguelensis* but clustering was weak in the pooled taxa scores plot. The loading weights plots (Fig. 3-5 c & f) showed similar trends for both the pooled taxon and *F. kerguelensis* with regard to trends in protein, phosphorylated molecules, silicate/silicic acid and carbohydrate levels between sites. In spite of this, the contribution of phosphorylated molecules to variation between cell spectra was stronger for *F. kerguelensis* alone.

The PLSDA by station for *F. kerguelensis* also served to examine the phenotypic plasticity of the species between high and moderate Fe stations (Fig. 3-5 d-f). The degree to which models can discriminate between cell spectra from different stations is indicative of the magnitude of change in macromolecular composition of those cells (Sackett et al. 2013). Factors 1 and 3 of the scores plots from PLSDA models explained 49% of the variation in the spectral dataset, with good clustering by station. *Pseudo-nitzschia* spp. did not show a similar pattern of clustering and model discrimination accuracy was poor (Fig. 3-6). This indicated that *F. kerguelensis* demonstrated a higher level of phenotypic plasticity under conditions of high and moderate Fe than did *Pseudo-nitzschia* spp.

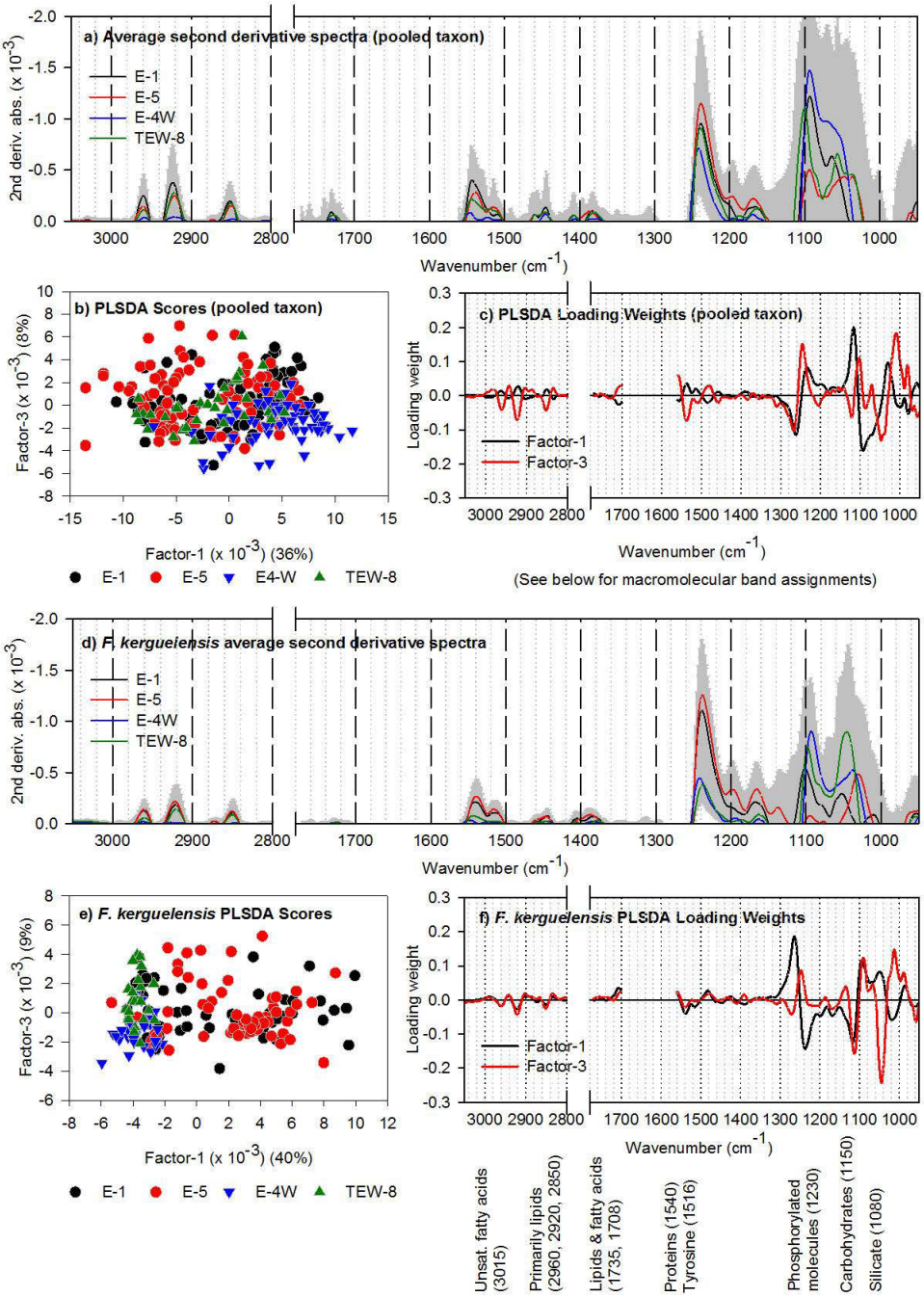

Figure 3-5 Variations in macromolecular composition for four taxon pooled (a-c) and separately for *F. kerguelensis* (d-f).

Average second derivative spectra (a & d) and loading weights plots (c & f) indicate the source of the variation between the taxonomic groups, including strong bands related to phosphorylated molecules, silicate and carbohydrates (~1240-1000 cm^{-1}). Weaker contributions from lipids and proteins are indicated by the presence of bands at 1730 cm^{-1} and 1540 cm^{-1}, respectively. Scores plots (b & e) show clustering by station and differences in intrapopulation variability.

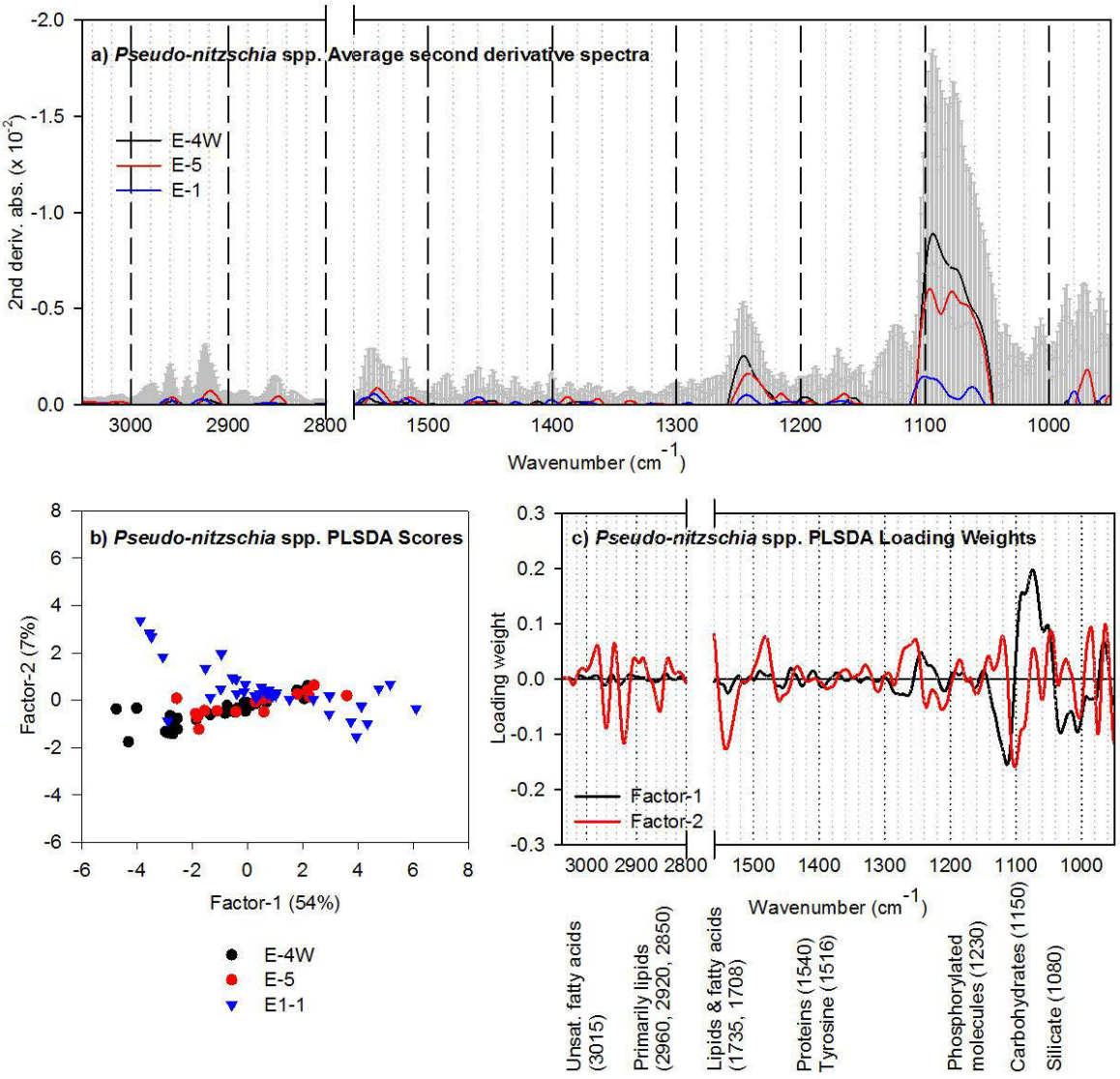

Figure 3-6 Average second derivative spectra (a), PLSDA scores plot (b) and PLSDA loading weights plot for *Pseudo-nitzschia* spp. at stations E-1, E-5 and E4-W.

Although the average second derivative spectra show differences between treatments, intra and interspecific variability are both high, resulting in weak clustering by station in the scores plot. The loading weights plot shows that variability between cell spectra is largely driven by protein levels (~1540 cm^{-1}) carbohydrates (1150 cm^{-1}) and silicate (1080 cm^{-1}).

3.4 Discussion

The taxon-specific analysis of *F. kerguelensis* cell spectra revealed that stations with lower Fe availability demonstrated higher levels of intraspecific variability (Fig. 3-5 e). The sources of variation between cell spectra were multivariate, including most of the major macromolecular

bands (proteins, phosphorylated molecules, amino acids, silicate/silicic acid and carbohydrates). Differences in variability were not observed when data was pooled across the four taxa, suggesting that community averages may not necessarily reflect the macromolecular composition of *F. kerguelensis*, despite its relatively high abundance within the assemblage. Although studies of intraspecific variability in microalgae are rare, higher levels of population variability have been previously reported for laboratory cultured microalgae under nutrient stress using SR-FTIR microspectroscopy (P. Heraud et al. 2008). Also, in a previous study of the Southern Ocean diatoms *Fragilariopsis cylindrus*, *Chaetoceros simplex* and *Pseudo-nitzschia subcurvata*, higher intraspecific variability was shown, particularly for *F. cylindrus*, under extreme salinity and temperature conditions (Sackett et al. 2013). Given that dissolved and particulate Fe levels appeared to be decreasing during the time series stations (indicated by a decrease from E-3 to E-5; (Bowie et al. 2014), high intraspecific variability in *F. kerguelensis* could be indicative of a population in transition towards Fe-limitation. Thus, the increased intraspecific variability may have been a sign that the population was in transition, relative to the Fe-enriched stations; however, further studies are required with controlled laboratory trials to confirm that the observed macromolecular changes were due solely to the influence of Fe supply.

Based on the SR-FTIR spectra, levels of silicate/silicic acid were higher in *F. kerguelensis* cells from the Fe-enriched stations (E4-W and TEW-8) compared to the moderate Fe stations (E-1 and E-5). This result contradicts some previous studies which have shown a negative correlation between Fe availability and silicification (Marchetti & Cassar 2009), but is not unprecedented. During the SOFeX experiment, Twining et al. (2004) observed a 16% increase in cellular Si after Fe addition for individual *Fragilariopsis* spp. cells, and Hoffmann et al. (2007) measured an increased ratio of biogenic silica (BSi) to particulate organic phosphate with bulk measurements of Fe-enriched Southern Ocean diatoms during the EIFEX project.

At the Fe-enriched stations (E4-W and TEW-8), the growth rate of the bulk population was substantially elevated compared to the moderate Fe stations (E-1 and E-5; Table 3-1). In their review of silicon metabolism in diatoms, Martin-Jézéquel et al. (2000) reported that the widely accepted inverse relationship between silicification and growth rate does not always hold, particularly when extracellular silicon is not limiting (Martin-Jézéquel et al. 2000). Thus, it is possible that Fe enrichment, in the presence of adequate ambient Si levels (Table 3-1), stimulated both high growth rate and high levels of biogenic silica. In conjunction with silicate/silicic acid, absorbance from phosphorylated molecules was also higher in cell spectra from the moderate-Fe stations (E-1 and E-5; Fig. 3-3 a & b). This is interesting because a previous spectroscopic study found that absorbance from phosphorylated molecules was positively correlated with growth rate

(Jebsen et al. 2012). Recently however, a proteomics study of acclimation to Fe-limited conditions in the diatom *Thalassiosira pseudonana*, measured substantial up-regulation of proteins related to the pentose phosphate pathway and to amino acid biosynthesis/degradation pathways, including some specifically related to the amino acid tyrosine (Nunn et al. 2013). That study found proteins related to sucrose metabolism (including photosynthesis, oxidative phosphorylation and carbon fixation) that were unique to Fe-limited cultures and can therefore be considered indicative of Fe-limitation. The up-regulation of these proteins would be consistent with observations from cell spectra at the moderate Fe stations (E-1 and E-4) of increased absorbance from proteins, tyrosine, and phosphorylated molecules (indicative of increased cellular concentrations) relative to Fe-enriched stations (E4-W and TEW-8).

BSi to particulate organic carbon (POC) ratios for the 20 μm size fraction of the phytoplankton community (which includes the diatoms *F. kerguelensis*, *Chaetoceros* spp. and *E. antarctica*, plus other species of microalgae) were found to be lower at Fe-enriched stations (0.57 and 0.23 at stations E4-W and TEW-8, respectively) and higher at stations with moderate Fe availability (0.63 at stations E-1 and E-5) (Trull et al., this issue). It may seem counter-intuitive that an increase in cellular Si levels could result in a decrease in the BSi/POC ratio; however, looking at the magnitude of difference in BSi and POC between stations shows that BSi increased by a factor of ~4.5, whereas POC increased ~12 fold at TEW-8 compared to E-1 (Table 3-1). Thus, the drop in BSi/POC at the Fe enriched station could be explained by increases in both the POC and BSi pools, with the increase in POC being ~3 times that of BSi. Although diatoms were the dominant group within the 20 μm size fraction, it should be noted that a decrease in BSi from bulk measurements could have been contributed to by a shift from siliceous diatoms to other, non-siliceous groups. Additionally, samples from the Fe enriched stations were observed to have substantially higher carbon productivity, which could have led to increased concentrations of cellular carbon (Jacquet et al. 2014). Increased cellular carbon under Fe enrichment has been reported in several recent diatom studies (Twining, Baines & Fisher 2004; Marchetti & Harrison 2007; Brzezinski et al. 2011). If the decrease in BSi/POC was caused primarily by a large increase in cellular C concentrations, calculations of cellular C from cell volume may provide overestimates under Fe enrichment, because cell size is constrained by the frustule and most regressions of cell volume versus carbon content are based on Fe replete cells (Twining, Baines & Fisher 2004).

Such changes in cellular carbon and Si content are consistent with changes in macromolecular composition observed by SR-FTIR microspectroscopy. The PLSDA loading weights plot for *F. kerguelensis* shows that cell spectra from station TEW-8 had the highest absorbance from

silicate/silicic acid (~1080 cm^{-1}) and carbohydrates (~1040 cm^{-1}) among the four stations (Fig. 3-5 f). Southern Ocean diatoms have been observed to accumulate carbohydrates to a maximum in the evening, providing a source of carbon skeletons for protein production over night (van Oijen et al. 2004). Given that station TEW-8 was sampled at 10 PM (whereas the other three stations were sampled between 12:00 and 17:30), it is possible that cellular carbohydrate levels were at a maximum at this time. Although carbohydrates contain a relatively lower proportion of carbon (gC/gDW) compared with lipids and proteins (~0.4, ~0.76 and ~0.53 respectively), it is plausible that a substantial increase in carbohydrate storage levels could cause an increase in cellular carbon (Geider & La Roche 2002). The pattern of changes in silicate/silicic acid and carbohydrate levels between stations was more complex for the pooled data set than for *F. kerguelensis* alone, indicating that community average measurements may not always reflect the composition of the dominant taxa, which can differ widely, and should therefore be interpreted cautiously.

This study adds to the growing evidence that SR-FTIR microspectroscopy has great value as a tool for quantifying various traits (e.g. growth rate, nutrient status, nutritional value, taxonomic identification) in phytoplankton and other microorganisms (Jebsen et al. 2012; Heraud et al. 2005; Heraud, Wood, et al. 2007; Sackett et al. 2013; Ngo-Thi et al. 2003). Trait-based approaches are a powerful, relatively untapped resource for improving predictions of phytoplankton community composition and dynamics in response to environmental change (Litchman & Klausmeier 2008). For example, phenotypic plasticity provides great potential for a species to cope with rapid and prolonged environmental changes (Charmantier et al. 2008). Accurate, taxon-specific models that describe a broad range of phenotypic parameters, referred to here as *phenomic models*, will enhance our ability to predict the response of the phytoplankton community to future climate scenarios. The power of these multivariate phenomic models depends largely on our ability to collect phenotypic data using high-throughput, robust and inexpensive techniques. Multivariate modeling approaches are recognised as integral tools for the analysis of ecophysiological traits (Litchman & Klausmeier 2008), however less attention has been paid to the power of multivariate *measurement* techniques, such as SR-FTIR microspectroscopy and X-ray Fluorescence Microprobe Analysis, for data collection. Encouraging the use of such multivariate measurement techniques, which can be used to predict multiple traits simultaneously, will dramatically increase the speed of trait data collection for microorganisms. Moreover, the advent of commercially available portable infrared and Raman spectrometers means that spectroscopic measurements can now be made in real time in the field.

This study demonstrated the taxon-specific responses of four dominant diatom taxa in association with natural Fe enrichment. These responses were not entirely reflected by the pooled data which

was viewed as analogous to bulk community averages. *Fragilariopsis kerguelensis* showed distinct phenotypic differences (i.e. plasticity) between high and moderate Fe stations, whereas *Pseudo-nitzschia* spp. did not (Figs. 3-5 and 3-6). Understanding differences between taxa is important for improving our ability to predict phytoplankton community composition and dynamics in response to environmental change (Arrigo 2005). The current lack of taxon-specific data is related to methodological challenges that limit *in situ* studies to bulk-community measurements. Methods which permit the analysis of individual cells, such as SR-FTIR microspectroscopy, present a pathway for the collection of taxon-specific data to fill this gap. It is likely that the broad use of the approach outlined in this paper would be limited by access to synchrotron facilities. However, burgeoning new technology in laboratory-grade instruments will soon make it possible to conduct measurements in single microalgal cells without the need for a synchrotron light source. For example, the newest focal plane array detectors have a higher magnification which allows infrared images to approach the spatial resolution possible using single-point mapping with an infrared microscope. Further, the advent of new extremely brilliant laboratory sources of IR light such as the quantum cascade laser are likely to further reduce the need for synchrotron sources in the future (Brandstetter et al. 2010). Taxon-specific data is in great demand from carbon cycle and ecosystem modelers, particularly for the Southern Ocean (Carr et al. 2006), and is necessary for advancing our ability to predict the effect of environmental changes, including climate change, on Earth's marine and terrestrial ecosystems.

3.5 Acknowledgments

We thank Prof. Stephane Blain (Chief Scientist) and Prof. Bernard Queguiner (Voyage Leader) for inviting and supporting L.A.'s and O.S.'s participation in the KEOPS2 programme. The captain of the RV Marion Dufresne II, Cmd. B. Lassiette, and his crew, and all scientific members of KEOPS2 community are acknowledged. L.A.'s participation in KEOPS2 was supported by an Australian Antarctic Division grant (#3214). This research was undertaken on the infrared microscopy beamline at the Australian Synchrotron, Victoria, Australia with beamtime awarded on the basis of merit, as part of a peer-reviewed provision process. We thank beamline scientists, Drs. Mark Tobin and Keith Bambery, for their assistance with the synchrotron measurements.

4 Snapshot prediction of carbon productivity, carbon and protein content in a Southern Ocean diatom using FTIR spectroscopy

In response to research questions iii and v (Figure 1-1), an experiment was designed to test the predictive accuracy of multivariate models based on FTIR microspectroscopy. Given previous reports that FTIR cell spectra had been used to accurately predict growth rate in microalgae (Jebsen et al. 2012), the current experiment tested the hypothesis that cell spectra could be used to accurately predict carbon productivity in *Chaetoceros simplex*. The experiment also tested the accuracy of multivariate models based on the same FTIR spectra to simultaneously predict cellular levels of proteins and carbon (per unit dry weight). This chapter is a reformatted version of the manuscript submitted to the International Society for Microbial Ecology (ISME) Journal. The paper is listed in Appendix II as Sackett, O. et al., 2014. Snapshot prediction of carbon productivity, carbon and protein content in a Southern Ocean diatom using FTIR spectroscopy. *The ISME Journal (submitted November 2014)*.

4.1 Introduction

Each year, growth of marine phytoplankton produces ~48.5 $\times 10^9$ tonnes of organic carbon, roughly equivalent to terrestrial photosynthesis (Field et al. 1998). More than 40% of the marine primary production is attributed to diatoms, a group of silicifying microalgae (Nelson et al. 1995). In the Southern Ocean, massive diatom blooms occur on a seasonal basis, covering thousands of square kilometers (Blain et al. 2007), providing carbon, nutrients and energy to the Southern Ocean ecosystem (Bernard et al. 2012). Annual freezing and thawing of the Southern Ocean means that diatoms are subject to major fluctuations in physicochemical (salinity, temperature, nutrients and light) conditions. These seasonal fluctuations are known to stimulate changes in diatom phenotypes, such as photophysiology (Ralph et al. 2007), macromolecular composition (Mock & Hoch 2005) and morphology (Morgan-Kiss et al. 2006). The ability to acclimate via phenotypic plasticity is essential for cells to satisfy physiological requirements and maximize fitness in variable environments. Antarctic diatoms have been shown to adjust their photophysiology to maximize photosynthesis for growth (Ralph et al. 2007; Petrou & Ralph 2011) and vary their macromolecular pools to changing environmental conditions, increasing lipid concentrations for maintaining membrane structure and for energy storage (Mock and Kroon 2002) or altering protein concentrations in response to osmoregulation and cryoprotection (Krell et al. 2008). Although species-specific data are scarce, increasing evidence suggests that

phenotypic responses are highly variable within and between taxonomic groups (Sackett et al. 2013; Petrou & Ralph 2011; Petrou et al. 2011).

Understanding phenotypic variation and acclimation is of great importance, as the phenotypes of marine phytoplankton determine ocean biogeochemistry and the efficiency with which carbon, nutrients and energy are transferred to higher trophic levels (Arrigo 2005; Hessen et al. 2004). In variable environments, like those in the Southern Ocean, the caloric value of food can be of critical importance, particularly in winter when sunlight and food are scarce. For example, lipids, which are the most energy-rich macromolecule, are known to vary under different environmental conditions (Mock & Kroon 2002b), therefore changes in macromolecular composition and energy partitioning in the cell will determine the nutritional value of the food and productivity of the entire food web (Diekmann et al. 2009b). Quantifying a species' capacity for phenotypic variation can inform predictions of its' ability to survive environmental change (Charmantier et al. 2008), and may provide insight into which species could dominate under future environmental conditions in the Southern Ocean, such as a reduction in sea ice thickness, duration and extent. Investigating the phenotypic responses of organisms, using high-throughput, high-dimensional methods, referred to as phenomics (Houle et al. 2010), may be particularly informative in the Southern Ocean ecosystem, where shifts in the phytoplankton communities may occur in response to the recent rapid pace of environmental change (Ducklow et al. 2013) provide insight into which species may dominate under future environmental conditions.

Investigating the phenotypic responses of Southern Ocean organisms is of growing importance for furthering our understanding of ecosystem processes into the future. As shifts in the phytoplankton communities may occur in response to the current rapid pace of environmental change already being measured, such as a reduction in sea ice thickness, duration and extent (Ducklow et al. 2013). However, field-based phenotypic data is in short supply, largely because of the great expense associated with sample collection and the slow turn-around time between collection and analysis. Current methods for quantitative studies of phytoplankton phenotypes involve lengthy protocols and/or expensive analytical techniques. The use of ^{14}C involves phytoplankton being incubated under desired conditions, and productivity determined by calculating the relative change in isotopic enrichment over a given period (typically 1-24h). While measuring incorporation of ^{14}C by the entire phytoplankton community is relatively rapid and inexpensive; the analysis of individual taxa within mixed natural samples is a time-consuming process (isolation and analysis of cells from individual taxa), and impractical for high-throughput studies. Additionally, the radioactivity of this isotope limits its application in the field (Hama et al. 1983). Methods based on ^{13}C avoid the use of radioactive isotopes; however, analysis can be

relatively expensive. Regardless of the advantages and disadvantages of these two methods, a common limitation to both is that measurements need to be taken over time. This methodological limitation has resulted in a slow supply of phenotypic data relative to demand from research groups such as biogeochemical and ecosystem modelers (Carr et al. 2006; Graff et al. 2012).

Spectroscopic approaches offer substantial benefits over traditional methods, being inexpensive, quantitative, objective, rapid, high throughput, sensitive and inherently multivariate (Jebsen et al. 2012; P. Heraud et al. 2008; Heraud et al. 2005; Heraud, Beardall, et al. 2007; Hirschmugl et al. 2005; Sackett et al. 2013). The use of spectroscopic techniques such as Raman and Fourier Transform Infrared (FTIR) spectroscopy in phytoplankton studies has been widely explored (Domenighini & Giordano 2009; P. Heraud et al. 2008; Heraud, Wood, et al. 2007; Dean et al. 2012; Dean et al. 2010). These techniques involve irradiating a sample with specific wavelengths of light and measuring light scattering (Raman spectroscopy) or absorbance (FTIR spectroscopy) by the sample. The resulting spectra consist of absorbance bands associated with macromolecules that can be interpreted to reveal quantitative variations in cell phenotype in terms of physiology, pigment content revealed quantitative variations in cell phenotype in terms of physiology (Li et al. 2012), pigment content (Andreeva & Velitchkova 2005) and macromolecular composition (Heraud, Wood, et al. 2007). In a recent study, Jebsen, Norici, Wagner, Palmucci, Giordano & Wilhelm (Jebsen et al. 2012) predicted growth rates from FTIR spectra of microalgal cells, showing that FTIR spectroscopy can provide a valuable alternative to time-series measurements for the collection of physiological rate data. Adopting this approach, here we develop a method to predict a number of phenotypic traits including rates of carbon production in phytoplankton cells.

Specifically, we combined ^{13}C mass spectrometry (quantitative elemental measurements) and FTIR microspectroscopy (rapid, high throughput, semi-quantitative, multivariate macromolecular measurements) to provide a quantitative and rapid approach for the collection of phytoplankton phenotypic data. Using mass spectrometry to build a calibration dataset, we predict multiple phenotypic traits; including cellular carbon and protein content, based on the FTIR spectra from intact *Chaeteceros simplex* cells. We also use the predictive model to obtain rates of carbon productivity. This is the first study, to our knowledge, that demonstrates the derivation of carbon productivity from a measurement taken at a single time-point, providing the first ever 'snapshot prediction' of phytoplankton carbon production rates.

4.2 Materials and Methods

4.2.1 Microalgal culturing and experimental conditions

Cultures of the Antarctic diatom *C. simplex* were grown from isolated cells from the coastal waters of Antarctica, Prydz Bay (CS 624, Australian National Algae Culture Collection, CSIRO, Hobart, Australia) and maintained at 4°C in filtered (0.2 µm) natural Antarctic seawater (collected from 145.9 °S 54.0 °S, 72 m, during SAZ-Sense, Jan.-Feb. 2007, *RV Aurora Australis*) supplemented with F/2 nutrients. The experiment was conducted as described in Petrou et al. (2011). Briefly, culturing was maintained in specially designed 1 L glass culturing vessels using natural seawater (salinity 34) enriched with F/2 nutrients (Guillard & Ryther 1962), with continuous air bubbling and maintained at 4 °C. Cultures received a 16:8 h light:dark cycle at 50 µmol photons m^{-2} s^{-1} (Grolux, GMT lighting, Northmead, Australia). Exponential growth phase (estimated with regular *in vivo* fluorescence measurements as a proxy for biomass where relative fluorescence units were converted to chlorophyll concentration by a conversion factor determined using a calibration standard (Wood et al. 2005); Trilogy, Turner Designs Inc., Sunnyvale CA, USA) was maintained for the duration of the experiment by diluting (up to 90%) with fresh medium every 3-5 days. To initialize experimental treatments, cultures were concentrated by gentle vacuum filtering using 2 µm polycarbonate membrane filters (Millipore, MA, USA) and re-suspended in approximately 150 mL of medium in 250 mL culture flasks at four different salinities (31, 34, 55 and 70 (± 0.5; n=4). The salinity of the F/2 medium was adjusted either by the addition of MilliQ water or sodium chloride salt (Sigma, USA) and measured using a refractometer. Flasks were then assigned to three different temperature treatments (-1.8, 2 and 5 °C (± 0.3 °C)), provided by temperature-controlled incubators. Cell cultures were given 72 h to acclimate (based on a previously reported acclimation period for the sea ice diatom *Fragilariopsis cylindrus* (Mock & Valentin 2004) before subsamples were removed and analysed spectroscopically for macromolecular composition, and by mass spectrometry for cellular carbon (^{12}C and ^{13}C) and nitrogen content (see description below). Treatments were applied in quadruplicate, using a fully factorial design to capture a range of salinity and temperature regimes characteristic of the Southern Ocean annual freeze-thaw cycle, namely, sea ice (-1.8 °C, salinity 70), meltwater (2 °C, salinity 30 and pelagic (5 °C, salinity 34) conditions, respectively.

4.2.2 FTIR spectroscopy for macromolecular 'snapshot' measurements

Approximately 15 mL of cell suspension was filtered onto 1 µm polycarbonate filter membrane (Millipore) using a hand-operated vacuum filter tower. Cells collected on the filter were then re-suspended in isotonic saline solution (NaCl (Sigma, USA) and MilliQ water) to wash the cells to remove F/2 medium which contains compounds that can absorb infrared radiation and possibly

confound the FTIR measurements (Heraud, Wood, et al. 2007). The saline solution was kept at the same temperature as the incubation temperature of the cells. This rinsing process was repeated three times for each replicate. To minimize the chance of spectral artifacts resulting from the use of transflection measurements, washed cells were deposited on Kevley MirrIR Low-e Microscope Slides (Kevley Technologies, Ohio, USA) using a Shandon Cytospin Centrifuge (Cytospin III, Thermo Fischer Scientific, Waltham, MA) and immediately stored in a vacuum desiccator at room temperature until analysis (Heraud, Wood, et al. 2007; Cao et al. 2013). This method has been shown to result in cellular monolayers with homogenous thickness (Cao et al. 2013; Heraud & Wood 2013) and therefore minimise issues related to the previously reported electric field standing wave effect (Bassan et al. 2009; Filik et al. 2012; Bassan et al. 2013). Flow cytometry confirmed that minimal changes in cell forward scatter (proxy for size) occurred between treatment conditions (mean ± 5%, data not shown), further reducing the likelihood of spectral artefacts which have been shown to relate to differences in sample thickness (Heraud & Wood 2013).

Spectral data were collected using a FTIR Spectrometer (Digilab FTS 7000 Series) fitted with a UMA 600 Microscope and a Mercury Cadmium Telluride detector cooled with liquid nitrogen. Spectral acquisition and instrument control were performed using Win-IR Pro software. Spectra were acquired over the measurement spectral range 4000 - 800 cm^{-1}. The microscope objective had a Plexiglas hood which was purged with dehumidified air. The measurements were performed in the single point mode, with the focal plane aperture of the FTIR microscope open, at a spectral resolution of 8 cm^{-1}, with 256 scans co-added. The number of co-added scans was chosen as a good compromise between achieving spectra with good signal to noise characteristics and the rapid acquisition of data. FTIR spectral data was exported from Win-IR Pro for multivariate analysis using The Unscrambler X v 10.2 (CAMO, Norway). An initial quality control procedure was performed over the spectral range 3000-950 cm^{-1} where spectra with maximum absorbance greater than 0.85, which resulted from spectral acquisition of regions of the sample where cells were clumped, were rejected. Spectra were then pre-processed taking the second derivative using the Savitzky-Golay algorithm with 9 smoothing points, and normalization using Extended Multiplicative Signal Correction (EMSC).

4.2.3 Calibration data for predictive models

Mass spectrometry was used to measure total nitrogen, carbon and ^{13}C enrichment. Mass spectrometry was conducted by the Australian Rivers Institute (Griffith University, Queensland) using an Isoprime Mass Spectrometer (GV Instruments, Manchester, UK) instrument with an EA 3000 inlet (Eurovector, Milan Italy). Protein content was calculated from particulate organic

nitrogen (PON) using the protein to nitrogen conversion factor of 4.78 (± 0.62) for phytoplankton (Lourenço et al. 2004). Because this study focused on improving the time and cost-efficiency of generating phenomic data, biomass contributions from lipids and carbohydrates were estimated using calculations which incorporated factors available in the literature (see equations below), rather than by direct extraction. Further, avoiding the use of extraction protocols may reduce uncertainty in lipid and carbohydrate levels since previous studies have reported large variations in lipid extraction efficiencies between different species of microalgae and with different extraction methods (Lee et al., 2010). Protein levels (based on nitrogen concentration) and carbon mass fraction were measured using mass spectrometry.

Carbon productivity was measured using the method described by Fernandez and coauthors (Fernandez et al. 2005). Briefly, ~100 mL of culture from each replicate flask was transferred into a 250 mL Erlenmeyer flask and 0.5 mL of tracer solution (3.64 mg^{13}C mL^{-1}, which is equivalent to 0.5 μmol.mL^{-1}) was added. Replicate cultures (n=4) were incubated for 4 h under 50 μmol photons m^{-2} s^{-1} of growth irradiance before microalgae were vacuum filtered onto pre-combusted GF/F filters, rinsed with isotonic saline solution and dried in an oven at 60°C overnight. Control samples were incubated in the dark for 4 h and natural background ^{13}C levels were measured in culture sub-samples taken prior to the addition of the tracer solution. Samples were stored under vacuum desiccation until analysis by mass spectrometry.

Carbon productivity was calculated from the level of ^{13}C enrichment relative to natural background levels following the equations in Fernandez et al. (2005). These mass spectrometry measurements were used as the calibration and validation data from which multivariate models of carbon productivity were created based on spectral data (see *Multivariate Modeling* below).

Carbon content was taken as the total particulate organic carbon (POC) per unit dry weight (DW). Energy from protein was calculated based on the average caloric equivalent of protein (20.08 kJ/g.DW) reported by Whyte et al (1987). Minimum and maximum energy content for the remaining fraction of the biomass was calculated based on the caloric equivalents of carbohydrates (17.57 kJ/g DW) and lipids (41.00 kJ/g DW) (Whyte 1987) and the approximate proportion of carbon by mass of proteins, lipids and carbohydrates (0.52, 0.76 and 0.40, respectively) (Geider & La Roche 2002) derived from phytoplankton, using the following equations.

$$protein\ (g/g.DW) = PON_{biomass}(g/g.DW) \times 4.78$$

$$carbon_{protein}(g/g.DW) = protein\ (g/g.DW) \times 0.52$$

$$carbohydrates_{\max.}(g/g.DW) = \frac{POC_{biomass}(g/g.DW) - carbon_{protein}(g/g.DW)}{0.40}$$

$$lipids_{\max.}(g/g.DW) = \frac{POC_{biomass}(g/g.DW) - carbon_{protein}(g/g.DW)}{0.76}$$

$$energy_{protein}(kJ/g.DW) = protein\ (g/g.DW) \times 20.08$$

$$\min energy_{biomass-protein}(kJ/g.DW) = carbohydrate_{\max.}(g/g.DW) \times 17.57$$

$$\max energy_{biomass-protein}(kJ/g.DW) = lipid_{\max.}(g/g.DW) \times 41.00$$

where 'min *energy* $_{\text{biomass-protein}}$' is the theoretical minimum energy content of the non-protein biomass calculated using caloric equivalent for carbohydrates, which have the lowest caloric equivalent of the major macromolecules. The parameter 'max *energy* $_{\text{biomass-protein}}$' is the theoretical maximum energy content of the non-protein biomass calculated using the caloric equivalent for lipids, which have the highest caloric equivalent of the major macromolecules.

4.2.4 Predictive model calibration and validation

Due to the highly multivariate nature of spectroscopic data, Partial Least Squares Regression (PLSR) modeling was used to probe the data in more detail and predict phenomic parameters in 'unknown' independent samples (known as the validation set). The PLS approach is useful for dealing with complicated data sets where univariate regression is difficult or impossible to apply. Since its first publication in 1966, the PLS approach has become a standard tool in chemometrics (Wold et al. 2001; Barker & Rayens 2003). In this study, PLSR models were built using the data generated through mass spectrometry to calibrate the spectroscopic data. Data from mass spectrometry was divided into two groups using a stratified-random method so that two-thirds of the data formed the calibration data set and the remaining third formed the independent validation test set. Replicates included in the calibration set were not included in the validation set. PLSR models were then built using The Unscrambler X 10.2 (CAMO, Norway) where each "Y" variable was the independently measured composition and productivity data (i.e. protein, carbon and productivity) and each "X" variable was an infrared absorbance spectrum. In other words, to estimate the rate of carbon productivity from the spectrum of a single sample (i.e. a single time-point), a linear regression was created using PLSR modeling to associate the spectral data with a rate of carbon productivity measured from multiple samples (i.e. two time-points) using mass spectrometry. The rate of carbon productivity of 'new' independent samples could then be predicted from samples taken at a single time-point based on this PLSR model.

The regions 3050-2800 and 1540-1000 cm^{-1} were selected for analysis since they contain all the major biological bands and avoided possible issues related to spurious absorbance values for the amide I band (~1650 cm^{-1}) due to variability in background atmospheric water vapour and differences in the levels of bound water within samples (Vaccari et al. 2012). Outliers were identified by inspecting the leverage and residual X and Y variance plots, with a threshold of 5% (set nominally). Additional regions of the spectrum were excluded (i.e. "feature selection") through a process of trial and error until each PLSR model was optimized (final spectral range included in the model was 3050-2800, 1250-1000 cm^{-1}). The models were validated using the test set data and summary statistics reported were based on the predictive performance of the models.

4.2.5 *Significance testing*

Data from the different simulated habitats (pelagic, meltwater, sea ice) and treatment conditions were compared by two-factor ANOVA (for salinity and temperature), post-hoc Tukey-tests and a significance level of α=0.05 (SigmaPlot 11.0 Systat, U.S.A.). Two-way ANOVA for productivity failed the test of normality, so significance was calculated using the Scheirer-Ray-Hare non-parametric test (Holmes et al. 2010).

4.3 Results

4.3.1 *FTIR spectroscopy for macromolecular 'snapshot'*

Visual inspection of infrared spectra identified obvious changes in the macromolecular composition of *C. simplex* between treatments. In cells from all treatments, the average second derivative spectrum showed strong bands associated with unsaturated fatty acids (3015 cm^{-1}), saturated CH stretches (2960, 2920, 2850 cm^{-1}), anti-symmetric phosphodiester vibrations (~1240 cm^{-1}), carbohydrates (1155 cm^{-1}) and silicate/silicic acid bands (~1076 cm^{-1}; Fig. 4-1; see Appendix I for band assignments). Variation in absorbance intensity between treatments was particularly strong for bands associated with carbohydrates and silicate/silicic acid, the dominant compounds in diatom frustules. Variation in cell spectra with salinity treatments was most obvious at 5 °C, whereas cell spectra from salinity levels 30 and 35 were notably different from those at the 55 and 70 levels (Fig. 4-1 c).

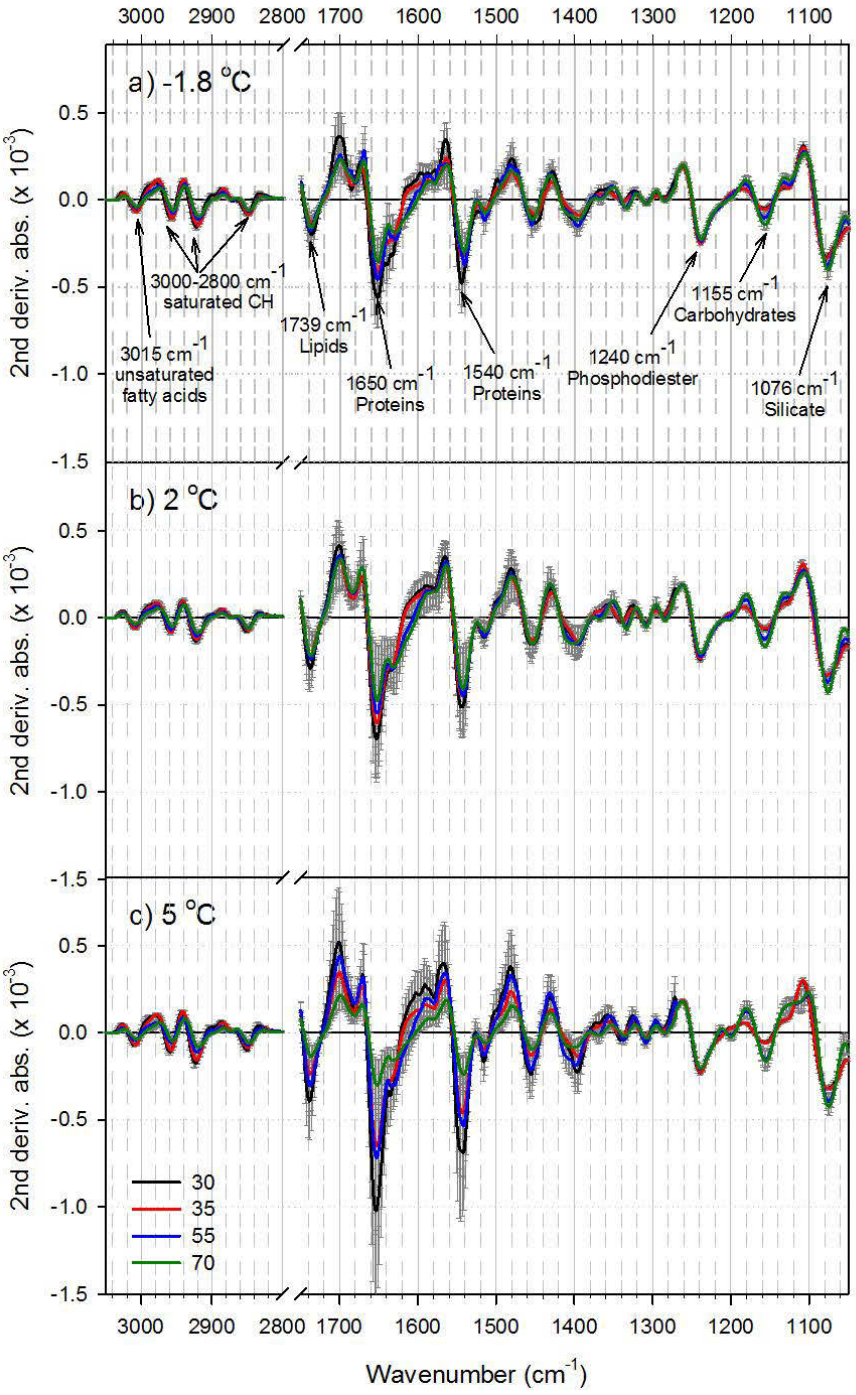

Figure 4-1 Average second derivative spectra for *C. simplex* under various temperature and salinity treatments.

The sea ice treatment is shown in green in plot (a), meltwater is shown in black on plot (b) and the pelagic is shown in red on plot (c). Bands related to lipids, proteins, carbohydrates and silicate are visible under all treatment conditions. Negative peaks indicate a positive absorbance. Differences in the height and area under peaks correspond to differences in the concentration of associated macromolecules. Error bars indicate one standard deviation from the mean.

4.3.2 Predictive model calibration and validation

The PLSR model constructed for the prediction of carbon productivity is shown in Fig. 4-2, as an example of the PLSR models constructed for cellular protein and carbon content. For carbon productivity, cell spectra clustered in PLSR scores plots by treatment conditions with 5 °C treatments towards the top of the scores plot and -1.8 °C treatments towards the bottom (Fig. 4-2 a) along the direction of Factor 2. Cell spectra from lower salinity treatments tended to cluster towards the right and higher salinity towards the left. The loading weights plot indicated that variation between the cell spectra was multivariate, with contributions from regions associated with lipids and proteins (~3015, ~2960, ~2920, ~2850 cm^{-1}), phosphorylated molecules (~1240 cm^{-1}), carbohydrates (~1155 cm^{-1}) and silicate/silicic acid (~1076 cm^{-1}; Fig. 4-2 b). Comparing the loading weights plot with the second derivative average spectra confirmed the absorbance from lipids in the region 2800-3000 cm^{-1} (Fig. 4-1). The reference versus predicted plot showed a linear trend with cell spectra from higher salinity treatments clustering towards the left of the plot and lower salinity treatments towards the right along the direction of Factor 1 (Fig 4-2 c). Cell spectra from the -1.8 °C temperature treatments clustered towards the left hand side of the plot, whereas 5 °C treatments occurred along the entire range of the plot. The predictive accuracy of all three models (carbon, protein and productivity) was relatively high. All models were linear and achieved R^2 values between 0.762 and 0.844, with the Root Mean Square Error of the prediction (RMSEP) ranging between 10 and 15% of the maximum Y-value (Table 4-1). The residual predictive deviation (RPD), which is often used to assess the quality of PLSR models, showed that all models presented were of "Excellent" quality (RPD > 8; Table 4-1) (Williams & Norris 2001).

Mass spectrometry data for treatments associated with -1.8 °C and 5 °C are presented along with data predicted using PLSR models for treatments associated with 2 °C (Fig. 4-3). Primary productivity reached a maximum (0.0018 g C/g DW/d or 1.64 ± 0.26 µg C L^{-1} d^{-1}) in conditions similar to those found in Southern Ocean pelagic habitats (salinity 35, 5 °C) and a minimum (7.9 x 10^{-5} g C/g DW/d or 0.18 ± 0.03 µg C L^{-1} d^{-1}) in conditions representative of sea ice habitats (salinity 70, -1.8 °C ; Fig. 4-3 a). Productivity predictions for treatments associated with 2 °C fell within the range of values measured for the -1.8 °C and 5 °C treatments, with a moderate rate of production predicted for cells in the simulated meltwater treatment (salinity 30, 2 °C). Cellular carbon content followed a similar trend to productivity, with a maximum measured in cells from the pelagic treatment and a minimum measured at a salinity level of 70 (sea ice brine treatment) for both the -1.8 °C and 5 °C treatments (Fig. 4-3 b). Carbon content predicted for treatments associated with 2 °C fell within the range of values measured for the -1.8 °C and 5 °C treatments.

Two-way ANOVA showed that the fraction of carbon partitioned into proteins was significantly different between salinity treatments ($P<0.001$), but not temperature treatments. In contrast, carbon partitioned into 'other' macromolecules (i.e. lipids, carbohydrates and phosphorylated molecules) was related to both salinity and temperature variation (interaction: salinity × temperature: $P=0.015$). Energy from proteins was maximal in cells from the pelagic treatment (5 °C and salinity 35). Proteins tended to contribute just less than 50 % of total cellular caloric content. Cellular carbon, protein and energy content showed a significant positive relationship with carbon productivity ($P<0.001$ in all cases), with R^2 values ranging between 0.678 and 0.733 (Fig. 4-4). In all cases, the standard error of prediction was about 10% of the maximum Y-value.

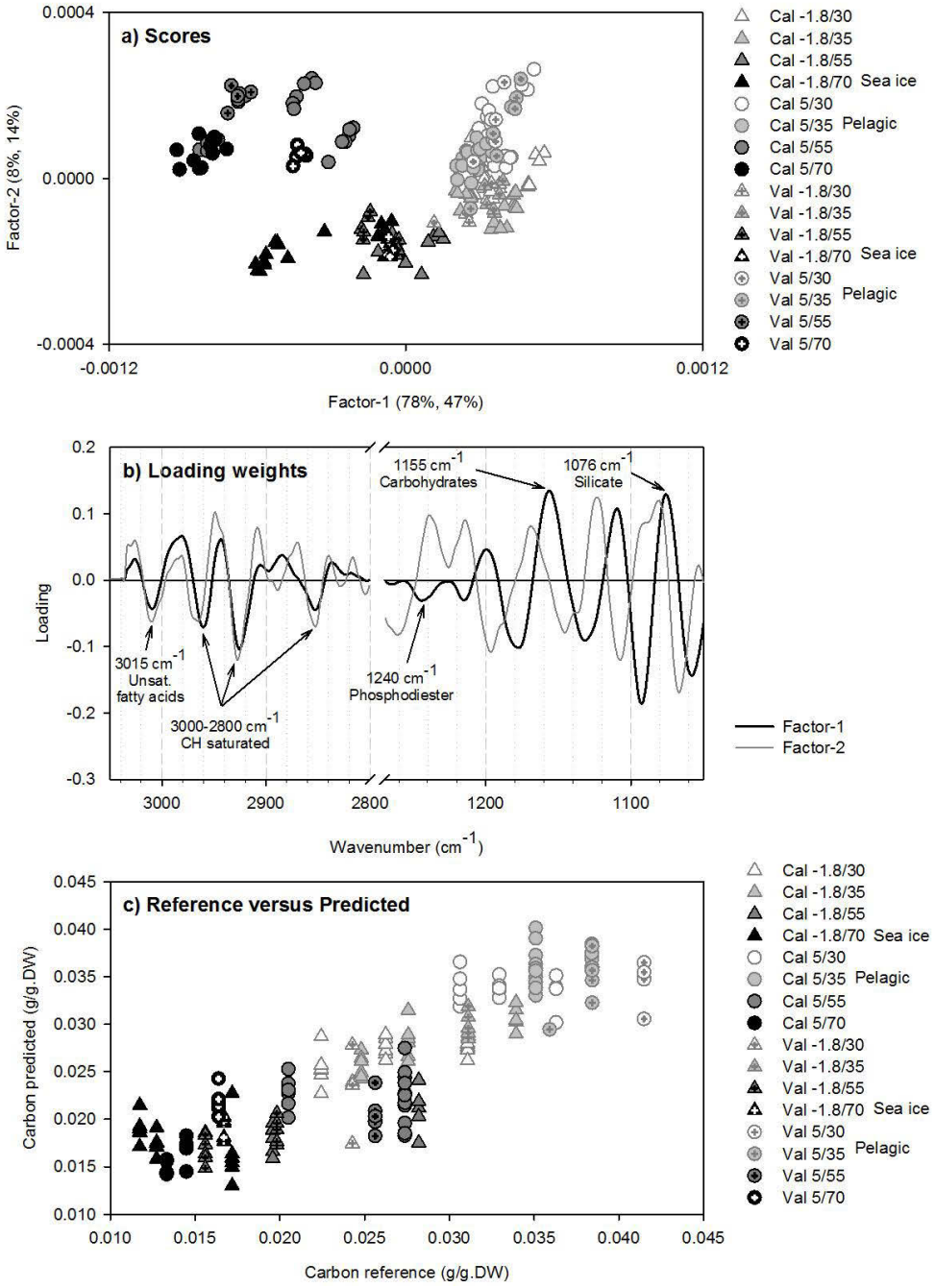

Figure 4-2 PLSR prediction model for cellular carbon content.

The scores plot for Factors 1 & 2 (a) shows cell spectra from lower salinity treatments (white and light grey), higher salinity treatments (dark grey and black), 5˚C treatments (circles) and -1.8˚C treatments (triangles). Validation samples are indicated by a cross hair in the centre of the symbol. Loading weights associated with the Factor 1 and 2 scores are shown in (b). Validation results are shown as the reference versus predicted plot (c) and validation statistics are shown in Table 4-1.

Table 4-1 PLSR predictive model validation statistics

Model	Protein	Carbon	Productivity
Units	g/g.DW	g/g.DW	ug.C/g.DW/h
n (cal)	131	130	129
n (val)	53	53	53
n (pred)	60	60	60
Factors	5	5	5
Pearson R-square	0.844	0.829	0.762
Max Y-value	0.0336	0.0415	0.0018
RMSEP[a]	0.0038	0.0041	0.0003
RMSEP/Max Y-value	±11%	±10%	±15%
RPD[b]	9.2	9.8	13.2
Quality[c]	Excellent	Excellent	Excellent

[a]Root Mean Squared Error of the Prediction
[b]Residual Predictive Deviation
[c]Quality evaluation based on RPD (models with RPD > 8 are considered to be of "Excellent" quality.

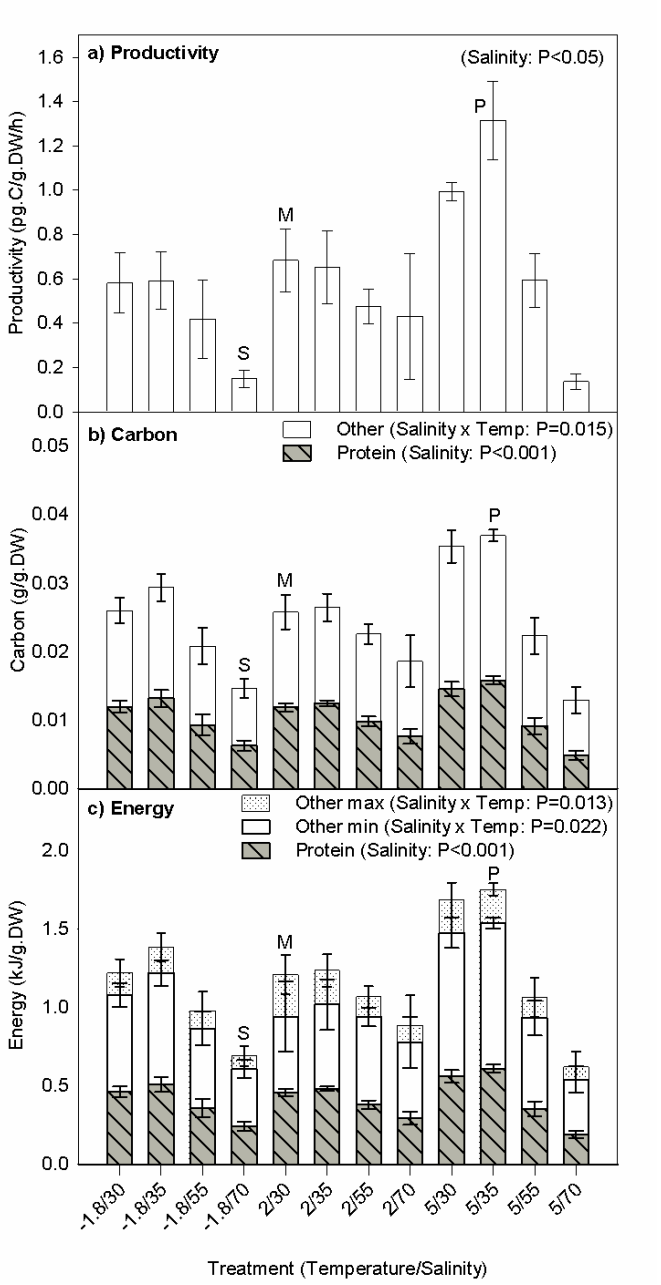

Figure 4-3 Productivity (a), carbon (b) and energy (c) content for C. simplex versus salinity and temperature treatments.

Treatments characteristic of sea ice, meltwater and pelagic habitats are indicated by the letters 'S', 'M' and 'P', respectively. Text in brackets indicates the results of two-factor ANOVA, where 'Salinity x Temp' refers to the interaction of the two factors. Error bars show the standard error of the mean.

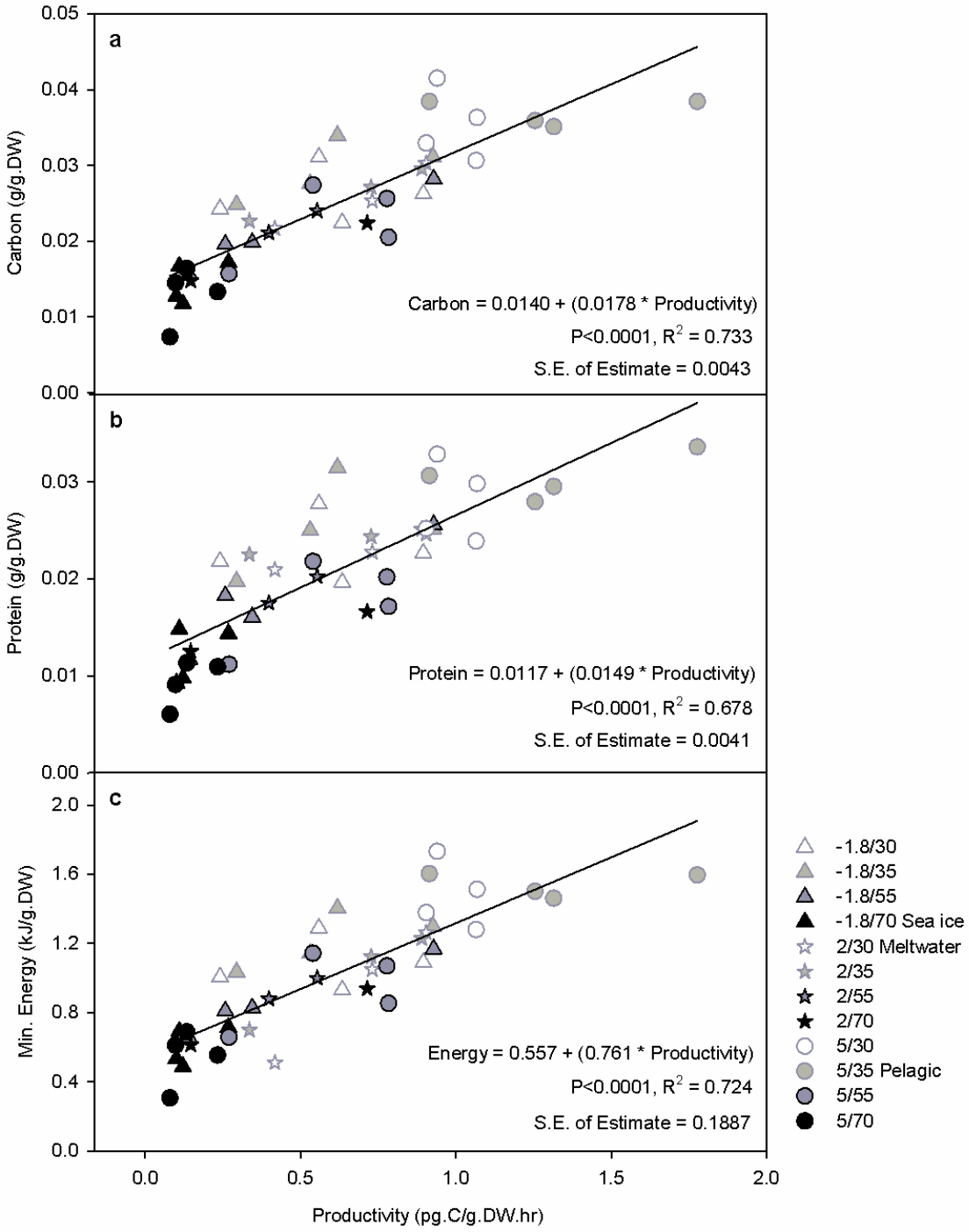

Figure 4-4 Carbon productivity versus cellular carbon (a), protein (b) and minimum total energy content (c).

Regression equations and statistics are indicated by text on each plot. Treatments characteristic of sea ice, meltwater and pelagic conditions are indicated in the legend.

4.4 Discussion

This study demonstrated the efficient and robust measurement of phenotypic traits from intact phytoplankton cells via FTIR microspectroscopy, complemented by mass spectrometry. The method enabled the concurrent measurement of changes in macromolecular composition and carbon productivity, which required minimal sample biomass and preparation. This approach enabled us to probe cellular carbon metabolism in response to salinity and temperature treatments, including those characteristic of the sea ice, meltwater and pelagic habitats found in the seasonally ice covered Southern Ocean.

Carbon productivity in *C. simplex* cells showed a significant positive correlation with cellular carbon, protein and energy content (Figure 4-4). This indicated that when carbon productivity was high, cells were actively growing and storing carbon as macromolecules, rather than simply exhibiting high carbon turn-over rates. High salinity (i.e. 70; commonly found in sea ice habitats) caused a reduction in cellular carbon, protein, energy and carbon productivity, regardless of the temperature (Figure 4-3). Cells from the pelagic treatment (salinity = 35 and 5 °C), had the highest cellular carbon, protein, energy and carbon productivity (Figure 4-3). This evidence suggests that *C. simplex* is tolerant of cold temperatures and high salinities, rather than being an extremophile *per se*, which is consistent with the species' propensity to form resting spores during the winter sea ice season. Given the rapid warming trend observed in some regions of Antarctica, particularly the West Antarctic Peninsula (Ducklow et al. 2013), species such as *C. simplex* which prefer milder temperatures and salinities may become increasingly competitive with truly extremophilic species.

Lipid accumulation in natural populations of sea ice algae has been reported for communities in both the Antarctic and Arctic, and it has been suggested that these lipids may constitute an important source of high energy biomass for organisms such as juvenile krill (Fahl & Kattner 1993; Lee et al. 2008). Krill, which have recently declined in numbers in some coastal Antarctic regions (Bernard et al. 2012), are one of the most numerous multicellular organisms on Earth, considered a keystone species in the Southern Ocean ecosystem and constitute the largest Southern Ocean fishery (Croxall & Nicol 2004). Consistent with these reports, cellular lipid concentrations in *C. simplex* cells were indeed found to be slightly higher (~10%) in the sea ice treatment (reported previously in Sackett et al. (2013)). However, increased lipid concentrations were associated with decreased energy per unit biomass (~60%), related to a substantial drop (~50%) in protein content (Figure 4-3). Given that sea ice algae are considered to be the main food source for juvenile krill, reduced protein, carbon and energy content in winter diatom communities could help explain why winter growth rates in Antarctic krill are half those in

summer (Meyer 2011). It should be noted that Sackett et al. (2013) found increases in lipid content in *Fragilariopsis cylindrus*, a dominant Southern Ocean sea ice diatom, to be substantially greater than in *C. simplex* under the same treatment conditions. Hence, variations in energy content and associated changes in macromolecular composition are likely to be taxon-specific. Consequently, shifts in phytoplankton assemblage composition have the potential to effect the amount of energy, carbon and protein available to juvenile krill and higher trophic levels in the Southern Ocean foodweb.

Demand for phytoplankton phenotypic data (e.g. carbon productivity, growth rate, elemental quotas and morphological characteristics) from biogeochemical and ecosystem modelers is currently outstripping supply (Carr et al. 2006). The supply of such data is relatively slow due to reliance on traditional methods that are often labour intensive and/or expensive (e.g. visible microscopy, mass spectrometry, chromatography and isotopic incubations). This paper demonstrates how FTIR microspectroscopy can be used to rapidly acquire phenotypic data (protein and carbon content, energy content and carbon productivity) from phytoplankton. We show how complementing the spectroscopic approach with mass spectrometry can reduce the cost of sample analysis by providing multiple phenotypic traits simultaneously in unseen samples, which have not been analysed via mass spectrometry. Furthermore, successful application of FTIR microspectroscopy to estimate the rate of carbon production over time (i.e. productivity) via a measurement taken at a *single time-point* is of great value for microbial ecologists, especially in situations where conducting incubation experiments may be impractical and/or expensive. A valid criticism of the method presented here is that predictive models based on cultured organisms may have limited applicability in the field. For example, physicochemical factors will likely diverge between field and laboratory conditions. However, this limitation can be overcome by using the calibration data from cultures as a starting point, then progressively updating the calibration set with field data over time. In particular, NanoSIMS is capable of measuring carbon and other elements in individual cells, making the collection of taxon-specific productivity data from natural populations a real possibility. Further, it may turn out that models developed for groups of taxa (for example, genera) provide sufficiently accurate predictions of phenotypic parameters to avoid the need for species-specific models.

Over the past 30 years, infrared spectroscopy has gained momentum as a powerful phenomics tool, particularly for the study of microorganisms (Giordano et al. 2001; Heraud et al. 2005, 2007; Heraud et al. 2008; Sackett et al. 2013; Naumann et al. 1991). To date, the suite of parameters that have been successfully measured or predicted in phytoplankton using FTIR

spectroscopy includes: levels of various macromolecules (e.g. proteins, lipids, carbohydrates and phosphorylated molecules), silicate concentration, physiological parameters (plasticity, growth rate and productivity) and the carbon mass fraction (Wagner et al. 2010; Sackett et al. 2013; Sackett et al. 2014; Stehfest et al. 2005). Given that all these parameters can be inferred from a single, non-destructive spectroscopic measurement, FTIR spectroscopy is well suited to provide rapid, robust and inexpensive phenotypic analysis of phytoplankton. In addition, a range of instruments is now available to suit a diversity of applications. For example, portability has been improved by the development of modern hand-held devices which enable measurements to be made in the field (Mukhopadhyay 2004), while efficiency has been increased with the integration of focal plane array detectors into spectrometers, enabling the collection of thousands of spectra at a time (Miller & Smith 2005).

This research builds on previous spectroscopic studies of phytoplankton by demonstrating the successful use of FTIR microspectroscopy to simultaneously and accurately estimate three different phenomic parameters (carbon productivity, protein and carbon content). The multivariate modeling approach adopted circumvented the need for productivity measurements to be taken over time (once data for a robust calibration set has been collected), with productivity being accurately estimated based on a single time-point. Simultaneously, an accurate estimate of cellular carbon and protein content was provided. Further, since microspectroscopy permits the measurement of individual cells, this approach provides an opportunity for the collection of taxon-specific phenotypic data.

The next phase in this promising research area will involve the development of holistic, multivariate phenomic models to describe the taxon-specific responses of phytoplankton to a range of environmental conditions, and the use of the technique to conduct on-line, real-time measurements of natural phytoplankton communities *in situ*. Field-based spectroscopic research has recently become possible with the introduction of portable, relatively user -friendly spectroscopic instruments. Phenomic models will greatly improve our ability to predict the responses of natural phytoplankton communities to environmental (including climate) change. This will intern improve our ability to predict changes in biogeochemical cycling.

FTIR microspectroscopy is currently an under-utilised resource in microbial phenotypic studies, with great potential to expedite our understanding of many microorganisms, including phytoplankton. We assert that the widespread application of spectroscopy to the study of microorganisms, including phytoplankton, could greatly increase the speed of phenomic data acquisition. Recent technological advances in focal plane multi-detector arrays provide an additional opportunity to up-scale spectroscopic studies from sequential cellular measurements

to thousands of measurements at a time. With such powerful analysis tools now available, the time is ripe for an advance in our understanding of microorganisms, including phytoplankton, and their interactions with marine ecosystems. Such advances could have far-reaching benefits across many sectors, including fisheries management, marine conservation and carbon cycle and ecosystem modeling.

4.5 Acknowledgements

We would like to thank Dr Scarlett Trimborne for the identification of *Chaetoceros simplex* by electron microscopy at the Alfred Wegener Institute for Polar and Marine Research. Thank you to Finlay Shanks at the Monash Centre for Biospectroscopy for continued instrument technical support. Sackett was supported by a UTS Doctoral Scholarship.

5 Synthesis

Phytoplankton play a key role in Earth's biogeochemical cycles and in fuelling marine and terrestrial ecosystems. Despite their importance, supply of phenotypic data from phytoplankton, particularly Southern Ocean species, is greatly outweighed by its demand from ecosystem and biogeochemical modelers, worldwide. The bottleneck is in part due to the technical challenges associated with analysing microscopic organisms and partly due to the expense and logistical difficulties associated with oceanographic voyages. There is growing observational evidence that climate change is having measurable impacts on Southern Ocean sea ice dynamics and consequently on ecosystem structure and function. Enhancing our ability to predict the effects of climate change on Southern Ocean phytoplankton, and hence biogeochemical cycling and ecosystem structure and function, relies on the development of new phenotypic methods that will greatly improve the efficiency of microbial phenotypic data acquisition. Arming ourselves with knowledge of how phytoplankton communities may change, in terms of their community structure and biogeographical distributions, will enable better predictions of how ecosystems and elemental cycling will change in future. In turn, this will provide us an opportunity to alter management practices for industries such as fisheries (e.g. krill and fish) and tourism, which have the potential to increase pressure on systems already under strain.

To address this critical knowledge gap, this study was designed to investigate the phenotypic responses of ecologically important taxa of Southern Ocean diatoms to environmental conditions, including a range of salinity and temperature levels and the phenomenon of natural iron enrichment from upwelling along the Kerguelen Island and Plateau. In addition, FTIR microspectroscopy was chosen as the primary method for measuring phenotypic traits in order to assess the power of the technique to provide the necessary increase in both data acquisition efficiency and sensitivity to taxon-specific traits. FTIR microspectroscopy was selected because of its' capacity for high-throughput sample analysis, rapid analysis time, high spatial-resolution, multivariate output and cost-effectiveness. The key research questions posed by this thesis are summarised in Figure 5-1 while Table 5-1 identifies the sections of this thesis which address each question.

Figure 5-1 Key Research Questions (repeated from Chapter 1)

Southern Ocean microalgae show great resilience to environmental stress.

i. Is this resilience related to phenotypic plasticity?
ii. Are taxon-specific phenotypic changes related to observed biogeography?
iii. Do such changes in microalgal phenotypes have the potential to affect the Southern Ocean ecosystem and biogeochemical cycling?
iv. Do bulk-community phenotypic measurements reflect those of key taxa?

There is currently a bottleneck in the rate of acquisition of phenotypic data.

Can FTIR Spectroscopy be used to:

v. increase the efficiency and cost-effectiveness of phenotypic data collection?
vi. measure taxon-specific traits in phytoplankton?

Table 5-1 Key research findings summarized by thesis chapter

Ch.	Title and key findings	Research Questions addressed					
		i	ii	iii	iv	v	vi
2	***Phenotypic plasticity of Southern Ocean diatoms: key to success in the sea ice habitat?***						
	▪ Phenotypic plasticity is taxon-specific and related to observed biogeography	✓	✓	✓			
	▪ FTIR Spectroscopy revealed taxon-specific changes in macromolecular composition and intra-population variability					✓	✓
3	***Taxon-specific responses of Southern Ocean diatoms to Fe-enrichment revealed by FTIR microspectroscopy***						
	▪ FTIR Microspectroscopy revealed taxon-specific responses to iron availability in natural, mixed communities	✓	✓			✓	✓
	▪ Challenged commonly held view that Fe-limitation causes increased silicification in diatoms			✓			
	▪ First study to measure taxon-specific changes in macromolecular composition and intra-specific variability in natural, mixed Southern Ocean communities				✓	✓	✓
4	***Phytoplankton phenomics through FTIR spectroscopy: rapid, simultaneous estimation of multiple traits***						
	▪ Expanded the range of phytoplankton phenotypic traits successfully measured by FTIR spectroscopy to include cellular carbon and carbon productivity					✓	
	▪ First study to demonstrate a method of estimating a rate of carbon production using samples from a single time-point					✓	
	▪ Productivity and the caloric content of the biomass was ~50% lower in sea ice relative to pelagic treatment. This is consistent with observations that winter growth rates in Antarctic krill are half those in summer			✓			

This thesis demonstrates the appropriateness of FTIR microspectroscopy as a powerful phenomics tool. In particular, the technique makes possible the analysis of individual taxon within mixed populations and the measurement of multiple phenotypic traits simultaneously (Chapter 4). Further, the technique circumvents the need to sample and measure at multiple time-steps for rate measurements such as carbon productivity (Chapter 4) and growth rate (Jebsen et al. 2012). Given the time-intensive nature of carbon productivity measurements and the demand for them by biogeochemists and carbon cycle modelers, FTIR microspectroscopy could help advance this field of research by increasing the pace of data collection in addition to untangling bulk-community measurements from those of key taxa.

FTIR microspectroscopy makes possible the analysis of individual taxa through its capacity for single-cell analysis. This thesis, in addition to providing taxon-specific measurements of phenotypic traits, demonstrates how single-cell measurements made using FTIR microspectroscopy revealed differences in variability both within and between taxa. Such differences can be related to, for example, populations in transition from Fe- enrichment to Fe-limitation (Chapter 3), or to levels of phenotypic plasticity when comparing the responses of individual phytoplankton to changes in environmental conditions (Chapter 2). Further, increases in intra-specific variation have been tied to phytoplankton responses to environmental stressors, such as salinity, temperature (Chapter 2) and nutrient limitation (e.g. Chapter 3 and P. Heraud et al. 2008). This thesis suggests that phenotypic plasticity and intrapopulation variability are separate traits, where plasticity is characterised by a population shift from one phenotypic "state" to another, while intrapopulation variability is characterised by the level of variability between organisms (in this case, cells) whether within or between phenotypic "states". Given that FTIR microspectroscopic datasets can capture such a multitude of information at once, the technique provides great scope for accelerating the pace of phenotypic studies of microorganisms, including phytoplankton.

Chapter 3 presents a potentially controversial finding of this thesis in relation to the use of elemental ratios in oceanographic studies. According to the taxon-specific FTIR microspectroscopic data collected from samples of phytoplankton found blooming near the Kerguelen Island and Plateau, cells from naturally Fe-enriched regions were higher in silicate than those from Fe-limited regions. At first this finding seemed to contradict previous studies, which widely showed increasing ratios of silica to carbon under Fe-limitation. Upon further investigation however, it became apparent that the few studies which presented absolute values for elemental quotas in phytoplankton had indeed measured an increase in silica levels in phytoplankton cells under Fe-enrichment. This highlights that the use of elemental ratios should

be approached with caution, given that differential rates of change in the numerator and denominator can lead to counter-intuitive results. For example, the ratio of Si/C can decrease in response to increases in both Si and C, so long as the increase in Si is of a lower magnitude than that of C. Thus, the causes of changes in elemental ratios should be carefully considered as part of biogeochemical studies.

Although this thesis does not focus specifically on the policy and legislative implications of phytoplankton research, a brief explanation of the link between such research and management of resources in the Southern Ocean is warranted. As previously mentioned, investing in research which improves our understanding of the Southern Ocean ecosystem and biogeochemical cycling is critical to managing our use of this precious resource. Although the Southern Ocean ecosystem is the most productive ecosystem on Earth, as an ice-dependent system it is also highly vulnerable to warming temperatures. Krill is the largest fishery in the Southern Ocean, with precautionary catch limits currently set to ~5 million tonnes per year across the South Atlantic, south-east Indian and south-west Indian Oceans (Croxall & Nicol 2004). Ideally, catch limits would be responsive to fluctuations in krill reproductive and larval success, which are currently not well understood but known to be related to changes in microalgal primary production and the seasonal duration and extent of sea ice. Hence studies which can improve understanding of the sea ice-phytoplankton-krill system could be used to improve management of the Southern Ocean krill fishery.

Previous studies which have tried to use phytoplankton productivity to predict fisheries yields have had some success (e.g. Friedland et al. 2012), however the complex relationships between trophic levels still presents a great challenge to this field of research. Studies of ecosystem stoichiometry have shown that differences in stoichiometry of biomass between trophic levels can substantially influence the trophic transfer efficiency of elements and energy (Andersen et al. 2004). Moreover, the taxon-specific changes in macromolecular composition revealed in this thesis suggest that changes in the community structure of phytoplankton (for example, taxonomic shifts throughout a bloom period) could affect both the efficiency of grazing and the elemental stoichiometry of the phytoplankton biomass. Taxon-specific macromolecular and elemental data may thus improve understanding of the link between primary production and fisheries yields.

Given the complex interactions between phytoplankton, environmental conditions and ecosystem structure and function, future phytoplankton research should aim to increase the collection of phenotypic data from natural, mixed populations. Portable spectroscopic instruments are becoming cheaper and more powerful, making their use on oceanographic voyages a real possibility. Theoretically, utilising spectroscopic instruments *in situ* would enable the collection

of data in real-time and thus the conduct of sampling designs that are flexible and responsive to preliminary results acquired during sampling. Such methods could improve the efficiency of data collection by increasing the effectiveness of sampling designs by making use of highly portable "spectrometer in a suitcase" systems, which are currently available for both Raman and FTIR spectroscopy. Further, the now commonplace use of focal plane array detectors, which can take thousands of spectral measurements at a time, will drastically increase the speed of data acquisition back at the laboratory. In summary, this thesis highlights how FTIR spectroscopy presents us with an exciting opportunity to move phenotypic studies towards truly high-throughput, high dimensional phenotyping – or *Phenomics*.

References

Agrawal, A.A., 2001. Phenotypic Plasticity in the Interactions and Evolution of Species. *Science*, 294(5541), pp.321–326. Available at: http://www.sciencemag.org/content/294/5541/321.abstract.

Almandoz, G.O. et al., 2008. Distribution and ecology of Pseudo-nitzschia species (Bacillariophyceae) in surface waters of the Weddell Sea (Antarctica). *Polar Biology*, 31(4), pp.429–442. Available at: http://dx.doi.org/10.1007/s00300-007-0369-9.

Andersen, T., Elser, J.J. & Hessen, D.O., 2004. Stoichiometry and population dynamics. *Ecology Letters*, 7(9), pp.884–900. Available at: http://dx.doi.org/10.1111/j.1461-0248.2004.00646.x.

Andreeva, A. & Velitchkova, M., 2005. Resonance Raman spectroscopy of carotenoids in Photosystem I particles. *Biophysical Chemistry*, 114(2-3), pp.129–135. Available at: http://www.sciencedirect.com/science/article/B6TFB-4F085D3-1/2/579f21cfb470c48d6c8cc4ca0de17e73.

Armand, L.K. et al., 2005. The biogeography of major diatom taxa in Southern Ocean sediments: 1. Sea ice related species. *Palaeogeography, Palaeoclimatology, Palaeoecology*, 223(1–2), pp.93–126. Available at: http://www.sciencedirect.com/science/article/pii/S003101820500163X.

Armbrust, E.V., 2009. The life of diatoms in the world's oceans. *Nature*, 459(7244), pp.185–192. Available at: http://dx.doi.org/10.1038/nature08057.

Arrigo, K.R., 2005. Marine microorganisms and global nutrient cycles. *Nature*, 437(7057), pp.349–355. Available at: <Go to ISI>://000231849100041.

Arrigo, K.R., 2012. Massive Phytoplankton Blooms Under Arctic Sea Ice. *Science*, 336, p.1408. Available at: http://chishr09lsap.hosted.exlibrisgroup.com:9003/monash2?sid=google&auinit=KR&aulast=Arrigo&atitle=Massive Phytoplankton Blooms Under Arctic Sea Ice&id=doi:10.1126/science.1215065&title=Science&volume=336&issue=6087&date=2012&spage=1408&issn=0036-8075.

Arrigo, K.R. & Thomas, D.N., 2004. Large scale importance of sea ice biology in the Southern Ocean. *Antarctic Science*, 16(4), pp.471–486. Available at: <Go to ISI>://000226060800009.

Assmy, P. & Smetacek, V., 2009. Algal Blooms. In M. Schaechter, ed. *Encyclopedia of Microbiology*. Oxford: Academic Press, pp. 27–41. Available at: http://www.sciencedirect.com/science/article/pii/B9780123739445000018.

Atkinson, A. et al., 2004. Long-term decline in krill stock and increase in salps within the Southern Ocean. *Nature*, 432(7013), pp.100–103. Available at: http://dx.doi.org/10.1038/nature02996.

Barbarino, E. & Lourenço, S.O., 2005. An evaluation of methods for extraction and quantification of protein from marine macro- and microalgae. *Journal of Applied Phycology*, 17(5), pp.447–460. Available at: http://www.springerlink.com/index/10.1007/s10811-005-1641-4 [Accessed October 27, 2012].

Barker, M. & Rayens, W., 2003. Partial least squares for discrimination. *Journal of Chemometrics*, 17(3), pp.166–173. Available at: http://doi.wiley.com/10.1002/cem.785 [Accessed September 23, 2013].

Barth, A., 2000. The infrared absorption of amino acid side chains. *Progress in biophysics and molecular biology*, 74(2000), pp.141–173. Available at: http://www.sciencedirect.com/science/article/pii/S0079610700000213 [Accessed June 12, 2013].

Bassan, P. et al., 2009. Resonant Mie scattering in infrared spectroscopy of biological materials - understanding the “dispersion artefact.” *Analyst*, 134(8), pp.1586–1593. Available at: <Go to ISI>://WOS:000268131500011.

Bassan, P. et al., 2013. The inherent problem of transflection-mode infrared spectroscopic microscopy and the ramifications for biomedical single point and imaging applications. *Analyst*, 138(1), pp.144–157. Available at: http://dx.doi.org/10.1039/C2AN36090J.

Bayer-Giraldi, M. et al., 2010. Antifreeze proteins in polar sea ice diatoms: diversity and gene expression in the genus Fragilariopsis. *Environmental Microbiology*, 12(4), pp.1041–1052. Available at: <Go to ISI>://WOS:000277029900018.

Benning, L.G. et al., 2004. Molecular characterization of cyanobacterial silicification using synchrotron infrared micro-spectroscopy. *Geochimica Et Cosmochimica Acta*, 68(4), pp.729–741. Available at: <Go to ISI>://WOS:000188882500004.

Bernard, K.S., Steinberg, D.K. & Schofield, O.M.E., 2012. Summertime grazing impact of the dominant macrozooplankton off the Western Antarctic Peninsula. *Deep Sea Research Part I: Oceanographic Research Papers*, 62, pp.111–122. Available at: http://linkinghub.elsevier.com/retrieve/pii/S0967063712000052 [Accessed December 16, 2013].

Blain, S. et al., 2014. Distributions and stoichiometry of dissolved nitrogen and phosphorus in the iron fertilized region near Kerguelen (Southern Ocean). *Biogeosciences*, (KEOPS2 Special Issue).

Blain, S. et al., 2007. Effect of natural iron fertilization on carbon sequestration in the Southern Ocean. *Nature*, 446(7139), pp.1070–4. Available at: http://www.ncbi.nlm.nih.gov/pubmed/17460670 [Accessed August 8, 2013].

Blain, S. et al., 2014. The natural iron fertilization experiment KEOPS 2 (KErguelen Ocean and Plateau compared Study 2): An overview. *Biogeosciences*, (KEOPS2 Special Issue).

Bowie, A.R. et al., 2014. Iron budgets for three distinct biogeochemical sites around the Kerguelen plateau (Southern Ocean) during the natural fertilization experiment KEOPS-2. *Biogeosciences*, (KEOPS2 Special Issue).

Boyd, P.W. et al., 2010. Environmental control of open-ocean phytoplankton groups: Now and in the future. *Limnology and Oceanography*, 55(3), pp.1353–1376. Available at: http://www.scopus.com/inward/record.url?eid=2-s2.0-77954231948&partnerID=40&md5=8e3d27464fbb5ef412253c3cd47928ce.

Brandstetter, M. et al., 2010. Tunable external cavity quantum cascade laser for the simultaneous determination of glucose and lactate in aqueous phase. *The Analyst*, 135(12), pp.3260–5. Available at: http://www.ncbi.nlm.nih.gov/pubmed/21046025 [Accessed July 29, 2014].

Brzezinski, M.A. et al., 2011. Co-limitation of diatoms by iron and silicic acid in the equatorial Pacific. *Deep Sea Research Part II: Topical Studies in Oceanography*, 58(3-4), pp.493–511.

Available at: http://www.sciencedirect.com/science/article/pii/S0967064510002225 [Accessed January 1, 2015].

Busalacchi, A.J., 2004. The role of the Southern Ocean in global processes: an earth system science approach. *Antarctic Science*, 16(04), pp.363–368. Available at: http://journals.cambridge.org/action/displayAbstract?fromPage=online&aid=265059&fulltextType=RA&fileId=S0954102004002196.

Bylesjö, M. et al., 2006. OPLS discriminant analysis: combining the strengths of PLSDA and SIMCA classification. *Journal of chemometrics*, 20(810), pp.341–351. Available at: http://chishr09lsap.hosted.exlibrisgroup.com:9003/monash2?sid=google&auinit=M&aulast=Bylesj&atitle=OPLS discriminant analysis: combining the strengths of PLS?DA and SIMCA classification&id=doi:10.1002/cem.1006&title=Journal of chemometrics&volume=20&issue=8?10&date=2006&spage=341&issn=0886-9383.

Cao, J. et al., 2013. Fourier transform infrared microspectroscopy reveals that tissue culture conditions affect the macromolecular phenotype of human embryonic stem cells. *The Analyst*, 138(14), pp.4147–60. Available at: http://www.ncbi.nlm.nih.gov/pubmed/23745179 [Accessed January 28, 2014].

Carr, M.-E. et al., 2006. A comparison of global estimates of marine primary production from ocean color. *Deep Sea Research Part II: Topical Studies in Oceanography*, 53(5-7), pp.741–770. Available at: http://www.sciencedirect.com/science/article/B6VGC-4K1X5GH-1/2/3608867914ae399460737d622b786faa.

Charmantier, A. et al., 2008. Adaptive phenotypic plasticity in response to climate change in a wild bird population. *Science (New York, N.Y.)*, 320(5877), pp.800–3. Available at: http://dx.doi.org/10.1126/science.1157174 [Accessed January 20, 2014].

Closset, I. et al., 2014. Seasonal evolution of net and regenerated silica production around a natural Fe-fertilized area in the Southern Ocean estimated from Si isotopic approaches. *Biogeosciences Discussions*, 11(5), pp.6329–6381. Available at: http://www.biogeosciences-discuss.net/11/6329/2014/ [Accessed July 25, 2014].

Cochlan, W.P., Bronk, D.A. & Coale, K.H., 2000. Trace metals and nitrogenous nutrition of Antarctic phytoplankton: experimental observations in the Ross Sea. In Brest, France, pp. 3365–3390. Available at: <Go to ISI>://000176691300016.

Croxall, J.P. & Nicol, S., 2004. Management of Southern Ocean fisheries: global forces and future sustainability. *Antarctic Science*, 16(4), pp.569–584. Available at: http://www.journals.cambridge.org/abstract_S0954102004002330 [Accessed June 10, 2013].

Dean, A., Estrada, B., et al., 2008. Molecular response of Anabaena flos-aquae to differing concentrations of phosphorus: A combined Fourier transform infrared and X-ray microanalytical study. *Phycological Research*, 56(3), pp.193–201. Available at: http://dx.doi.org/10.1111/j.1440-1835.2008.00501.x.

Dean, A. et al., 2010. Using FTIR spectroscopy for rapid determination of lipid accumulation in response to nitrogen limitation in freshwater microalgae. *Bioresource Technology*, 101(12), pp.4499–4507. Available at: http://www.sciencedirect.com/science/article/B6V24-4YC8RBM-3/2/0a977e59c4ab6920a4900cddfeb74c11.

Dean, A., Nicholson, J. & Sigee, D., 2012. Changing patterns of carbon allocation in lake phytoplankton: an FTIR analysis. *Hydrobiologia*, 684(1), pp.109–127. Available at: http://dx.doi.org/10.1007/s10750-011-0973-0.

Dean, A., Nicholson, J. & Sigee, D., 2008. Impact of phosphorus quota and growth phase on carbon allocation in Chlamydomonas reinhardtii: an FTIR microspectroscopy study. *European Journal of Phycology*, 43(4), pp.345–354. Available at: http://www.informaworld.com/10.1080/09670260801979287.

Devos, N. et al., 1998. RUBISCO adaptation to low temperatures: a comparative study in psychrophilic and mesophilic unicellular algae. *Journal of Phycology*, 34(4), pp.655–660. Available at: http://dx.doi.org/10.1046/j.1529-8817.1998.340655.x.

Diekmann, A.B.S. et al., 2009a. Variation in diatom biochemical composition during a simulated bloom and its effect on copepod production. *Journal of Plankton Research*, 31(11), pp.1391–1405. Available at: <Go to ISI>://000270710900010.

Diekmann, A.B.S. et al., 2009b. Variation in diatom biochemical composition during a simulated bloom and its effect on copepod production. *Journal of Plankton Research*, 31(11), pp.1391–1405. Available at: <Go to ISI>://000270710900010.

Domenighini, A. & Giordano, M., 2009. Fourier Transform Infrared Spectroscopy of microalgae as a novel tool for biodiversity studies, species identification, and the asssessment of water quality. *Journal of Phycology*, 45(2), pp.522–531. Available at: <Go to ISI>://000264959600021.

Ducklow, H.W. et al., 2007. Marine pelagic ecosystems: the West Antarctic Peninsula. *Philosophical Transactions of the Royal Society B: Biological Sciences*, 362(1477), pp.67–94. Available at: http://rstb.royalsocietypublishing.org/content/362/1477/67.abstract.

Ducklow, H.W. et al., 2013. West Antarctic Peninsula: An ice-dependent coastal marine ecosystem in transition. *Oceanography*, 26(3), pp.190–203.

Eicken, H. et al., 2000. Magnetic resonance imaging of sea-ice pore fluids: methods and thermal evolution of pore microstructure. *Cold Regions Science and Technology*, 31(3), pp.207–225. Available at: http://linkinghub.elsevier.com/retrieve/pii/S0165232X00000161.

El-Sayed, S.Z., 2005. History and evolution of primary productivity studies of the Southern Ocean. *Polar Biology*, 28(6), pp.423–438. Available at: <Go to ISI>://000229110300001.

Fahl, K. & Kattner, G., 1993. Lipid content and fatty acid composition of algal communities in sea-ice and water from the Weddell Sea (Antarctica). *Polar Biology*, 13(6), pp.405–409. Available at: http://dx.doi.org/10.1007/BF01681982.

Falkowski, P.G., Barber, R.T. & Smetacek, V., 1998. Biogeochemical Controls and Feedbacks on Ocean Primary Production. *Science*, 281(5374), pp.200–206. Available at: http://www.sciencemag.org/cgi/content/abstract/281/5374/200.

Falk-Petersen, S. et al., 1998. Lipids and fatty acids in ice algae and phytoplankton from the Marginal Ice Zone in the Barents Sea. *Polar Biology*, 20(1), pp.41–47.

Fernandez, C. et al., 2005. An estimation of annual new production and carbon fluxes in the northeast Atlantic Ocean during 2001. *J. Geophys. Res.*, 110(C07S13). Available at: http://dx.doi.org/10.1029/2004JC002616.

Field, C.B. et al., 1998. Primary Production of the Biosphere: Integrating Terrestrial and Oceanic Components. *Science*, 281(5374), pp.237–240. Available at: http://www.sciencemag.org/cgi/doi/10.1126/science.281.5374.237 [Accessed May 21, 2013].

Filik, J. et al., 2012. Electric field standing wave artefacts in FTIR micro-spectroscopy of biological materials. *Analyst*, 137(4), pp.853–861. Available at: http://dx.doi.org/10.1039/C2AN15995C.

Finkel, Z. V et al., 2010. Phytoplankton in a changing world: Cell size and elemental stoichiometry. *Journal of Plankton Research*, 32(1), pp.119–137. Available at: http://www.scopus.com/inward/record.url?eid=2-s2.0-71949084247&partnerID=40&md5=86ad9e52ecfa55ac3fd9672b1c122125.

Flynn, K.J. et al., 2012. Changes in pH at the exterior surface of plankton with ocean acidification. *Nature Climate Change*, 2(7), pp.510–513. Available at: http://dx.doi.org/10.1038/nclimate1489.

Friedland, K.D. et al., 2012. Pathways between Primary Production and Fisheries Yields of Large Marine Ecosystems. *PLoS ONE*, 7(1), p.e28945. Available at: http://dx.doi.org/10.1371/journal.pone.0028945.

Geider, R.J. & La Roche, J., 2002. Redfield revisited: variability of C : N : P in marine microalgae and its biochemical basis. *European Journal of Phycology*, 37(1), pp.1–17. Available at: <Go to ISI>://000174629800001.

Giordano, M. et al., 2001. Fourier transform infrared spectroscopy as a novel tool to investigate changes in intracellular macromolecular pools in the marine microalga Chaetoceros muellerii (Bacillariophyceae). *Journal of Phycology*, 37(2), pp.271–279. Available at: <Go to ISI>://000168389200010.

Giordano, M., Ratti, S. & Domenighini, A., 2009. Spectroscopic classification of 14 different microalga species: first steps towards spectroscopic measurement of phytoplankton biodiversity. *Plant Ecology & Diversity*, 2(2), pp.155–164. Available at: http://www.tandfonline.com/doi/abs/10.1080/17550870903353088.

Graff, J.R., Milligan, A.J. & Behrenfeld, M.J., 2012. The measurement of phytoplankton biomass using flow-cytometric sorting and elemental analysis of carbon. *Limnology and Oceanography: Methods*, 10(Banse 1977), pp.910–920. Available at: http://www.aslo.org/lomethods/free/2012/0910.html [Accessed August 10, 2014].

Green, J., Bohannan, B. & Whitaker, R., 2008. Microbial biogeography: from taxonomy to traits. *Science*, 320(5879), pp.1039–1043. Available at: http://dx.doi.org/10.1126/science.1153475.

Guillard, R.R.L. & Ryther, J.H., 1962. Studies of marine olanktonic diatoms: I. Cyclotella nana Hustedt, and Detonula confervacea (Cleve) gran. *Canadian Journal of Microbiology*, 8(2), pp.229–239. Available at: http://dx.doi.org/10.1139/m62-029.

Gwak, I. et al., 2010. Antifreeze Protein in Antarctic Marine Diatom, Chaetoceros neogracile. *Marine Biotechnology*, 12(6), pp.630–639. Available at: http://dx.doi.org/10.1007/s10126-009-9250-x.

Hama, T. et al., 1983. Measurement of Photosynthetic Production of a Marine Phytoplankton Population Using a Stable 13C Isotope. *Marine Biology*, 73(1), pp.31–36. Available at: <Go to ISI>://WOS:A1983QK35200004.

Hasle, G.R. & Syvertsen, E.E., 1997. Marine Diatoms. In C. R. Tomas, ed. *Identifying marine phytoplankton*. New York: Academic Press, pp. 5–361.

Heraud, P., Beardall, J., et al., 2007. In vivo prediction of the nutrient status of individual microalgal cells using Raman microspectroscopy. *Fems Microbiology Letters*, 275(1), pp.24–30. Available at: http://dx.doi.org/10.1111/j.1574-6968.2007.00861.x.

Heraud, P. et al., 2008. Intercolonial variability in macromolecular composition in P-starved and P-replete Scenedesmus populations revealed by infrared microscopy. *Journal of Phycology*, 44(5), pp.1335–1339. Available at: http://dx.doi.org/10.1111/j.1529-8817.2008.00564.x.

Heraud, P. et al., 2008. Intercolonial variability in macromolecular composition in P-starved and P-replete Scenedesmus populations revealed by infrared microscopy. *Journal of Phycology*, 44(5), pp.1335–1339. Available at: http://dx.doi.org/10.1111/j.1529-8817.2008.00564.x.

Heraud, P. et al., 2005. Mapping of nutrient-induced biochemical changes in living algal cells using synchrotron infrared microspectroscopy. *FEMS microbiology letters*, 249(2), pp.219–25. Available at: http://www.ncbi.nlm.nih.gov/pubmed/16006070 [Accessed March 2, 2011].

Heraud, P., Wood, B., et al., 2007. Probing the influence of the environment on microalgae using infrared and raman spectroscopy. In K. Kneipp et al., eds. *New Approaches in Biomedical Spectroscopy*. American Chemical Society, Washington, DC, ETATS-UNIS (1974) (Revue), pp. 85–106. Available at: http://cat.inist.fr/?aModele=afficheN&cpsidt=18976319.

Heraud, P. & Wood, B., 2013. Editorial - the latest thinking and developments in optical diagnosis. *The Analyst*, 138(14), pp.3861–2. Available at: http://www.ncbi.nlm.nih.gov/pubmed/23757481 [Accessed June 19, 2013].

Hessen, D.O. et al., 2004. Carbon Sequestration in Ecosystems: The Role of Stoichiometry. *Ecology*, 85(5), pp.1179–1192. Available at: http://www.jstor.org/stable/3450161.

Hirschmugl, C.J. et al., 2005. Analysis of the nutritional status of algae by Fourier transform infrared chemical imaging. *Infrared Physics & Technology*, 49(1-2), pp.57–63.

Hoffmann, L.J., Peeken, I. & Lochte, K., 2007. Effects of iron on the elemental stoichiometry during EIFEX and in the diatoms Fragilariopsis kerguelensis and Chaetoceros dichaeta. *Biogeosciences*, 4(4), pp.569–579. Available at: <Go to ISI>://000249046600009.

Holmes, D., Moody, P. & Dine, D., 2010. Hypothesis testing: do my samples come from the same population? Non-parametric data. In *Research methods for the biosciences*. Oxford University Press, p. 488. Available at: http://ukcatalogue.oup.com/product/9780199545766.do.

Horner, R. et al., 1992. Ecology of sea ice biota 1. Habitat, Terminology and Methodology. *Polar Biology*, 12(3-4), pp.417–427. Available at: <Go to ISI>://WOS:A1992JP99800010.

Houle, D., Govindaraju, D.R. & Omholt, S., 2010. Phenomics: the next challenge. *Nature reviews. Genetics*, 11(12), pp.855–66. Available at: http://www.ncbi.nlm.nih.gov/pubmed/21085204 [Accessed October 28, 2012].

Ingall, E.D. et al., 2013. Role of biogenic silica in the removal of iron from the Antarctic seas. *Nature Communications*, 4, p.1981. Available at: http://search.proquest.com/docview/1366360256?accountid=12528.

Jacquet, S.H.M. et al., 2014. Variability of mesopelagic organic carbon mineralization efficiency in the naturally ion-fertilized Kerguelen area. *Biogeosciences*, (KEOPS2 Special Issue).

Jakob, T. et al., 2007. A complete energy balance from photons to new biomass reveals a light- and nutrient-dependent variability in the metabolic costs of carbon assimilation. *Journal of Experimental Botany*, 58(8), pp.2101–2112.

Jebsen, C. et al., 2012. FTIR spectra of algal species can be used as physiological fingerprints to assess their actual growth potential. *Physiologia plantarum*, 146(4), pp.427–38. Available at: http://www.ncbi.nlm.nih.gov/pubmed/22540209 [Accessed June 4, 2014].

Jungandreas, A., Wagner, H. & Wilhelm, C., 2012. Simultaneous measurement of the silicon content and physiological parameters by FTIR spectroscopy in diatoms with siliceous cell walls. *Plant and Cell Physiology*, 53(12), pp.2153–2162.

Kansiz, M. et al., 1999. Fourier transform infrared microspectroscopy and chemometrics as a tool for the discrimination of cyanobacterial strains. *Phytochemistry*, 52(3), pp.407–417. Available at: http://dx.doi.org/10.1016/S0031-9422(99)00212-5.

Krell, A. et al., 2008. A new class of ice-binding proteins discovered in a salt-stress-induced cDNA library of the psychrophilic diatom Fragilariopsis cylindrus (Bacillariophyceae). *European Journal of Phycology*, 43(4), pp.423–433. Available at: http://www.informaworld.com/10.1080/09670260802348615.

Kroon, B.M.A. & Thoms, S., 2006. From electron to biomass: a mechanistic model to describe phytoplankton photosynthesis and steady-state growth rates. *Journal of Phycology*, 42(3), pp.593–609. Available at: 10.1111/j.1529-8817.2006.00221.x.

Laskowski, R.A., 2001. PDBsum: summaries and analyses of PDB structures. *Nucleic Acids Research* , 29 (1), pp.221–222. Available at: http://nar.oxfordjournals.org/content/29/1/221.abstract.

Laws, E.A., 1991. Photosynthetic quotients, new production and net community production in the open ocean. *Deep Sea Research Part A. Oceanographic Research Papers*, 38(1), pp.143–167. Available at: http://www.sciencedirect.com/science/article/pii/019801499190059O.

Lee, J.-Y. et al., 2010. Comparison of several methods for effective lipid extraction from microalgae. *Bioresource technology*, (1), pp.S75–7. Available at: http://www.ncbi.nlm.nih.gov/pubmed/19386486 [Accessed January 22, 2014].

Lee, S.H., Whitledge, T.E. & Kang, S.-H., 2008. Spring time production of bottom ice algae in the landfast sea ice zone at Barrow, Alaska. *Journal of Experimental Marine Biology and Ecology*, 367(2), pp.204–212. Available at: http://www.sciencedirect.com/science/article/B6T8F-4TW9WHW-2/2/86cc2bd5d7567b73c8e22df5272148b7.

Li, M. et al., 2012. Rapid resonance Raman microspectroscopy to probe carbon dioxide fixation by single cells in microbial communities. *The ISME journal*, 6(4), pp.875–85. Available at: http://www.pubmedcentral.nih.gov/articlerender.fcgi?artid=3309358&tool=pmcentrez&rendertype=abstract [Accessed June 24, 2014].

Litchman, E. & Klausmeier, C. a., 2008. Trait-Based Community Ecology of Phytoplankton. *Annual Review of Ecology, Evolution, and Systematics*, 39(1), pp.615–639. Available at: http://www.annualreviews.org/doi/abs/10.1146/annurev.ecolsys.39.110707.173549 [Accessed October 17, 2013].

Lizotte, M.P., 2001. The contributions of sea ice algae to Antarctic marine primary production. *American Zoologist*, 41(1), pp.57–73. Available at: http://icb.oxfordjournals.org/content/41/1/57.short.

Lohrenz, S.E. & Taylor, C.D., 1987. Primary production of protein: I. Comparison of net cellular carbon and protein synthesis with 14c-derived rate estimates in steady-state cultures of marine phytoplankton. *Mar Ecol Prog Ser*, 35, pp.277–292.

Long, J.D. & Hay, M.E., 2006. When intraspecific exceeds interspecific variance: Effects of phytoplankton morphology and growth phase on copepod feeding and fitness. *Limnology and Oceanography*, 51(2), pp.988–996. Available at: <Go to ISI>://000236343600018.

Lourenço, S.O. et al., 2004. Distribution of intracellular nitrogen in marine microalgae: Calculation of new nitrogen-to-protein conversion factors. *European Journal of Phycology*, 39(1), pp.17–32. Available at: http://www.tandfonline.com/doi/abs/10.1080/0967026032000157156 [Accessed May 22, 2013].

MacLeod, N., Benfield, M. & Culverhouse, P., 2010. Time to automate identification. *Nature*, 467(7312), pp.154–155. Available at: http://dx.doi.org/10.1038/467154a.

Marchetti, A. et al., 2010. Iron and silicic acid effects on phytoplankton productivity, diversity, and chemical composition in the central equatorial Pacific Ocean. *Limnology and Oceanography*, 55(1), pp.11–29. Available at: http://www.aslo.org/lo/toc/vol_55/issue_1/0011.html.

Marchetti, A. & Cassar, N., 2009. Diatom elemental and morphological changes in response to iron limitation: a brief review with potential paleoceanographic applications. *Geobiology*, 7(4), pp.419–31. Available at: http://www.ncbi.nlm.nih.gov/pubmed/19659798 [Accessed May 31, 2013].

Marchetti, A. & Harrison, P.J., 2007. Coupled changes in the cell morphology and elemental (C, N, and Si) composition of the pennate diatom Pseudo-nitzschia due to iron deficiency. *Limnology and Oceanography*, 52(5), pp.2270–2284. Available at: http://doi.wiley.com/10.4319/lo.2007.52.5.2270.

Martin-Jézéquel, V. et al., 2000. Review of silicon metabolism in diatoms: implications for growth. *Journal of Phycology*, 840(February), pp.821–840.

McMinn, A. et al., 2007. Spring sea ice photosynthesis, primary productivity and biomass distribution in eastern Antarctica, 2002-2004. *Marine Biology*, 151(3), pp.985–995. Available at: <Go to ISI>://WOS:000246098900015.

Meyer, B., 2011. The overwintering of Antarctic krill, Euphausia superba, from an ecophysiological perspective. *Polar Biology*, 35(1), pp.15–37. Available at: http://link.springer.com/10.1007/s00300-011-1120-0 [Accessed June 11, 2013].

Miller, L.M. & Smith, R.J., 2005. Synchrotrons versus globars, point-detectors versus focal plane arrays: Selecting the best source and detector for specific infrared microspectroscopy and

imaging applications. *Vibrational Spectroscopy*, 38(1-2), pp.237–240. Available at: http://linkinghub.elsevier.com/retrieve/pii/S0924203105000676 [Accessed January 24, 2014].

Mock, T. & Hoch, N., 2005. Long-term temperature acclimation of photosynthesis in steady-state cultures of the polar diatom Fragilariopsis cylindrus. *Photosynthesis Research*, 85(3), pp.307–317. Available at: <Go to ISI>://WOS:000231949800004.

Mock, T., Junge, K. & Seckbach, J., 2007. Psychrophilic Diatoms. In J. Seckbach, ed. *Algae and Cyanobacteria in Extreme Environments*. Springer Netherlands, pp. 343–364. Available at: http://dx.doi.org/10.1007/978-1-4020-6112-7_18.

Mock, T. & Kroon, B.M.A., 2002a. Photosynthetic energy conversion under extreme conditions - I: important role of lipids as structural modulators and energy sink under N-limited growth in Antarctic sea ice diatoms. *Phytochemistry*, 61(1), pp.41–51. Available at: <Go to ISI>://WOS:000178189500007.

Mock, T. & Kroon, B.M.A., 2002b. Photosynthetic energy conversion under extreme conditions - II: the significance of lipids under light limited growth in Antarctic sea ice diatoms. *Phytochemistry*, 61(1), pp.53–60. Available at: <Go to ISI>://WOS:000178189500008.

Mock, T. & Thomas, D.N., 2005. Recent advances in sea-ice microbiology. *Environmental Microbiology*, 7(5), pp.605–619. Available at: 10.1111/j.1462-2920.2005.00781.x.

Mock, T. & Valentin, K., 2004. Photosynthesis and Cold Acclimation: Molecular Evidence From a Polar Diatom. *Journal of Phycology*, 40(4), pp.732–741. Available at: http://doi.wiley.com/10.1111/j.1529-8817.2004.03224.x [Accessed March 7, 2011].

Montechiaro, F. et al., 2006. Homeostasis of cell composition during prolonged darkness. *Plant Cell and Environment*, 29(12), pp.2198–2204. Available at: <Go to ISI>://WOS:000241739000008.

Mora, C. et al., 2009. Management Effectiveness of the World's Marine Fisheries. *PLoS Biol*, 7(6), p.e1000131. Available at: http://dx.doi.org/10.1371/journal.pbio.1000131.

Morgan-Kiss, R.M. et al., 2006. Adaptation and acclimation of photosynthetic microorganisms to permanently cold environments. *Microbiology and Molecular Biology Reviews*, 70(1), pp.222–252. Available at: <Go to ISI>://000236410100008.

Mukhopadhyay, R., 2004. Portable FTIR spectrometers get moving. *Analytical chemistry*, 76(19), p.369A–372A. Available at: http://www.ncbi.nlm.nih.gov/pubmed/15487052.

Murdock, J.N., Dodds, W.K. & Wetzel, D.L., 2008. Subcellular localized chemical imaging of benthic algal nutritional content via HgCdTe array FT-IR. *Vibrational Spectroscopy*, 48(2), pp.179–188. Available at: http://www.sciencedirect.com/science/article/B6THW-4RGFCY1-1/2/f5ee6fb7a2f4e90d2f1546684dbe7fd2.

Murdock, J.N. & Wetzel, D.L., 2009. FT-IR Microspectroscopy Enhances Biological and Ecological Analysis of Algae. *Applied Spectroscopy Reviews*, 44(4), pp.335–361. Available at: http://www.informaworld.com/10.1080/05704920902907440.

Naumann, D., 2000. Infrared Spectroscopy in Microbiology. In R. A. Meyers, ed. *Encyclopedia of Analytical Chemistry*. pp. 102–131.

Naumann, D., Helm, D. & Labischinski, H., 1991. Microbiological characterisations by FT-IR spectroscopy. *Nature*, 351(7a0052f4-e298-4dc2-918b-6fcbeea18c3a), pp.81–82. Available at: <Go to ISI>://WOS:A1991FK19300066.

Nelson, D.M. et al., 1995. Production and dissolution of biogenic silica in the ocean: Revised global estimates, comparison with regional data and relationship to biogenic sedimentation. *Global Biogeochemical Cycles*, 9(3), pp.359–372. Available at: http://dx.doi.org/10.1029/95GB01070.

Ngo-Thi, N., Kirschner, C. & Naumann, D., 2003. Characterization and identification of microorganisms by FT-IR microspectrometry. *Journal of Molecular Structure*, 661, pp.371–380. Available at: http://dx.doi.org/10.1016/j.molstruc.2003.08.012.

Nichols, P.D. et al., 1989. Changes in the lipid composition of Antarctic sea-ice diatom communities during a spring bloom: an indication of community physiological status. *Antarctic Science*, 1(02), pp.133–140. Available at: http://journals.cambridge.org/action/displayAbstract?fromPage=online&aid=223201&fulltextType=RA&fileId=S0954102089000209.

Nunn, B.L. et al., 2013. Diatom proteomics reveals unique acclimation strategies to mitigate fe limitation. *PloS one*, 8(10), p.e75653. Available at: http://www.pubmedcentral.nih.gov/articlerender.fcgi?artid=3797725&tool=pmcentrez&rendertype=abstract [Accessed October 30, 2013].

Van Oijen, T. et al., 2004. Light rather than iron controls photosynthate production and allocation in Southern Ocean phytoplankton populations during austral autumn. *Journal of Plankton Research*, 26(8), pp.885–900. Available at: <Go to ISI>://000223144400006.

Pankowski, A. & McMinn, A., 2009. Iron availability regulates growth, photosynthesis, and production of ferredoxin and flavodoxin in Antarctic sea ice diatoms. *Aquatic Biology*, 4(3), pp.273–288. Available at: <Go to ISI>://000263642500007.

Patel, S.A. et al., 2008. Spatial metabolic fingerprinting using FT-IR spectroscopy: investigating abiotic stresses on Micrasterias hardyi. *Analyst*, 133(12), pp.1707–1713. Available at: <Go to ISI>://000261005100009.

Petrou, K., Doblin, M. & Ralph, P., 2011. Heterogeneity in the photoprotective capacity of three Antarctic diatoms during short-term changes in salinity and temperature. *Marine biology*, 158(5), pp.1029–1041. Available at: http://dx.doi.org/10.1007/s00227-011-1628-4.

Petrou, K. & Ralph, P.J., 2011. Photosynthesis and net primary productivity in three Antarctic diatoms: possible significance for their distribution in the Antarctic marine ecosystem. *MEPS*, 437, pp.27–40.

Pollard, R.T. et al., 2009. Southern Ocean deep-water carbon export enhanced by natural iron fertilization. *Nature*, 457(7229), pp.577–580. Available at: http://dx.doi.org/10.1038/nature07716.

Quéguiner, B., Blain, S. & Trull, T., 2007. High primary production and vertical export of carbon over the Kerguelen Plateau as a consequence of natural iron fertilization in a high-nutrient, low-chlorophyll environment. In G. Duhamel & D. Welsford, eds. *The Kerguelen Plateau: marine ecosystem and fisheries, Proceedings of the 1st international Science Symposium on the Kerguelen Plateau, Société Française d'Ichtyologie*. pp. 167–172.

Le Quere, C. et al., 2005. Ecosystem dynamics based on plankton functional types for global ocean biogeochemistry models. *Global Change Biology*, 11(11), pp.2016–2040. Available at: http://dx.doi.org/10.1111/j.1365-2486.2005.1004.x.

Ralph, P.J. et al., 2007. Melting out of sea ice causes greater photosynthetic stress in algae than freezing in. *Journal of Phycology*, 43(5), pp.948–956. Available at: <Go to ISI>://000249827400010.

Raymond, J.A., 2000. Distribution and partial characterization of ice-active molecules associated with sea-ice diatoms. *Polar Biology*, 23(10), pp.721–729. Available at: http://dx.doi.org/10.1007/s003000000147.

Richardson, A.J., 2009. Plankton and Climate. In J. H. Steele & S. A. Thorpe, eds. *Encyclopedia of Ocean Sciences*. Oxford: Academic Press, pp. 455–464. Available at: http://www.sciencedirect.com/science/article/pii/B9780123744739006597.

Rivkin, R.B., 1985. Carbon-14 labelling patterns of individual marine phytoplankton from natural populations. *Marine Biology*, 89(2), pp.135–142. Available at: http://dx.doi.org/10.1007/BF00392884.

Rivkin, R.B. & Voytek, M.A., 1987. Photoadaptations of photosynthesis and carbon metabolism by phytoplankton from McMurdo Sound, Antarctica. 1. Species-specific and community responses to reduced irradiances. *Limnology and Oceanography*, 32(1), pp.249–259.

Sackett, O. et al., 2013. Phenotypic plasticity of Southern Ocean diatoms: key to success in the sea ice habitat? *PLoS ONE*, 8(11), p.e81185. Available at: http://www.plosone.org/article/info:doi/10.1371/journal.pone.0081185.

Sackett, O. et al., 2014. Taxon-specific responses of Southern Ocean diatoms to Fe enrichment revealed by synchrotron radiation FTIR microspectroscopy. *Biogeosciences Discussions*, 11(KEOPS2 Special Issue), pp.1–31.

Saibo, N.J.M., Lourenco, T. & Oliveira, M.M., 2009. Transcription factors and regulation of photosynthetic and related metabolism under environmental stresses. *Annals of Botany*, 103(4), pp.609–623. Available at: <Go to ISI>://000263162300006.

Sarthou, G. et al., 2005. Growth physiology and fate of diatoms in the ocean: a review. *Journal of Sea Research*, 53(1–2), pp.25–42. Available at: http://www.sciencedirect.com/science/article/pii/S1385110104000644.

Sigee, D.C. et al., 2007. The influence of phosphorus availability on carbon allocation and P quota in Scenedesmus subspicatus: A synchrotron-based FTIR analysis. *Phycologia*, 46, pp.583–592. Available at: <Go to ISI>://WOS:000249353600009.

Smetacek, V., Assmy, P. & Henjes, J., 2004. The role of grazing in structuring Southern Ocean pelagic ecosystems and biogeochemical cycles. *Antarctic Science*, 16(4), pp.541–558. Available at: <Go to ISI>://WOS:000226060800014.

Smetacek, V. & Nicol, S., 2005. Polar ocean ecosystems in a changing world. *Nature*, 437(7057), pp.362–368. Available at: <Go to ISI>://WOS:000231849100043.

Stehfest, K., Toepel, Jã. & Wilhelm, C., 2005. The application of micro-FTIR spectroscopy to analyze nutrient stress-related changes in biomass composition of phytoplankton algae. *Plant Physiology & Biochemistry*, 43(7), pp.717–726. Available at: 10.1016/j.plaphy.2005.07.001.

Suárez, I. & Marañón, E., 2003. Photosynthate allocation in a temperate sea over an annual cycle: the relationship between protein synthesis and phytoplankton physiological state. *Journal of Sea Research*, 50(4), pp.285–299. Available at: http://www.sciencedirect.com/science/article/pii/S1385110103000923.

Tang, K.W. et al., 2009. Survival and recovery of Phaeocystis antarctica (Prymnesiophyceae) from prolonged darkness and freezing. *Proceedings of the Royal Society B-Biological Sciences*, 276(1654), pp.81–90. Available at: <Go to ISI>://000262004900011.

Thomas, D.N. & Dieckmann, G.S., 2002. Antarctic sea ice-a habitat for extremophiles. *Science*, 295(5555), pp.641–644.

Tobin, M.J. et al., 2010. FTIR spectroscopy of single live cells in aqueous media by synchrotron IR microscopy using microfabricated sample holders. *Vibrational Spectroscopy*, 53(1), pp.34–38. Available at: http://www.sciencedirect.com/science/article/pii/S0924203110000299.

Tomczak, M. & Godfrey, S.J., 2003. *Regional Oceanography: an Introduction* 2nd edn., Daya Publishing House, Delhi. Available at: http://www.es.flinders.edu.au/~mattom/regoc/pdfversion.html.

Trovato, M., Mattioli, R. & Costantino, P., 2008. Multiple roles of proline in plant stress tolerance and development. *Rendiconti Lincei*, 19(4), pp.325–346. Available at: http://dx.doi.org/10.1007/s12210-008-0022-8.

Trull, T. et al., 2014. Phytolankton size and compositions variations in naturally iron fertilised Southern Ocean waters: evidence for differing propensities for carbon export in waters downstream versus over the Kerguelen plateau. *Biogeosciences*, (KEOPS2 Special Issue).

Twining, B.S., Baines, S.B., Fisher, N.S., et al., 2004. Cellular iron contents of plankton during the Southern Ocean Iron Experiment (SOFeX). *Deep-Sea Research Part I-Oceanographic Research Papers*, 51(12), pp.1827–1850. Available at: <Go to ISI>://WOS:000226044500003.

Twining, B.S. et al., 2008. Exploring Ocean Biogeochemistry by Single-Cell Microprobe Analysis of Protist Elemental Composition. *Journal of Eukaryotic Microbiology*, 55(3), pp.151–162. Available at: http://dx.doi.org/10.1111/j.1550-7408.2008.00320.x [Accessed March 5, 2013].

Twining, B.S., Baines, S.B. & Fisher, N.S., 2004. Element stoichiometries of individual plankton cells collected during the Southern Ocean Iron Experiment (SOFeX). *Limnology and Oceanography*, 49(6), pp.2115–2128. Available at: <Go to ISI>://WOS:000225137100020.

Vaccari, L. et al., 2012. Synchrotron radiation infrared microspectroscopy of single living cells in microfluidic devices: advantages, disadvantages and future perspectives. *Journal of Physics: Conference Series*, 359, p.012007. Available at: http://stacks.iop.org/1742-6596/359/i=1/a=012007?key=crossref.39973d303808f08f77a36f800ba33ed4 [Accessed October 30, 2013].

Venyaminov SYu & Kalnin, N.N., 1990. Quantitative IR spectrophotometry of peptide compounds in water (H2O) solutions. I. Spectral parameters of amino acid residue absorption bands. *Biopolymers*, 30(13-14), pp.1243–57. Available at: http://www.ncbi.nlm.nih.gov/pubmed/2085660.

Vongsvivut, J. et al., 2012. Quantitative determination of fatty acid compositions in micro-encapsulated fish-oil supplements using Fourier transform infrared (FTIR) spectroscopy. *Food chemistry*, 135(2), pp.603–9. Available at: http://www.ncbi.nlm.nih.gov/pubmed/22868135 [Accessed May 23, 2013].

Wagner, H. et al., 2010. The use of FTIR spectroscopy to assess quantitative changes in the biochemical composition of microalgae. *Journal of biophotonics*, 3(8-9), pp.557–66.

Westberry, T. et al., 2008. Carbon-based primary productivity modeling with vertically resolved photoacclimation. *Global Biogeochem. Cycles*, 22. Available at: http://dx.doi.org/10.1029/2007GB003078.

Whyte, J.N.C., 1987. Biochemical composition and energy content of six species of phytoplankton used in mariculture of bivalves. *Aquaculture*, 60(3–4), pp.231–241. Available at: http://www.sciencedirect.com/science/article/pii/0044848687902900.

Williams, P. & Norris, K. eds., 2001. Implementation of Near-infrared Technology. In *Near-infrared technology in the agricultural and food industries*. American Association of Cereal Chemist, St. Paul, MN, USA, p. 145.

Wold, S., Sjöström, M. & Eriksson, L., 2001. PLS-regression: a basic tool of chemometrics. *Chemometrics and intelligent laboratory systems*, 58(2), pp.109–130. Available at: http://dx.doi.org/10.1016/S0169-7439(01)00155-1.

Wood, A.M., Everroad, R. & Wingard, L., 2005. Measuring growth rates in microalgal cultures. In R. A. Andersen, ed. *Algal culturing techniques*. Elsevier Academic Press, pp. 269–286.

Xie, Y. et al., 2012. Rapid identification and classification of staphylococcus aureus by attenuated total reflectance fourier transform infrared spectroscopy. *Journal of Food Safety*, 32(2), pp.176–183. Available at: http://www.scopus.com/inward/record.url?eid=2-s2.0-84859879283&partnerID=40&md5=86547ded8fb7c9e77dbd7e29e6e1dba0.

Appendix I: Infrared Band Assignments

Wavenumber (cm^{-1})	[a]Assignment	Reference (& refs. therein)
1200-900	ν(C-O-C) of polysaccharides, dominated by ring vibrations of carbohydrates	(Giordano et al. 2001; Naumann 2000)
1080	ν(Si-O) from the silicate frustule	(Giordano et al. 2001)
1230	ν_{as}(P=O) from phosphorylated molecules (includes nucleic acids, phosphorylated proteins and phosphorylated lipids)	(Giordano et al. 2001)
1240	ν(C–N) and δ(N–H) of amides associated with proteins (amide III band)	(Vongsvivut et al. 2012)
1516	Phenol group (ring vibration), possibly from Tyrosine	(Naumann 2000; Venyaminov SYu & Kalnin 1990)
1400	Protein side chain	(Barth 2000)
1450	$\delta_{as}(CH_3)$ and $\delta_{as}(CH_2)$ of proteins	(Heraud et al. 2005)
1540	δ(N-H) of amides associated with proteins	(Heraud et al. 2007; Giordano et al. 2001)
1735	ν(C=O) of ester functional groups, primarily from lipids and fatty acids	(Vongsvivut et al. 2012)
1708	ν(C=O) of free fatty acids	(Murdock & Wetzel 2009)
2850	ν_s(C-H) from methylene ($-CH_2$) groups, primarily from lipids	(Vongsvivut et al. 2012)
2920	ν_{as}(C-H) from methylene (CH_2) groups, primarily from lipids	(Vongsvivut et al. 2012)
2960	ν_{as}(C-H) from methyl (CH_3) groups, primarily from lipids	(Vongsvivut et al. 2012)
3015	ν(C–H) of cis-alkene –HC=CH–, from unsaturated fatty acids	(Vongsvivut et al. 2012)

[a] ν_{as} - asymmetric stretch; ν_s - symmetric stretch; δas - asymmetric deformation (bend); δs - symmetric deformation (bend)

Appendix II: Publications resulting from this thesis

Below is a list of publications resulting from this thesis along with the associated author contributions.

Sackett, O., Petrou, K., Reedy, B., Grazia, A. De, Hill, R., Doblin, M., Beardall, J., Ralph, P. and Heraud, P.: Phenotypic plasticity of Southern Ocean diatoms: key to success in the sea ice habitat?, PLoS One, 8(11), doi:10.1371/journal.pone.0081185, 2013.

- Designed experiments: O.S., K.P., R.H., M.D., P.R.
- Conducted experiments: O.S., K.P., B.R., A.G., P.H., J.B.
- Analysed data: O.S., P.H., J.B.
- Wrote manuscript: O.S., K.P., P.H., J.B., M.D., P.R., R.H.

Sackett, O., Armand, L., Beardall, J., Hill, R., Doblin, M., Connelly, C., Howes, J., Stuart, B., Ralph, P., and Heraud, P.: Taxon-specific responses of Southern Ocean diatoms to Fe enrichment revealed by synchrotron radiation FTIR microspectroscopy, Biogeosciences, 11, 5795-5808, doi:10.5194/bg-11-5795-2014, 2014.

- Designed experiments: O.S., L.A., P.H.
- Conducted experiments: O.S., L.A., P.H., C.C, J.H.
- Analysed data: O.S., P.H., J.B.
- Wrote manuscript: O.S., P.H., J.B., L.A., P.R., M.D., R.H.

Sackett, O., Petrou, K., Reedy, B., Hill, R., Doblin, M., Beardall, J., Ralph, P. and Heraud, P.: Snapshot prediction of carbon productivity, carbon and protein content in a Southern Ocean diatom using FTIR spectroscopy, ISME J. *(submitted November 2014)*.

- Designed experiments: O.S., K.P., R.H., M.D., P.R.
- Conducted experiments: O.S., K.P., B.R., P.H., J.B.
- Analysed data: O.S., P.H., J.B.
- Wrote manuscript: O.S., K.P., P.H., J.B., M.D., P.R.

Please see the below literature for further physiological data related to Chapter 2 and 4.

Petrou, K., Doblin, M. & Ralph, P., 2011. Heterogeneity in the photoprotective capacity of three Antarctic diatoms during short-term changes in salinity and temperature. *Marine biology*, 158(5), pp.1029–1041.

Petrou, K. & Ralph, P.J., 2011. Photosynthesis and net primary productivity in three Antarctic diatoms: possible significance for their distribution in the Antarctic marine ecosystem. *MEPS*, 437, pp.27–40.